Functional Oxides for Photo-Neuromorphic Engineering: towards a *Solar Brain*

Amador Pérez-Tomás*

Catalan Institute of Nanoscience and Nanotechnology (ICN2), CSIC and the Barcelona Institute of Science and Technology, Barcelona, Spain
E-mail: amador.perez@icn2.cat

New device concepts and new computing principles are needed to balance our ever-growing appetite for data and information with the realization of the goals of increased energy efficiency, reduction in CO_2 emissions and the circular economy. Neuromorphic or synaptic electronics is an emerging field of research aiming to overcome the current computer's Von-Neumann bottleneck by building artificial neuronal systems to mimic the extremely energy efficient biological synapses. The introduction of photovoltaic and/or photonic aspects into these neuromorphic architectures will produce self-powered adaptive electronics but may also open up new possibilities in artificial neuroscience, artificial neural communications, sensing and machine learning which would enable, in turn, a new era for computational systems owing to the possibility of attaining high bandwidths with much reduced power consumption. This perspective is focused on recent progress in the implementation of functional oxide thin-films into photovoltaic and neuromorphic applications towards the envisioned goal of self-powered photovoltaic neuromorphic systems or a *solar brain*.

Index

1. Introduction

1.1. It is the Energy Issue

A *living technology* [1] based on a largely distributed networks of wireless sensors with artificial intelligence have great potential for a better internet-of-things (IOT) implementation in areas such as robotics, transportation, health care, environmental monitoring or safety. However, to alleviate the problems associated with the increasingly number of batteries (e.g. monitoring, replacing and recycling) and/or the additional electrical energy consumption from the grid; the new generation of IOT devices should be *self-powered* [2], [3], [4], [5]. The electrical energy to power the electronics would be generated primarily from *light* [6], [7], *kinetic* [8], [9], *electromagnetic* [10], [11] or *thermal energy* [12], [13] (Fig. 1). The obtained energy can then be used to recharge a secondary battery or, in some cases, to power directly the electronics. Among these environmental energy sources, the sun light interacts with Earth's atmosphere and lifeforms to act as the main source of energy in our planet [14]. New device concepts [15] and, perhaps equally importantly, new computing principles [16] are needed to balance our ever-growing appetite for data and information with the realization of the goals of increased energy efficiency, reduction in CO_2 emissions and the circular economy [17]. In a prominent place, neuromorphic or synaptic electronics is an emerging field of research focused in creating artificial synaptic devices to mimic the computation carried out by biological synapses (see e.g. [18] [19] [20] [21] [22] [23] [24] [25] [26] [27] [28]). The renewed research efforts on synaptic electronics and brain-inspired computing can be understood by regarding the energy consumption issue, the increasing signaling of the end of the Moore's Law for nanoelectronics scaling era and the inefficiency of conventional (aka *Von-Neumann*) computational systems [29] (Fig. 2). Today's Von-Neumann computers are shockingly wasteful; modern microprocessors are orders of magnitude less efficient than human brains. While there are $\sim 10^{10}$ neurons in the human cortex, there are only $\sim 10^5$ of processors in powerful parallel computers (e.g. Blue Gene supercomputer with $\sim 140,000$ microprocessors and 144 TB of memories consuming a power of 1.4 MW [30]). The "reduced" number of processors is compensated by their speed; CMOS transistors are much faster ($\sim 10^{-9}$ s) compared with the operating speed of biological neurons ($\sim 10^{-3}$ s), but at much higher energy cost; the human brain is extremely energy efficient, using $\sim 10^{-16}$ J/s per operation, whereas the best computers today consume around $\sim 10^{-6}$ J/s. The hardware of neuromorphic systems is either *extrinsic* (silicon-based CMOS artificial neurons sorted in neural networks [31]) or

intrinsic that are constructed with synaptic devices that inherently possess key figures such as plasticity [32] non-linearity [33] or spiking processing capabilities [34], [35], [19], [36]. Nevertheless, artificial neural networks with the computing capability of a human brain composed solely of silicon CMOS-based hardware would demand extremely high resources in terms of power consumption. Several projections point out that a just a bunch of these brain-like *Von-Neumann* computing machines would require a sizable fraction of the global energy produced worldwide while the human brain uses only about ~10 watts of power [37]. Therefore, the *Von-Neumann* paradigm must be shifted to build energetically viable computing machines with the learning and adaptive capabilities of biological brains. Or in other words, we need to rethink computers from scratch (and the way they are powered) if we want living technologies that think like us. But the energy issue does not restrict to computers; there is a consensus that energy consumption is one of the grand challenges facing our planet today [38] and one of the IOT main global challenges [39],[40]. Functional oxide thin-films is, at the time being, perhaps the only platform [41] to conceive *intrinsic* photo-neuromorphic engineering and to analyze this fact is devoted this progress report. Advances in photo-neuromorphic devices could pave the way to artificial live hardware mimicking biological systems [42], [43], [44] but at *zero metabolic cost* [45] (Fig. 2). Besides the energy issue, the introduction of photonic aspects into these neuromorphic architectures may also open up new possibilities in artificial neural communications, sensing and learning which may open up a new era for computational systems owing to the possibility of attaining high bandwidths and the low-computation-power requirements [46].

1.2. Functional Metal Oxides for Photo-Neuromorphic Engineering

1.2.1. Oxide Resistivity

Oxides are a very relevant class of materials for emerging self-powered electronic (Fig. 3) systems owing to their semiconductor and ionic properties [47], [48], [49], [50], [51], [52]. They are the most abundant material system in nature (Earth's crust) owing the large oxygen electronegativity that easily creates stable chemical bonds with almost all elements thereby forming binary (e.g. SiO_2) and complex oxides (e.g. $PbTi_xZr_{1-x}O_3$). They present a number of various basic crystalline structures including rocksalt (TiO, VO, NbO, EuO, FeO, NiO…), corundum (Al_2O_3, Ga_2O_3, V_2O_3…), rutile (TiO_2,SnO_2,VO_2,RuO_2,OsO_2), ReO_3, WO_3, perovskite ($CaTiO_3$, $SrTiO_3$, $BaTiO_3$, $PbZrO_3$, $PbTiO_3$…), spinel ($MgAl_2O_4$, $NiFe_2O_4$,

CoFe$_2$O$_4$, MnFe$_2$O$_4$, LiV$_2$O$_4$, Fe$_3$O$_4$…), pyrochlore (Y$_2$Ti$_2$O$_7$, La$_2$Zr$_2$O$_7$, Y$_2$Mo$_2$O$_7$, Cd$_2$Re$_2$O$_7$) or tungsten bronzes (M_xWO$_3$, Sr$_x$Ba$_{1-x}$Nb$_2$O$_6$). In these structures, the oxygen is usually bounded to three metals (e.g. rutile) or six metals (e.g. rocksalt) although there are many non-stoichiometric and/or amorphous compounds. Besides, many oxides are also polymorph an example being TiO$_2$ which can present phases of rutile, anatase, and brookite. Most metal oxides (such as Al$_2$O$_3$, Ga$_2$O$_3$, TiO$_2$, Cu$_2$O, WO$_3$, or NiO) have a much wider bandgap than that of silicon (1.12 eV) and are generally insulating at room temperature if they are stoichiometric and undoped [53]. It is usual that the metal-*s* or *d* orbitals overlap with the ligand oxygen-2*p* orbitals forming molecular bands; the conduction band being the metal bands and the valence band related to the oxygen *p*-band. Nevertheless, the oxide's electronic conductivity modulation required for defining solid-state devices (e.g. *p-n* or Schottky junctions) can be accomplished either *extrinsically* (involving external impurities) or *intrinsically* (due to their own oxide/cation vacancies and interstitials) [54]. Extrinsic doping implies substitutional atoms of different valence while free carriers can also be produced by the thermal (entropically driven) excitations of intrinsic defects such as interstitials and vacancies. Some metal oxides can, for example, be both optically transparent and highly conductive (i.e. *transparent conducting oxides* (TCOs)) when degenerately doped (e.g. In$_2$O$_3$, SnO$_2$ or ZnO). Such TCOs are currently the standard choice for use in transparent electrode applications [55] and are also hugely important for information and communication technologies such as displays, touch screens, solar cells or light emitting diodes [56]. Another key factor in the adoption of oxide semiconductors is that they are compatible with the strict manufacturing requirements of large-scale, large-volume, flexible, low cost and disposable/reusable devices [57], [58]. These constraints are particularly relevant for thin-film photovoltaics where extremely large-scale, large volume fabrication requires low cost fabrication in order to be competitive with dominant Si-based photovoltaic technologies. Non-degenerate *transparent semi-conducting oxides* (TSOs) are also widely investigated as the semiconductor platform for many applications, including; solar cells (see e.g. [59], [51]), display's thin-film transistors (see e.g. [60]), photodetectors [61] or transparent power transistors [62] among other applications. *Transparent insulating oxides* (TIOs) usually are the platform of choice for defining the insulation layers (either gate or passivation - e.g. SiO$_2$, Al$_2$O$_3$, HfO$_2$) [63], [64], [65] in several semiconductor industries (i.e. silicon, SiC or GaN) [66], [67] and insulating oxides are also ubiquitous as electronic substrates (sapphire, Ga$_2$O$_3$) [68],[69], optoelectronic transparent substrates (soda-lime and borosilicate glasses, sapphire, YSZ) and optical lenses.

1.2.2. Oxide Resistive Switching

Functional insulating oxide thin-films also are one of the most promising material systems for neuromorphic engineering [21], [24], [22]. As neuronal synaptic connections are strengthened or weakened in biological brains, the sudden resistivity changes of insulating oxide thin-films imitates the way a new memory is acquired or forgotten in bio-synapses. Oxides have arguably shown the highest flexibility and prospects of all investigated material systems where *resistive switching* (RS) phenomena is observed. A resistive switching device can be defined as a variable resistor with memory in which its internal electrical resistivity depends on the applied electric field (or current) and its previous history [70], [71], [72]. Once the field is removed, a RS event can be irreversible (non-volatile), when it stays in the new resistivity state, or transitory (volatile), when it comes back to the original resistivity value after a characteristic time. Oxide thin-films singularity lies in the fact that they merge an almost universal non-volatile RS phenomenological behavior with other uncommon electronic properties owing to unusual electronic-lattice and electronic-electronic quantum interactions [73], [74], [75]. The common physical origin of *non-volatile RS* relies on *ionic drift* within the insulating oxide thin-film which creates defects (generally oxygen vacancies) and induces their migration due to the multi-valence states of metal oxides [76]. For some of these metal oxides, the free electron (and free hole) drift on conduction (and valence) band framework fails when second order effects (usually neglected in the basic band theory) become larger that the width of the energy band. These non-conventional effects include non-periodic potentials, electron-phonon exchanges and strong electron-electron correlations giving rise to the reversible Mott transition (also known as metal insulation transition - MIT) which eventually is a route for implementing *volatile RS* [77]. Complex transition metal oxide materials also exhibit a broad range of supplementary electronic and magnetic properties such as ferromagnetism, colossal magnetoresistance, spin-charge coupling, (anti)-ferroelectricity and high-temperature superconductivity which often come from their strongly correlated electrons in d or f orbitals [78], [79], [80]. Some of these unusual quantum material properties can also be engineered to implement additional sources for volatile and non-volatile RS. Therefore, metal oxides are especially appealing for neuromorphic engineering as they feature multiple routes for implementing both types of resistive switching. This inherent oxide versatility enables, in turn, a variety of routes for implementing the basic building blocks of neuromorphic hardware: *Neuristors* and *Synaptors* [24]. Neuristors emulate the action potential

signaling of cortical spiking neurons while synaptors emulate the memory behavior (the connection with variable strength in between two neurons) of biological synapses in response to a train of spikes, as will be shown further on.

1.2.3. Oxide Photo-Resistive Switching

The same resistive switching oxide layers are present in several kinds of light harvesting devices and they are multifunctional; as transparent conductive electrodes, as light absorbers, as semiconductor transport layers or bringing new functionalities into the structure such as ferroelectricity. Ferroelectric photovoltaics is, in particular, a growing field of research and is the class of materials for which the single-phase and *non-Shockley–Queisser* limited [81], [82] *bulk photovoltaic effect* (BPE) is strongest [83], [84], [85], [86], [87], [88]. In such arrangements, an often-overlooked property of a ferroelectric semiconductor is that the switchable bipolar surface arrangement also implies a switchable surface band-bending. In a heterojunction (with an oxide absorber or other efficient light harvester), this property is used to define cheap and large area compact self-powered neuromorphic two-terminal solar transistors and thus, paving the way to self-powered neuristors and synaptors [89], [90]. Oxide thin-films also exhibit other photonic properties with inherent photo-switchable and/or photo-memory features such as persistent photoconductivity [91], [92], [93], [94], photorefraction [95], [96], [97] and other electro-optic phenomena such as the Pockels Effect [98], [99]. Therefore, functional oxides are arguably the most promising material system for future *neuromorphic photovoltaic engineering* (or photo-neuromorphic engineering). In this progress report, it is succinctly overviewed recent progress in the implementation of functional oxide thin-films into photovoltaic and neuromorphic applications towards the envisioned goal of self-powered photovoltaic neuromorphic systems or a *solar brain*.

2. Oxide Thin-films for Photovoltaic Engineering

2.1. Photovoltaic Devices

Sunlight harvesting usually takes place in a *solar cell*. A solar cell is the optoelectronic device that converts light quanta energy (i.e. photons) in electric energy (i.e. free carriers - electrons and/or holes) by means of the photovoltaic effect [100], [101]. Solar cells are however commonly described as photovoltaic devices, irrespective of whether the source is sunlight or an artificial

light. In most photovoltaic devices, the light harvesting takes place in a semiconductor *p-n* junction (Fig. 4(a)). When its space-charge region is illuminated, an electric current is generated; excited electrons (in the conduction band) and the remaining holes (in the valence band) are swept in different directions by the built-in electric field of the depletion region. However, an electron and a hole can also meet and recombine (principle of detailed balance) thus limiting the electron per photon conversion. The theoretical maximum solar (unconcentrated, AM 1.5 solar spectrum) power conversion efficiency (PCE) for a single *p-n* junction is ~33% (peaking at a band gap of ~1.2-1.4 eV) and the maximum photovoltage possible is always below the semiconductor bandgap [102]. These figures are commonly known as the *Shockley-Queisser limit* which represents a fundamental limit of conventional solar cells [81]. The *bulk photovoltaic effect* (BPE) is a completely different approach where a photo-current is impressed with unpolarized light in the bulk of non-centric (Fig. 4(b) single-phase ferro- and pyroelectric crystals, and with polarized light even in non-pyroelectric piezoelectric crystals [103]. In traditional *p-n* light harvesting devices, the mechanism for separation of the photo-excited carriers is the built-in electric field inside *p–n* junctions. Several BPE mechanisms have been reported in the literature including quantum-coherent shift-current [104], circular photo-galvanic [105] or ballistic transport (due to absorption/scattering center's asymmetry) [106], [107]. In the shift current framework, the photo-carrier transport is ascribed to a quantum-mechanical coherent excitation instead of inelastic scattering [108]. As the shift-current driving force for carrier separation is believed to be the coherent evolution of photo-carrier wave-functions (not the *p-n* built-in electric field), the so-called Shockley–Queisser limit of conventional *p-n* solar cell could be surpassed [81]. This implies that photo-voltages much larger that the semiconductor bandgap (or above bandgap voltages) can be obtained [87] and it has also been argued that shift current carriers would rapidly propagate to the electrodes potentially reducing energy losses [88]. Mechanical strain has also been studied as a way to enhance photovoltaic conversion in piezoelectric semiconductors (e.g. ZnO) resulting in a *piezo-phototronic effect* [109], [110] (Fig. 4(c)) and, very recently, Yang *et al.* [111] expanded the class of materials capable of exhibiting the BPE effect by making ordinarily centrosymmetric materials, such as $SrTiO_3$ and TiO_2, lose their inversion symmetry by a strain gradient (i.e, flexoelectricity) (Fig. 4(d)). The *flexo-photovoltaic effect*, is expected to apply to most semiconductors by inducing a strain gradient [112] (e.g. by an atomic force microscope tip) resulting in photovoltaic currents under illumination.

Although there are a number of photovoltaic technologies (e.g. III-V, (single crystal) c-Si, CIGS, CdTe, halide organic-inorganic perovskite (HOIP), (amorphous) a-Si, CZT(S,Se), dye sensitized or organic bulk heterojunction (OPV)), the basic solar cell structure is a sandwich of a light harvester [113] layer (depleted of free carriers) in between two carrier extraction layers [114]. Solar cells are designed to maximize the light conversion into electricity (i.e. the power conversion efficiency) (Fig. 5). At the time being, III-V GaAs-based photovoltaic devices hold the world record for the highest-efficiency *p-n* single-junction at 28.8% [115] while c-Si, CIGS, CdTe and HOIP solar cells have also been reported to deliver efficiencies above 20% [116]. Oxides are widely used in solar cells (e.g. as light harvesters, conductors (TCOs), semiconductors (TSOs) and insulators (TIOs)) and are generally adopted because they deliver performance advantages, a lower cost and larger device stability or brings new functionalities into the structure such as ferroelectricity [51]. Other uses of oxide thin-films in the photovoltaic context include antireflection coatings [117] and back reflectors [118]. As it will be review in the next sections, oxide thin-films are used as solar cell's electrodes, buffers and absorbers. Being still a developing field, oxides absorbers are now producing solar cells with power conversion efficiencies around of ~8% as will be shown further on.

2.2. OTF as *Electrodes*: Transparent Metals

Any photovoltaic or light harvesting device in a vertical architecture (i.e., sandwiched in between two electrodes) requires one of these two electrodes to be a transparent conducting electrode for the light penetrating into the light absorbing core layers without attenuation [6],[119]. For some consumer electronics applications these transparent metals should be also flexible [120], [56], [121], [122]. In most optoelectronic systems, transparent conducting electrodes have been traditionally made of degenerately doped wide bandgap transparent metal oxides (TCO) [123], [124] while recently there is also interest in carbon materials such as graphene [125], [126] or flexible polymer/metal hybrid electrodes [127], [128]. The low resistivity in TCOs is generally achieved by increasing the oxide carrier concentration extrinsically (i.e. doping) while not degrading in excess its mobility (although there are intrinsic transparent conductors without extrinsic doping [129], [130]). While the largest impurity concentration achievable by doping is limited by the dopant solubility within the oxide lattice (typically ~10^{21} cm^{-3}), the free carrier mobility is degraded by its Coulomb scattering at the large number of ionized impurities (a common phenomenon taking place in any degenerately doped semiconductors [131]). Intrinsic semiconductor oxides are predominately *n*-type due to their ability to form

oxygen vacancies (e.g. In_2O_3, SnO_2, ZnO) [132]. Depositing or annealing in reduced oxygen partial pressure can increase the conductivity of the oxide by introducing more carriers. In contrast, there are few predominantly *p*-type oxide semiconductors due to cation vacancies such as Cu_2O, SnO or NiO [133],[134]. In any case, oxides generally exhibit an important doping asymmetry and bipolar oxide semiconductors [135] represent only a small subset (e.g. $CuInO_2$ [136], SnO [137], Ga_2O_3 [138], $Ni_xCd_{1-x}O_{1+\delta}$ [139], $SnNb_2O_6$ [140], ZrOS [141]).

2.1.1. *n*-type

Electron TCOs have a long history with the first reported being cadmium oxide (CdO) as early as in 1907 [142]. They have been (and continue to be) the usual material of choice for transparent electrodes since 1950s [143]. In practice, the industry standard has been primarily restricted to doped forms of In_2O_3, SnO_2 and ZnO and their alloys [55] (Fig. 6(a)). The surplus of free electrons in these well-known TCOs is usually achieved by foreign atom substitutional doping. Indium oxide doped with tin (ITO or In_2O_3:Sn) is, at the time being, the TCO exhibiting the lowest resistivity on an industrial scale (~1-2x10^{-4} Ωcm) [144], [145]. The resistivity of tin oxides (SnO_2) can be as low as 5x10^{-4} Ωcm, depending on the substitutional impurity [146]. Within the SnO_2 family, the industrial standard is commonly the fluorine-doped one (FTO or SnO_2:F) [146] due to its raw material and processing low costs (indium is an expensive precious metal). Zinc oxides (ZnO) either doped with gallium (GZO) or aluminum (AZO) may present resistivities lying somewhere in between ITO and FTO (~2-4x10^{-4} Ωcm) [147],[148],[149],[150]. During many years, titanium oxide (TiO_2) was considered too resistive to be used as a competitive *n*-type TCO. Nevertheless, it was demonstrated by mid 2000s that, low-temperature polymorph anatase epitaxially grown Nb- or Ta-doped TiO_2 may present resistivities as low as 5x10^{-4} Ωcm [151], [152].

There are other *n*-type more complex oxides (ternary or multicomponent oxides) exhibiting excelent TCO characteristics. These complex oxides are formed through combination of binary compounds. The most relevant cations can be grouped as divalent (Cd^{2+} and Zn^{2+}), trivalent (Ga^{3+} and In^{3+}), and tetravalent (Sn^{4+}). Examples of ternaries are Cd_2SnO_4, $CdSnO_3$, Zn_2SnO_4, $CdIn_2O_4$, $Zn_2In_2O_5$, $MgIn_2O_4$ or $In_4Sn_3O_{12}$ and quaternaries $Zn_2In_2O_5$-$MgIn_2O_4$, $ZnIn_2O_5$-$In_4Sn_3O_{12}$, $GaInO_3$-$In_4Sn_3O_{12}$ or In_2O_3-Ga_2O_3-ZnO [57]. There are some notable crystalline ternary oxides exhibiting particularly high mobility such as cadmium stannate (Cd_2SnO_4) and barium stannate ($BaSnO_3$). Single-phase spinel Cd_2SnO_4 is a ternary oxide used in the cadmium telluride (CdTe) photovoltaic technology which may exhibit the

remarkable low resistivity of ~1-2x10^{-4} Ωcm [153],[154]. Toxic cadmium is replaced with zinc in more environmentally friendly approaches but the resistivity of polycrystalline or amorphous zinc stanate (Zn_2SnO_4) is significantly higher (~1x10^{-3}Ωcm) [155], [156], [157]. Perovskite cadmium tellurate Cd_3TeO_6 [158] and In-doped Cd_3TeO_6 [159] have been reported to present conductivities of up to ~2×10^{-2} Ωcm and ~3×10^{-3} Ωcm, respectiviely (Hall mobilities in the range of 6-10 cm^2/Vs). Perovskite La-doped $BaSnO_3$ films have been reported with conductivity exceeding 10^4 S/cm with mobilities of up to 120 cm^2/Vs, even at carrier concentrations above 3×10^{20} cm^{-3} [160]. Many other perovskite-type ternary oxides have also been investigated as n-type TCOs including stannates, and titanates such as $SrSnO_3$, $SrTiO_3$, $ZnSnO_3$, $CaSnO_3$ or $CaTiO_3$. Strontium stannate ($SrSnO_3$) has been doped with lanthanum, antimony or neodymium - $SrSnO_3$:(La,Sb,Nd) [161], [162] while strontium titanate ($SrTiO_3$) has been doped with lanthanum or antimonium - $SrTiO_3$:(La,Sb) [163], [164]. $ZnSnO_3$, $CaSnO_3$ or $CaTiO_3$ have been doped with antimonium, Terbium-Magnesium (Tb-Mg-) or niobium (e.g. $ZnSnO_3$:Sb [165], $CaSnO_3$:Tb-Mg [166], and $CaTiO_3$:Nb [167]). Perovskite correlated vanadates such as $SrVO_3$ and $CaVO_3$ have been recently reported as n-type TCO alternative. Notably, this correlated oxide route represent an unconventional approach; the strong electron–electron interactions produce an electron effective mass enhancement (i.e., larger mobility), although their high carrier concentration (~10^{22} cm^{-3}), thus resulting in an overall conductivity as high as 1-3x10^4 S/cm [168].

In a similar fashion, tunable electrical conductivity (while maintaining superior mobility) is arguably the central technological advantage of an amorphous oxide TCO. The conduction band in amorphous oxides is generally composed of spherical and isotropic 5s orbitals which overlap is rather invariant despite the large structural disorders [169], [170]. This is in marked contrast to the previous (poly)crystalline semiconductor oxides, where the electron mobility is governed primarily by the scattering on ionized impurities, phonons, and grain boundaries. Ionic amorphous mixed oxides such as In–Zn–O (IZO) and In–Ga–Zn–O (IGZO) are prominent n-type amorphous oxide TCOs [171], [172], [173]. Amorphous oxides exhibit several additional technological advantages such as very large-area deposition at low temperature, mechanical stretchability and high carrier mobility (~10-100 cm^2/Vs), which is ×10-100 larger than of amorphous silicon (~ 1 cm^2/Vs). Since the first amorphous indium gallium zinc oxide (IGZO) was reported in 2004 [174], a number of advances during the last decade have boosted amorphous oxide-based transistors as an alternative for flexible and transparent electronics [175].

2.1.2. *p*-type

Hole majority or acceptor *p*-type TCOs have, in general, much larger resistivities than their *n*-type counterparts and no degenerately doped acceptor TCO is industrially viable as generic transparent conducting electrode yet (in contrast to the well-stablished *n*-type ITO, FTO or AZO) [176], [177]. Nevertheless, efficient *p*-type transparent conducting electrodes are still required in a number of optoelectronic applications (e.g. those involving the efficient carrier transport of both electron and holes) such as LEDs, solar cells or complementary logic circuits with TFTs. For the majority of oxides, to achieve sizable *p*-type conductivity is challenging because their valence band maximum consists of strongly localized O 2*p*-derived orbitals. In other words, the valence band of most oxides is rather *flat*, resulting in deep acceptor levels (lower free hole concentration at room temperature) and larger hole effective masses (lower mobilities) [176], [178]. There are however few notable *p*-type oxide exceptions to this *valence-band flatness* rule; oxides where free holes can drift with a similar drift velocity to the *n*-type free electron case. The archetypical example is cuprous oxide (Cu_2O), which exhibits acceptor mobilities larger than 100 cm^2/Vs [179]. A particularly parabolic valence band structure, owing to a pronounced covalent exchange between Cu (*d*) and O (*p*) orbitals, results in the Cu_2O exceptionally large *p*-type mobility. However, a shorter Cu-Cu separation implies stronger Cu *d-d* orbital exchanges also resulting in a relative narrow bandgap of around ~2.1 eV [180],[181]. A TCO should have a bandgap larger than 3eV to be transparent to the visible spectrum (400-700 nm), thus making Cu_2O rather unsuitable as transparent electrode but still interesting as efficient sunlight harvester (as will be shown in the next section). Tin monoxide (SnO) is a wider bandgap oxide (2.6-3.4 eV) which also exhibits particularly spatially extended cation orbitals (*s*-orbitals in this case) [182],[183],[184]. Although it has recently been shown that the incorporation of metallic Sn can remarkably improve the hole mobility (~20 cm^2/Vs), preparing acceptor stable SnO is still challenging [184]. Recently, it has been suggested that bismuth incorporation may lead to enhanced extended *s*-orbital applicability in *p*-type SnO [185]. Among *classic* wider bandgap *p*-type oxides, perhaps the most investigated acceptor TCO is nickel oxide (NiO). NiO usually presents a rock salt structure and a bandgap energy in the range of ~3.6-4.0 eV [186]. As a proper wide bandgap semiconductor, stoichiometric and undoped NiO is a very good insulator (~10^{13} Ωcm). However, the NiO *p*-type conductivity can be increased by creating defects (nickel vacancies), doping (incorporation of monovalent atoms such as lithium or cesium) and/or interstitial oxygen. In this sense, Ni vacancies in NiO_x thin-films (in oxygen-rich conditions) have been reported to result in much larger

conductivities of ~ 7 $\Omega^{-1}cm^{-1}$ [186]. The NiO hole mobility may also be relatively high. For example, values in excess of ~25 cm^2/Vs have been reported owing to an excess of oxygen (which produce additional free holes) in non-stoichiometric NiO_x films [187]. Doping NiO with Li^+ or Cs^+ at Ni sites is also a widely used method to enhance the NiO conductivity (up to values of ~10-20 $\Omega^{-1}cm^{-1}$) [188], [189], [190], [191]. Analogously, Li doped ZnO (~3.6 eV) has a *p*-type character, when Li is included as Zn substitutional dopant, but it turns into an *n*-type when Li is in interstitial sites [192], [193].

In complex oxides, the concept of chemical modulation of the valence band (introduced by Kawazoe, Hosono *et al.* [194] in 1997) is a well-known route to reduce the *p*-type oxide resistivity of Cu-based ternary compounds. The acceptor conductivity in these complex oxides increases due to the formation of tight covalent bindings and the hybridization of O 2*p* and (closed shell) Cu $3d^{10}$ orbitals. This results in a greater dispersion at the valence band maxima (i.e., a reduction of the hole localization) while the nature of the d^{10} closed shell avoids optical coloration. Following this rule, a series of *p*-type TCOs based on Cu^+ bearing oxides, such as delafossites (e.g. $CuGaO_2$, $CuInO_2$, $CuCrO_2$, $CuBO_2$, $CuScO_2$ or $SrCu_2O_2$) [195], [196], [197], [198], [199] has been discovered since then. Cu vacancies can further enhance the *p*-type conductivity in these material systems [200], [201], [202]. In this sense, Lunca-Popa *et al.* [203] reported $Cu_{0.66}Cr_{1.33}O_2$ thin films showing conductivities greater than 100 $\Omega^{-1}cm^{-1}$ and carrier concentrations around 10^{21} cm^{-3} owing to metastable Cu-vacancies chain defects. Substitutional doping (e.g. Mg-doped $CuCr_{1-x}Mg_xO_2$) has resulted in *p*-type layers with conductivities of up to ~200 $\Omega^{-1}cm^{-1}$. Analogously, the Mg and N substitution of Cr and O sites (in $CuCrO_2$) resulted in an increased conductivity of up to ~278 $\Omega^{-1}cm^{-1}$ [204], which arguably is the largest conductivity for *p*-type Cu-based delaffosite oxides reported to date. More recently, the valence band chemical modulation concept has been extended to other materials with quasi-closed shells such as d^6 and d^3. A series of novel *p*-type TCOs were identified following this approach such as ZnM_2O4 spinels (*M*=Rh,Ir) [205] and Sr-,Ca-,Ba-doped (substituting for La) $LaCrO_3$ [206], [207]. Hu *et al.* [208] reported in 2018 that substitution of La^{3+} by Sr^{2+} in the Mott-Hubbard insulator $LaVO_3$ can introduce high hole carrier concentration at the top of the valence band with *p*-type $La_{2/3}Sr_{1/3}VO_3$ conductivity of 872.3 $\Omega^{-1}cm^{-1}$ (Fig. 6(b)). The concept of chemical modulation was further extended introducing oxygen substitutional chalcogens atoms (S, Se and Te) owing to the greater hybridization level of Cu 3*d* orbitals and chalcogen *p* orbitals [209], [210], [211], [212], [213]. In this regard, Mg-doped NdCuOS has been reported to be an excellent *p*-type TSO [214] while layered Mg-doped

LaCuOSe exhibited a high *p*-type conductivity of 910 $\Omega^{-1}cm^{-1}$ [215], but a relatively narrow bandgap of ~2.8 eV somehow limits its optical transparency for TCO applications. One of the most promising transparent *p*-type kind of oxide material is the layered quinary oxychalcogenide system $[Cu_2S_2][A_3M_2O_5]$ [216]. In particular, the Cu-quinary compound $[Cu_2S_2][Sr_3Sc_2O_5]$, which is comprised of alternating $[Cu_2S_2]^{2-}$ layers and perovskite-like $[Sr_3Sc_2O_5]^{2+}$ layers. $[Cu_2S_2][Sr_3Sc_2O_5]$ has a large band gap of 3.1eV and hole mobilities of up to ~150 $cm^{2/}Vs$ [217]. Analogously, the quinary oxychalcogenide $[Cu_2S_2][Ba_3Sc_2O_5]$, was found to possess even wider optical band gap (3.24eV) and calculated *p*-type conductivities of up to ~2000 $\Omega^{-1}cm^{-1}$. This value is in the conductivity range of thin films of industry standard *n*-type TCOs and the largest conductivity predicted for any *p*-type TCO to date [216]. In a similar fashion to oxychalcogenides, some bismuth and antimony-based oxyhalides such as SbOF, BiO*X* (*X*=Cl,Br) and $Sb_4O_5X_2$ (*X*=Cl,Br) have also recently suggested as potentially high performing TCOs owing to their predicted large bandgap (>3 eV) and low effective electron mass [218]. Regarding two-dimensional oxide materials, 2D TeO_2 exhibits a direct bandgap when thinning from bulk (3.32 eV) to monolayer (3.70 eV); which is an energy range not accessible by conventional 2D materials (in between *h*-BN (~5eV) and transition metal dichalcogenides (~2eV)). Furthermore, monolayer TeO_2 is exceptional in high transport anisotropy, possessing not only high electron mobility (of the order of 1000 cm^2/Vs but also exceptionally high hole mobility (up to 9100 cm^2/V s) [219].

2.2. OTF as the *Core*: Light Harvesters

In conventional solar cells, a semiconductor junction is essential to host an internal built-in field to split photo-generated electron and hole pairs and to bring these carriers to their respective electrodes. This junction can be a metal-semiconductor Schottky interface, a *p-n* semiconductor homojunction or an (usually *p-n*) heterojunction of dissimilar semiconductors. In general, a bipolar *p-n* junction is the kind of photovoltaic interface delivering the highest (light to electricity) power conversion efficiency as it can harvest both, electron and holes (Schottky junctions are unipolar). In *p-n* solar cells, it is the *p*-type *absorber* layer the one that defines the main photo-physics (absorbance efficiency, direct vs indirect photo-excitations, active wavelength range, etc.) and the transport properties (conductivity, electron and hole mobilities, minority vs majority carrier transport, recombination etc.) [220]. It is common in the literature to refer to the other side of the *p-n* junction, the *n*-type layer, as the widow layer.

Due to the broad bandgap energy range covered by metal oxides (which is also tunable by varying their crystal structure, stoichiometry, alloying etc.), there are many oxides potentially suitable as light harvesters. However, as silicon and other III-V semiconductors (and, more recently, chalcogenides and halides) have historically received much more attention, only a bunch of metal oxides have been seriously investigated as the photon harvester media [221]. The copper oxide family (Cu-O) is, by far, the most studied oxide material system to harvest sunlight among all metal oxides. Stable binary oxide phases of copper oxides are Cu_2O (cuprite or cuprous oxide), CuO (tenorite or cupric oxide) and Cu_4O_3 (paramelaconite) where the CuO_x bandgap can be tuned to cover the entire range in between 1.4-2.2 eV [222]. Emerging oxides being investigated as photon harvesters include cobalt (Co-O), bismuth (Bi-O) and iron (Fe-O) oxides [223]. In contrast, because the BPE mechanism relies only on the crystal inversion asymmetry, it can be realized in single-phase materials (e.g. a *n*-type, *p*-type or insulating single thin-film) and this would allow for a much simpler implementation. Ferroelectric oxides, a small subset of polar materials which have a switchable polarization direction, have been the most investigated BPE materials. Since 1950s, the most studied and prominent class of ferroelectrics are the perovskite oxides; a wide group of oxides with composition ABO_3, where A and B each represent a cation element or mixture of two or more such cation atoms (e.g. $BaTiO_3$ or $Pb(Zr,Ti)O_3$). Sharing many structural features with perovskites oxides, lithium niobate ($LiNbO_3$) - and related materials such as $LiTaO_3$ - are ferroelectric oxides with a trigonal paraelectric structure and are crystallographically analogous to the R3c bismuth ferrite ($BiFeO_3$) [224]. Other relevant families include layered oxide ferroelectrics [225], tungsten bronzes (e.g. $Sr_xBa_{1-x}Nb_2O_6$) [226], gallium silicates and lead germinates (e.g. $X_3Ga_5SiO_{14}$ (X = Pr,La), $Pb_5Ge_3O_{11}$) [227]. Among non-perovskite ferroelectrics, the layered oxide ferroelectrics or Aurivillius phases, which are layered bismuth oxides formed by the regular stacking of Bi_2O_2 slabs and perovskite-like blocks (e.g. $Bi_4Ti_3O_{12}$, $Bi_5FeTi_3O_{15}$, $(Na,K)_xBi_{5-x}Ti_4O_{15}$ or $SrBi_2Ta_2O_9$), are particularly relevant [228]. Both, *p-n* and BPE oxide thin-films (mostly ferroelectric) are being investigated as light absorbers in oxide-based photovoltaic devices as will be reviewed in this section [229], [230], [231] (Fig. 6(c) and (d)).

2.2.1. Oxide *p-n* Solar Cells

2.2.1.1. Cu_2O

Cuprous oxide (Cu$_2$O) is a defect *p*-type oxide semiconductor with a bandgap of ~1.9-2.2 eV and the most prominent member of the Cu-O family for photovoltaic applications [232]. The natural acceptor nature of Cu$_2$O is due to their intrinsic defects (cooper vacancies), with the acceptor level typically lying relatively deep within the bandgap (>100 meV) [233],[234]. From the optoelectronic point of view, Cu$_2$O has a relatively large absorbance coefficient of α ~ 4x10^3 cm^{-1} (600 nm) [235] together with a large free hole mobility (for an acceptor oxide standard as mentioned earlier in the *p*-type TCO section) in excess of 110 cm^2/Vs for highly crystalline layers [236]. This hole mobility, however, critically depends on the Cu$_2$O grain size and the particular method of growth of the thin-film. Vacuum routes such as copper thermal oxidation, sputtering or atomic layer deposition produce bigger grains and overall larger hole mobility. In contrast, chemical routes (in principle more suited for inexpensive thin-film photovoltaics) such as spray pyrolysis or electrodeposition results in smaller grains and reduced hole mobility [229]. The first reports on Cu$_2$O electronic devices can be traced back to 1920s, two decades before than the pivotal germanium and subsequent silicon solid-state transistors [237]. Cu$_2$O also was one of the earliest materials where a photovoltaic effect was observed [238]. After a long latent period, the attention on Cu$_2$O for photovoltaics was somehow timidly reactivated in 1970s as a semiconductor platform for Schottky oxide-based solar cells [239]. It was not until recently (early 2000s) that Cu$_2$O has regained interest fueled by the light-to-electricity power conversion improvement [240],[241] (now PCE has reached values above ~8%) and its application as photocathode in photo-electrochemical cells [242], [229].

In a Cu$_2$O homojunction *p-n* solar cell, both, the *p*-type absorber and the *n*-type widow are composed of Cu$_2$O. However, highly conducting and stable *n*-type Cu$_2$O films for defining the window layer in copper oxide solar cells are still elusive as the intrinsic donor levels are located even deeper within the bandgap than the acceptor levels [243]. The donor microscopic origin remains unclear with O vacancies, Cu interstitials, inversion layers or extrinsic defects as possible candidates [244]. Due to a self-compensation effect and their reduced dopant solubility, only very few extrinsic impurity atoms have shown a sizable degree of donor doping [245],[246]. A Cu$_2$O *p-n* homojunction is therefore still challenging (i.e., small grains and poor *n*-type activation) [247],[248],[249] although it is technologically very relevant for optoelectronics owing its low electron affinity [56]. During the last decade, research efforts has been focused on enhancing the homojunction photovoltaic performances by approaches as tuning the Cu$_2$O orientation and surface morphology [250], adjusting the thin-film thickness

16

[251], incorporating *p*-type sulphidation [249] or by introducing extrinsic dopants atoms such as Zn [252] or Cl [253]. Currently, the largest PCE of Cu_2O photovoltaic homojunctions are in the range of ~2% [253-254].

Due to the long-lasting problems in achieving high quality *n*-type Cu_2O, in practice, a heterojunction *n*-type with a dissimilar oxide window layer has been a more common approach. A widely implemented class of *n*-window materials in Cu_2O solar cells are binary thin-film oxides such as ZnO, Ga_2O_3 or TiO_2. Among these oxides, perhaps the most investigated is ZnO, either, with planar [240],[255] or nanostructured [256] arrangements. The window layer can be produced by a number of methods, including electrochemical deposition [257], spray pyrolysis [258], ion beam sputtering [240], vaccum arc plasma evaporation [259], atomic layer deposition [260], pulsed layer deposition [261] or metal-organic chemical vapor deposition [262]. Planar Cu_2O/ZnO heterojunction PCE is now approaching ~5% [261] (where Cu_2O and ZnO are doped with Na and Cu, respectively). A number of Cu_2O/ZnO and few Cu_2O/TiO_2 nanostructures in the form of nanowires [263], nanopilars [264], nanorods [265], [256], [266],[267], nanofibrous networks [268] or nanotubes [269] have been demonstrated delivering up to ~2% of power conversion efficiency. Replacing ZnO by other conducting *n*-type oxide with wider bandgap has resulted in improved conduction-band offsets and less Cu^{2+}-related defects in planar junctions. For example, Ga_2O_3/Cu_2O heterojunctions showed enhanced PCE (5.38%) and a very large open-circuit of V_{oc}=1.2 V [270]. However, are ternary oxides the ones that have resulted in the best light harvesting efficiency; $Al_xGa_{1-x}O$ resulted in conversion efficiencies over 6% [271] while current PCE record of 8.1% is with a *n*-window thin-film of $Zn_{1-x}Ge_xO$ [241] (Fig. 6(c)). Other ternary oxides has been used as the *n*-window such as $ZnGa_2O_4$, $MgIn_2O_4$, $ZnSnO_3$, Zn_2SnO_4, $GaInO_3$, Zn_2SiO_4, Zn_2GeO_4, Zn_2FeO_4, $CuInO_2$, $CuGaO_2$ and $AgInO_2$ and multicomponents of two or more binary compounds such as ZnO, MgO, Ga_2O_3, Al_2O_3, In_2O_3 and SnO_2 being the largest efficiency observed for $ZnGa_2O_4$ (5.36%) with an open-circuit voltage of V_{oc}=0.81 V [272].

2.2.1.2. Other visible oxide absorbers

Another prominent member of the copper oxide family is cupric oxide (CuO). In a similar fashion to Cu_2O, CuO also is an intrinsically *p*-type semiconductor but with a more ideal (narrower) bandgap of ~1.4 eV for harvesting sunlight in the visible spectral region. Owing to its lower bandgap energy, the single CuO *p-n* junction predicted theoretical (detailed balance)

maximum conversion efficiency is ~31% thus significantly larger than the predicted maximum for Cu_2O (~22%) [273]. Nevertheless, the maximum power conversion efficiency achieved to date in CuO based solar cells is just ~2%. This largest PCE have been achieved when the *p*-type CuO layers were defined onto *n*-Si substrates [274], [275]. CuO-based oxide heterojunctions presents a light harvesting efficiency even smaller (~0.1% for nanostructured CuO/ZnO[276],[277] and 0.25% for planar $CuO/Zn_{1-x}Mg_xO$) [278]. The small power conversion efficiencies are ascribed to several reasons including the CuO absorber low hole concentration and conductivity [279], reduced CuO carrier lifetimes [273] and/or interface recombination at defects [278b]. CuO can be also combined heteroepitaxially with (either *n* or *p*-type) Cu_2O to enhance the light harvesting properties of CuO alone [280],[281]. Cobalt oxides (Co-O) are another family of intrinsic *p*-type semiconductors which may exhibit promising optical bandgaps. Co_3O_4 is a mixed valence compound with a normal spinel structure and is the most stable phase in the Co-O system. While the CoO band gap energy (5 eV) results in an insulator, the Co_3O_4 is an optical *p*-type semiconductor. First evaluation of Co_3O_4 as a *p*-type absorber (with TiO_2 as the *n*-type window layer) resulted in a low PCE of 10^{-2}-10^{-3} % [282], [283]. Dopants such as Li, Cu and Fe into the spinel Co_3O_4 layer has been reported resulting in much enhanced *p*-type conductivity [284], [285], [286]. Patel *et al.* [287] reported that a rapid thermal annealing effectively overcomes the native defects in the Co_3O_4, tuning the free carrier concentration (10^{17}–$10^{20}\,cm^{-3}$) and enhancing the hole mobility. The Co_3O_4/TiO_2 semitransparent *p-n* heterojunction exhibited enhanced PCE from 0.1 to 0.6%. A MoO_3 interfacial layer has a beneficial effect onto the V_{oc} in $TiO_2/Co_3O_4/MoO_3$ all-oxide solar cells [288]. All oxide cobalt-oxide based Co_3O_4/ZnO based *p-n* photovoltaic heterostructures (ZnO being planar or in a nanowire arrangement) were also reported [286], [289]. Bismuth oxides have also been investigated as potential oxides with an optical bandgap (Bi_2O_3 bandgap ~2.4-3 eV) [290], [291]. Morash *et al.* [292] reported open circuit voltages of ~680 mV and short-circuit currents of ~0.3 mA/cm^2 for an ITO/Bi_2O_3 all-oxide solar cell representing a maximum PCE of ~0.05%. Iron oxides are another prominent solar active oxide family. Hematite (α-Fe_2O_3) has attracted much attention because of its promising properties as photoanode in solar water splitting cells owing to its relatively narrow bandgap of 2.1 eV [293]. With the same corundum-type crystal structure, α-Rh_2O_3 has an ideal optical bandgap of ~1.2–1.4 eV [294]. The bandgap of α-Fe_2O_3 is narrowed by Rh substitution in hematite which, in turn, increasing its optical activity [295]. Analogously, the Bi–Fe (doped with V) families of oxides are also investigated as potential solar light harvesters with a special focus in the composition $Bi_4V_{1.5}Fe_{0.5}O_{10.5}$ [296]. The combination of two wide bandgap oxides may produce an oxide with better solar

harvesting properties. Although CeO_2 and NiO are both wide bandgap oxides (~3.3 eV), their alloys form oxides with an optical bandgap. In this sense, Barad *et al.* [297] investigated the Ce-Ni-O system by a combinatorial material science approach. They identified and implemented the $CeNiO_3$ reduced bandgap phase (1.48–1.77 eV) as the absorber layer in a solar cell where photovoltages of up to 550 mV were achieved. Oxynitrides (such as La-Ta-N-O) are another family of oxides being studied as the absorber in photovoltaic systems where the introduction of nitrogen greatly results in a reduction of the oxide band gap (e.g. $LaTaON_2$ *vs* La_3TaO_7) [298]. It possesses a narrow bandgap energy of 2.1 eV that allows for the absorption of up to 40% of solar spectrum. The bismuth oxyhalide BiOI has been reported to have a direct bandgap of ~2eV with an effective mass below m_0 and therefore it could harvest a part of the solar spectrum efficiently [218]. Two dimensional oxides are also investigated to harvest solar photons [299]. For example, 2D $GaInO_3$ (calculated bandgap of 1.56 eV) can exist stably at ambient condition and would be stable up to 1100 K [300].

2.2.2. Ferroelectric Oxide Solar Cells

2.2.2.1. Ferroelectric Photovoltaics Materials

Ferroelectric oxides, an exclusive subclass of polar materials possessing a switchable polarization, have been the most investigated materials of those exhibiting bulk photovoltaic effects (BPE) [88]. Indeed, the study of the anomalous photovoltaic effect in ferroelectrics is commonly referred as *ferroelectrics photovoltaics* [301], [302]. The field was mainly developed in three wide bandgap oxides families (typical reported optical bandgap in brackets); $LiNbO_3$ (~4 eV), $BaTiO_3$ (~3.2 eV), and $Pb(ZrTi)O_3$ (~3.6 eV). The first ferroelectric photovoltaics reports can be traced back to 1950s on investigating photo-generated surface fields in $BaTiO_3$ [303] or perhaps 20 years before on reporting photo-induced currents in tartaric acid crystals [304]. It was in 1974 when Glass and co-workers published their seminal paper reporting extremely large (over 1kV) anomalous above bandgap voltages in iron doped $LiNbO_3$ (Fe:$LiNbO_3$) crystals and ascribed this to a new photovoltaic effect which was dubbed as *bulk photovoltaic effect* [305]. Analogous large photovoltages were also reported in $BaTiO_3$ and $(Pb,La)(Zr,Ti)O_3$ ceramics as early as in 1973 and 1975, respectively [306],[307]. In 1985, Uchino and co-workers discovered a notable photostrictive effect in $(Pb,La)(Zr,Ti)O_3$ [308] following the Brody's optomechanical bimorph-type actuator [309]. These photostrictive actuators directly transform light energy into kinetical energy (mechanical motion) and may

find an application niche in future wireless remote-control photo-actuators and sensors. The field of ferroelectric photovoltaics has experimented a rejuvenation the last few years owing to a bunch of advances as the discovery of a photovoltaic effect and above bandgap voltages in multiferroic $BiFeO_3$ thin-films (~2.7 eV) [310] and the development of new ferroelectric oxides with even narrower optical bandgaps (e.g. Bi_2FeCrO_6 ~1.5 eV) to harvest sunlight more efficiently [311], [312], [313]. These ferroelectric oxides (and many other ferroelectric oxides) have been investigated in the form of single crystals [314] [315] [311], [316], [317], [318], ceramics [306] [319] [307] [308] [309] [320] or thin-films, e.g. $BaTiO_3$ [321] [322], $(Pb,La)(Zr,Ti)O_3$ [323] [324] [325] [326] [327] [328] [329] [330] [331] [332] [333] [334] [335], $BiFeO_3$ [336] [337] [338] [339] [340] [341] [342] [343] [344] [345] [346] [347] [348] [349] [350] [351] [352] [353] [354] [355] [356] [357] [358] [359] [360] [361] [362] [363] [364] [365] [366] [367] and Bi_2FeCrO_6 [368] [313]. Ferroelectric photovoltaic action has been investigated in other perovskite ferroelectric oxides such as $Na_xK_{1-x}NbO_3$ [369], $Pb(Mg,Nb)TiO_3$ [370] or $Pb(Fe,V)O_3$ [371]. Further, Aurivillius layered perovskite oxides such as, $Bi_4Ti_3O_{12}$ [372], [373], [374], [375], $Bi_5FeTi_3O_{15}$ [376], $(Na,K)_xBi_{5-x}Ti_4O_{15}$ [377] or $SrBi_2Ta_2O_9$ [378] have also been reported to exhibit ferroelectric photovoltaic phenomena. The ferroelectric anomalous photovoltaic features have also been studied in other non-perovskite ferroelectric such as tungsten bronzes $Sr_xBa_{1-x}Nb_2O_6$ [379], [380], gallium silicates $X_3Ga_5SiO_{14}$ (X=Pr,La) [381], [382], lead germanates $Pb_5Ge_3O_{11}$ [383] and non-oxide ferroelectrics such as (3-Pyrrolinium)(CdCl$_3$) [384], (benzylammonium)$_2$PbCl$_4$ [385] and polyvinylidene fluoride (PVDF), a ferroelectric polymer [386], [387].

2.2.2.2. Wide Bandgap Ferroelectric Oxide Thin-films

In general, the ferroelectric photovoltaic phenomena in *classic* wide bandgap (i.e., those with an optical bandgap in the near ultraviolet range of ~3-4 eV) ferroelectric oxide single crystals or ceramics may produce (but not always) large above bandgap photovoltages. However, in contrast, only very tiny photocurrents (typically ~pA/cm^2) are usually generated in these bulk oxides. When compared to single crystals and ceramics, ferroelectric oxide thin-films is a route to highly improve the device photocurrent as for example was demonstrated by Ichiki *et al.* [388] with a x100 enhanced photocurrent for $Pb(Zr,Ti)O_3$ thin-films. The thin-film arrangement for photovoltaics presents other well-known advantages; thin-films absorb and harvest light as crystals do but they require much less material (if the absorption coefficient is sufficiently high) which is highly desirable for any commercial application. However, the ferroelectric photovoltaic phenomena in oxide thin-films is not, in general, (only) ascribed to

a canonical BPE (developed for perfectly homogeneous single crystals) but may exist other symmetry breaking effects (grain boundaries, Schottky barriers, depletion regions, depolarization fields and/or domain walls to name a few (e.g. [389],[390])). Dharmadhikari et al. [321] reported the first ferroelectric thin-film photovoltaic device in 1982. $BaTiO_3$ layers were evaporated (0.3-0.5 μm) by rf sputtering on silicon. The first epitaxial $Pb(Zr,Ti)O_3$ thin-film solar cell (grown by pulsed layer deposition onto $Nb:SrTiO_3$) was reported in 2000 with a power conversion efficiency of ~0.6% under near UV light [325]. As a comparison, under simulated sunlight (AM1.5 100 mW/cm^2), Chen et al. [331] reported in 2012 the first thin-film $Pb(Zr,Ti)O_3$ solar cell onto photovoltaic graded glass coated with a TCO (glass/ITO) with a power conversion efficiency of ~0.2%. In contrast to single crystals and ceramics, only a bunch of ferroelectric devices with above bandgap voltages have been reported for thin-films of $Pb(Zr,Ti)O_3$ (and $BiFeO_3$) to date; e.g. Yang et al. [391], Yao et al. [392], Bhatnagar et al. [393] and Nakashima et al. [394]. In particular, Yao et al. [392] demonstrated in 2005 above bandgap voltages (larger than 7 V) for a $(Pb,La)(Zr,Ti)O_3$ thin-film (0.42 μm) having in-plane polarization and interdigitated in-plane electrodes with a 10 μm gap. Despite the above bandgap photo-generated voltage, the photovoltaic field of this lateral device was indeed rather small ($E_{pv} \sim 4$ kV/cm). Zenkevich et al. [322] reported in 2014, for much thinner $BaTiO_3$ epitaxial films (20-50 nm) on Pt/MgO (001), an out-of-plane photovoltaic field of ~300 kV/cm thus representing a giant BPE field. However, in this case, the photovoltage (~0.7 V) was well below the $BaTiO_3$ bandgap energy (~3.2 eV). In 2016, it was reported much large above bandgap photovoltages (120 V) and the largest photovoltaic field (more than 6 MV/cm) ever observed for any photovoltaic material in antiferroelectric $PbZrO_3$ (PZO) thin films under near ultraviolet (365 nm) illumination [87]. In anti-ferroelectric photovoltaics, the ferroelectric phase of $PbZrO_3$ (bandgap energy of ~3.8 eV) may be pinned under UV illumination thus resulting in an extraordinarily strong photo-induced field. Other wide bandgap ferroelectric oxides have been used to define thin-film photovoltaic devices including $(K,Na)NbO_3$ (KNNO) [369], and BiTs (the layered ferroelectric $Bi_4Ti_3O_{12}$ family) [375],[376],[377]. Park et al. [395] reported sizable photovoltaic properties on ferroelectric oxide KNNO nanotube solar cells with an improved power conversion efficiency of 0.02% when compared with the planar thin-film solar cell. Regarding the Aurivillius layered perovskite oxide thin-films, ferroelectric photovoltaics has been investigated in oxides such as $Bi_4Ti_3O_{12}$ [372],[373],[374],[375] $Bi_5FeTi_3O_{15}$ [376], $(Na,K)_xBi_{5-x}Ti_4O_{15}$ [377] and $SrBi_2Ta_2O_9$ [378]. The oxide thin-film solar cell efficiency in these layered ferroelectrics under withe light illumination (or AM1.5) is very low (10^{-6}-10^{-4} %). However, the oxide thin-film Aurivillius solar cell

performances have been progressively enhanced (0.04 %) for four-layer phase bismuth layered structure and it has been related to a larger remnant polarization.

2.2.2.3. Optical Bandgap Ferroelectric Oxide Thin-films

To harvest sunlight efficiently, the ferroelectric oxide should have smaller bandgaps than those of *classical* perovskite oxides. Bismuth ferrite ($BiFeO_3$ or BFO), one of the most promising multiferroic material (because its co-existing ferroelectricity and antiferromagnetism at room temperature), has a tunable optical bandgap of ~2.2-2.7 eV and has arguably been the most investigated ferroelectric photovoltaic oxide in the last decade. In 2009, Choi *et al.* [396] reported a switchable ferroelectric diode and a modest visible-light photovoltaic effect in $BiFeO_3$ single crystals. Yang *et al.* [336] published also in 2009 much enhanced photovoltaic currents in epitaxial $BiFeO_3$ thin-films grown on $SrRuO_3/SrTiO_3$ substrates under simulated sunlight (AM 1.5). The same authors reported in 2010 [391] in-plane above bandgap voltages for epitaxial $BiFeO_3$ thin-films grown on $DyScO_3$ substrates under white-light illumination. In $BiFeO_3/DyScO_3$, arrays of ordered 71° $BiFeO_3$ ferroelectric domain walls were achieved by tuning thermal treatments. The domain walls array orientation with respect to the in-plane electrodes was found to critically modulate their photovoltaic performances; either, above bandgap voltages (when perpendicular to the current flow) or just enhanced photocurrents (when parallel to the current flow). Following these works, many investigations have been focused on enhancing the photovoltaic properties of $BiFeO_3$ thin-films during the last decade, although the overall power conversion efficiency still remains low (below 1%) [393], [394],[337, 397], [398]. It has been common to substitute and/or to dope $BiFeO_3$ (with several atoms such as Sr, Cs, Mn, Ti, Sa, Na, La, K and/or Ni) to enhance the power conversion efficiency but, again, with only very limited success yet (BFO:D in Fig. 6(c)). With the same goal, other ferroelectric oxides with even lower bandgap energies have been intensively investigated during the last few years (see e.g. Fig. 6(d)), including $[KNbO_3]_{1-x}[BaNi_{1/2}Nb_{1/2}O_{3-\delta}]_x$ [311], Bi_2FeCrO_6 [313], [368], $KBiFe_2O_5$ [316], $Bi_xMn_{1-x}O_{3-\delta}$ [399], $Pb(Zr,Ti)O_3-NiO_\delta$ [400], [401] or $BaTi_{1-x}(Mn_{1/2}Nb_{1/2})_xO_3$ [402]. Some of these optical bandgap oxide (OBG) thin-film has certainly produced more promising results (in terms of power conversion) than previous wider bandgap oxides (WBG) as LNO, PZT, BTO and BFO (see Fig. 6(c)). In 2011, Nechache *et al.* [368] reported epitaxial Bi_2FeCrO_6 grown on $Nb:SrTiO_3$ substrates exhibiting a record high power efficiency of 6% with monochromatic illumination of 635 nm. In 2014, the same authors published [313] a optimized stack of three Bi_2FeCrO_6

layers resulting in an even higher power conversion efficiency of 8.1% under AM1.5 (100 mW/cm^2) simulated sunlight. They also reported ~2% efficiency in *p*-i-*n* NiO/Bi$_2$FeCrO$_6$/Nb:SrTiO$_3$ heterostructures [403]. In 2018, Chakrabartty *et al.* [404] reported a power conversion efficiency of ~4.2% under AM1.5 (100 mW/cm^2) simulated sunlight from Bi–Mn–O composite thin films (with mixed phases of ferroelectric BiMnO$_3$ (gap 1.2 eV) and BiMn$_2$O$_5$ (gap 1.23 eV)) which photocurrent mainly developed across grain boundaries rather than within the grains.

2.3. OTF as *Buffers*: Transparent Semiconductors

2.3.1. Transport Layers

Transparent semiconducting oxides (TSOs) have widely been used as barrier (or transport) layers (Fig. 7) in solution-processed thin-film photovoltaics [e.g. organic (OPVs), dye sensitized (DSSCs) or organic-inorganic halide perovskite (HPSCs) solar cells] since the very beginning [405],[406],[407],[408],[409]. Oxide buffers have also been implemented in many other (if not all other) thin-film photovoltaic technologies such as amorphous silicon (a-Si) (e.g. [410], [411]), cadmium telluride (CdTe) (e.g. [412],[413]), copper zinc tin sulfide - "CZTS" (Cu$_2$ZnSnS$_4$) (e.g. [414],[415]) and copper indium gallium selenide - "CIGS" (Cu(In,Ga)Se$_2$) (e.g. [416], [417]). Oxide thin-films have been also implemented in crystalline silicon solar cells (c-Si) (see e.g. [418],[419],[420],[421],[422],[423]), crystalline germanium solar cells (c-Ge) (see e.g. [424]) and single-crystal III-V (see e.g. InP [425]). In these structures, TSO thin-films deliver some critical advantages, including; (i) optical transparency, (ii) tunable conductivity, (iii) tunable band-alignment, (iv) sealing from the environment, and (v) easy and cheap processing. As a buffer layers, TSOs can be either *n*-type or *p*-type semiconductors with non-degenerate doping (not yet a metal as a TCO) but usually still highly conducting. The TSO buffer is usually located in between one of the carrier extraction metal electrodes and the light absorber core layer. A major role of TSOs in thin-film photovoltaics consists in selecting (or transporting) only the majority carrier type to avoid further electron-hole recombination at the metal electrodes. As *electron transport material* (ETM) in thin-film solar cells, the most used oxide semiconductor is arguably TiO$_2$ but many other *n*-type binary oxides (e.g. ZnO, SnO$_2$ or WO$_3$) and *n*-type ternary oxides such as BaSnO$_3$, SrTiO$_3$ and Zn$_2$SnO$_4$ are also being intensively investigated (see e.g. [426]). As *hole transport materials* (HTM), the most common oxide semiconductor probably is NiO$_x$ (see e.g. [427]) while other binary oxides such as CuOx, MoO$_3$, V$_2$O$_5$ or GeO$_2$

have also attracted a lot of attention. In a thin-film photovoltaic context, TSO thin-films can also be classified as *nanostructured* or *planar*. Nanostructured oxide thin-films are made of nanoparticles (e.g. mesoscopic), nanorods, nanoplates, quantum dots or any other nanostructure within the nanoscopic size range (1 to 100 nm) while in the planar configuration they are dense thin-films [428] (see Fig. 7).

2.3.1.1. Nanostructured Transport Layers

There are few thin-film photovoltaic technologies that are nanostructured in nature (e.g. dye sensitized (DSSCs)), there are other photovoltaic technologies that may or may not be nanostructured (e.g. organic-inorganic halide perovskite (HPSCs)) and there are other thin-film photovoltaic technologies that are not nanostructured in general (e.g. bulk organic heterojunctions). The buffer nanostructure is introduced in these solar cells as a route for enhancing the potential area for photon harvesting and carrier collection, to increase the overall power conversion efficiency or to achieve a larger degree of stability and durability of the solar cell. For example, TiO_2 is the most common oxide electron extraction layer in DSSCs [429], [430] and nanostructured normal (or *n*-i-*p*) HPSCs solar cells [431],[432], delivering power conversion efficiencies over 11% [433] and 20% [434], respectively. The most common nanostructure in this kind of solar cells is a mesoporous nanostructure of aggregated nanoparticles. State-of-the-art electron extraction layers in DSSC solar cells are made of a porous layer of TiO_2 nanoparticles, coated with a molecular dye (e.g. photosensitive ruthenium-polypyridine dye) that absorbs sunlight. In HPSC, this generally comprises a *n*-type bi-layer of mesoporous mp-TiO_2 nanoparticles of tens of nanometers (with a final thickness of ~100-500 nm) in diameter onto a much thinner dense d-TiO_2 blocking layer (typically ~10-20 nm). The mesoporous bi-layer is typically sandwiched in between a commercial TCO/glass substrate (the TCO being primarily ITO or FTO) and the light absorber layers. While the mp-TiO_2 nanostructure increases the area for photovoltaic conversion, the dense d-TiO_2 avoids hole recombination at the transparent electrode. The standard method for defining the blocking dense layer is by solution processing where a solution containing titanium (usually titanium iso-propoxide) is spin-coated and further annealed at high temperature in an oxygen ambient (~450 ^{o}C) [405], [406], [407], [435], [436], [437], [438], [439], [440], [441], [442], [443], [444], [445], [446], [447]. Larger area, spray pyrolysis [441], [448], [449], [450] and screen printing [450], [451], [450] are among the different methods to define the *n*-type buffer layer. Several other research directions regarding the engineering of the electron

extraction layer include crystal design (e.g. brookite mp-TiO$_2$ [452]), coatings (e.g. fullerene monolayers (C$_{60}$SAM) [453]) or doping to further reduce the TiO$_2$ resistivity (e.g. Nb:d-TiO$_2$) [454]. In DSSC solar cells, binary and ternary *n*-type mesoporous oxides such as mp-ZnO, mp-Nb$_2$O$_5$, mp-SrTiO$_3$, mp-BaSnO$_3$ and mp-Zn$_2$SnO$_4$ have already been investigated as an alternative to mp-TiO$_2$ to achieve enhanced power conversion efficiencies [455]. In HPSC solar cells, alternative mesoporous *n*-type oxides reported as ETM include mp-SrTiO$_3$ [456], [457] and mp-ZnO [458]. Other forms of nanostructured *n*-type electron transport ZnO has also been routinely implemented to improve the photo-carrier harvesting of various photovoltaic thin-film technologies, particularly in the form of columnar *nanorods* [459], [460], [461], [462], [463], [464]. The *inverted* (or *p*-i-*n*) HPSC structure presents the advantage of defining the high temperature oxide HTM before the perovskite absorber (maximum thermal budget typically limited to ~100 ^{o}C) thus widening the number of cheaper potential materials to be used as the hole extraction layer and is also compatible with more common low temperature *n*-type oxides [465]. This approach is a potential route for further improving the solar cell stability and reducing the overall cost of the HPSC solar cell (the most common organic polymeric HTM Spiro-OMeTAD is as expensive as gold) [466]. In the case of halide perovskite solar cells, the mesoporous mp-NiO is the most investigated nanostructured *p*-type oxide HTM which is located in between the TCO/glass substrate and the halide perovskite absorber [467], [468], [469], [470], [471], [472].

2.3.1.2. Planar Transport Layers

Planar solar cells present several advantages respect to their nanostructured counterparts such as simpler fabrication routes, better conformal coating characteristics, smoother surfaces, enhanced crystal quality with larger grains and lower cost [473]. Titanium oxide is, again, the most common oxide ETM in planar (*n*-i-*p*) organic (OPV) and normal (*n*-i-*p*) HPSCs solar cells [474], [475], [476], [477], [478], [479], [480], [481], [482], [483], [484], [485], [486], [487], [488], [489], [490], [491], [492], [493], [494], [495], [496], [497], [498]. Buffer semiconductor TiO$_2$ thin-films are usually grown by spin-coating in a similar fashion to the mesoporous one described earlier and may be doped to enhance the TiO$_2$ conductivity with atoms such as yttrium [482], molybdenum [494] or zirconium [495]. For example, yttrium doping resulted in larger HPSC photovoltaic currents, owing to a higher conductivity at the ETM buffer, and resulting in an overall efficiency in excess of 19 % [482]. There are other potential *n*-type oxides being investigated as planar electron extraction layers of normal halide perovskite solar cells including ZnO [462], [499], [500], [501], [502], [503], [504],

[505], [506], WO$_3$ [507], CeO$_2$ [465] and Zn$_2$SnO$_4$ [508]. Planar inverted (or *p*-i-*n*) HPSC solar cells containing *p*-type nickel oxide as the hole extraction buffer semiconductor have also been extensively studied, where the NiO layer was grown by various techniques including spin coating, magnetron sputtering or spray pyrolysis [509], [510], [511], [512], [513], [409], [514], [515], [516]. Doping the NiO layer with atoms as copper, cobalt, strontium and cesium has resulted in enhanced optoelectronic properties of the oxide-based hole transport media and better overall PCE [515], [517], [518], [191]. For example, Kim *et al.* [515] increased the NiO HTM conductivity up to a value of ~8x10^{-4} Ω^{-1}cm^{-1} for Cu-doped (the undoped conductivity was only 2x10^{-6} Ω^{-1}cm^{-1}) which, in turn, resulted in an increase of the HPSC photocurrent from 14.13 mA/cm^2 up to a value of 18.75 mA/cm^2 together with larger photovoltages (1.1 V) owing to better band alignment. In a similar fashion, other oxides have been investigated as HTM in various thin-film photovoltaic technologies including NiMgLiO [519], graphene oxide (GO) [520], molybdenum oxide (MoO$_3$) [521] and copper oxide (CuO$_x$) [522]. In 2018, a carefully designed tandem organic photovoltaic (OPV) device containing *n*-type and *p*-type ZnO and MoO$_x$ planar oxide buffers has been reported to achieve power conversion efficiency as high as 17.4% [523]. Molybdenum oxide also is a particularly used *p*-type oxide as hole carrier selective contact for high efficiency silicon heterojunction solar cells [524].

2.3.2. Insulating Scaffolds

Transparent insulating oxides (TIOs) also found its place within thin-film photovoltaic devices as insulating scaffolds, surface passivation [525], [526] or very thin tunneling contacts (oxide tunneling contacts [527], [528]). As insulating scaffolds, they must be nanostructured; otherwise they would block the current through the structure. The most studied nanoparticle insulating scaffolds in HPSC solar cells are based in Al$_2$O$_3$ [407], [529], [530], [531], [532], [533], [448], [534], [449], [450], [535], [536], ZrO$_2$ [537], [538], [539], [540], [408], [541] and SiO$_2$ [542], [543], [544]. Nanoparticles of Al$_2$O$_3$, ZrO$_2$ and SiO$_2$ are insulating owing to their wide band gaps (from 7 eV to 9 eV) and present optical transparency and high lowest unoccupied molecular orbitals. In a typical arrangement, there is enough interspace among nanoparticles which is infiltrated with the light absorbers (creating photo-conductive channels). Insulating scaffolds exhibit some interesting features in halide perovskite solar cells. For example, due to its insulating nature, electrons are inefficiently injected into the dielectric nanoparticle scaffolds allowing the electrons to be transported faster within the perovskite layer and thus producing larger photovoltages [407]. There are also reports that suggest that a mesoporous scaffold hinders

deleterious ionic migration thus recombination and hysteresis are reduced [545]. In practice, these potential advantages should be carefully balanced with the unavoidable current losses at highly resistive insulating nanoparticles. For example, Yu *et al.* [543] compared the photovoltaic characteristics of identical halide perovskite solar cells containing semiconductor *n*-type mp-TiO$_2$, and insulating mp-Al$_2$O$_3$ or mp-SiO$_2$. The overall HPSC average photocurrent of the mp-SiO$_2$ structures was 18.0 mA/cm^2, lower than those from mp-TiO$_2$ and mp-Al$_2$O$_3$ (~19.7 mA/cm^2). However, as the photovoltage and fill-factor was larger (in average) for the mp-SiO$_2$ structure, the more insulating scaffold produced the largest power conversion efficiency of 16.2 %. From the device engineering point of view, insulating scaffolds can add new practical aspects to thin-film solar-cell architectures (e.g. acting as spacer layers). For example, mesoporous nanoparticles of zirconium oxide (ZrO$_2$) are in the core of the so-called triple-layer perovskite junction [546]. Originally grown onto a FTO/glass substrate, the triple-layer structure is a stack of a mesoporous mp-TiO$_2$ layer (~1 mm-thick) acting as electron extraction layer, a mesoporous mp-ZrO$_2$ layer (~2 mm-thick) as insulating scaffold which is coated with a conductive carbon-based paste acting as counter-electrode. The triple-layer is infiltrated with the light harvesting halide perovskite from a chemical solution by drop-casting. This hole-conductor-free solar cell architecture is, therefore, fully printable [547] and avoids the implementation of expensive hole transport layers and precious metals as the counter-electrode (typically Au), which is replaced by low-cost carbon-based materials [548]. Further, this particular kind of HPSC can be readily implemented in larger photovoltaic modules (~40 cm^2) with power conversion exceeding 15% and, therefore, having prospects for commercialization [549]. Other similar HPSC architectures have been recently reported in which it was replaced the mp-ZrO$_2$ by other insulating oxides such as mp-Al$_2$O$_3$ [550], [551],[552] or a HTM was incorporated [450]. The hole extraction layer can be, indeed, a *p*-type mesoporous oxide as in the all-oxide mesoporous four-layer mp-TiO$_2$/mp-Al$_2$O$_3$/mp-NiO$_x$. This four-layer was infiltrated again with a halide perovskite light absorber solution and caped with a carbon electrode [450].

2.3.3. Switchable Buffers: Solaristor – *A neuromorphic phototransistor*

The oxide buffer layers mentioned in previous sections were incorporated in thin-films solar cells as semiconductor transport layers or as spacers thus exploiting primarily their optoelectronic properties (optical transparency, majority carrier conductivity or insulation). While oxide thin-films in photovoltaics may present several technological advantages as their

stability, inherent low cost or their potential for covering large areas by printable techniques, these optoelectronic properties are essentially common to many other potential non-oxide wide bandgap semiconductors (e.g. chalcogenides or halides). Nevertheless, many oxide thin-films do exhibit a range of unique complementary functionalities, (they are indeed sometimes referred to as *functional oxides*) or, at least, it is common that they are the class of materials where some of these unique functionalities are stronger. An example of this is the ferroelectric phenomena, which basically implies a switchable internal polarization and, in turn, space charges at the surface which polarity may be reversed. An often-overlooked property of a ferroelectric semiconductor is that a switchable surface charge arrangement also implies a switchable surface band-bending [553], [554], [555]. In a heterojunction with other more efficient light harvester, this property may be used to define compact two-terminal phototransistors or *solaristors* [89] (Fig. 8(a)-(b)). A way to improve the photovoltaic current of ferroelectric photovoltaic devices is through the combination with organic, inorganic or hybrid semiconductor light absorbers such as Cu_2O [556], a-Si [557], ZnO [558], OPV [89] or HOIPs [90]. The maximum PCE in this hybrid ferroelectric-oxide/light absorber heterojunctions is now above 11% [90]. In the context of switchable photovoltaic interfaces, ferroelectric oxides add these new functionalities to the structure (a ferroelectric layer can be seen as a semiconductor with switchable surface charge polarity). Because of its tuneable internal dipole effect, ferroelectrics bend their electronic band structure and offsets with respect to adjacent metals and/or semiconductors when switching the ferroelectric polarization so that the overall solar cell conductivity can be tuned orders of magnitude (Fig. 8(c)-(d).

Currently, any *transistor* (i.e., the basic building block of any Von-Neumann or Neuromorphic computing machine) is fueled by an external source and this represents an undesired and critical energetic requirement. A *phototransistor* [559], [560], [561], [562] can be defined as a three-terminal device whose output can be simultaneously and independently controlled by light or voltage. Ideally, phototransistors should be self-powered (i.e. producing its own energy) and integrated into a vertical two-terminal device for higher density miniaturization. In practice, these photo-transistors also must keep a normally-*off* state for mitigating the "sneak-path" problem (due to an excess of current leakage) [35], better dissipation efficiency (less Joule heating) and easier control [563]. Normally-*off* (or enhancement-mode) transistors are in general preferred by electric engineers and are those that, at a gate bias of 0V, do not transport current in between its source and drain terminals, so they are normally switched-off. Harvesting the photon energy, a photovoltaic junction would

already act as a self-powered current source, but conventional *p-n* junctions do not switch. There are however several photo-switchable mechanisms that can result in diverse types of photovoltaic responses; these include ferroelectric photovoltaics [397], [337], [367], [301], ionic drift in halide perovskites [564],[565] (or oxide perovskites [566]), photovoltaic resistive switching [567], and the photochromic effect [568]. However, these incipient photovoltaic switches do not have, in general, a stable low energy consumption state. The *solaristor* (a portmanteau of SOLAR cell transISTOR) is the compact two terminal self-powered phototransistor (with a normally-*off* state), or in other words, *a solar cell and a memristor in series* (Fig. 8 (a)-(b)). Solaristors, in their basic embodiment and working in a photovoltaic mode, should have no internal gain. Conventional phototransistors exhibit photoconductive gain, which is not seen in photodiodes (except avalanche photodiodes [569],[570]), and results in external quantum efficiencies (EQEs) well over 100%. For example, for an image sensor pixel in low lighting, photoconductive gain in the phototransistor enables higher EQEs than the photodiode-based pixel [571]. The combination of photoconductive gain and sublinear responsivity of a phototransistor-based pixel would lead to a wider dynamic range than a photodiode-based pixel. However, the sublinear photoresponse can be problematic in applications that require high-resolution and quantitative light detection, for which a linear photoresponse with constant EQE provided by photodiodes would be preferred [572].

The solaristor effect is achieved by controlling the internal field properties or the overall conductivity of the solar cell. As will be reviewed in the next sections, there are several phenomena resulting in changes in a material resistivity [16] including an internal resistivity change (e.g. creation of conductive filaments), a structural change of phase, spin-driven or ferroelectricity-driven effects as shown in Fig. 8(e). In oxide-based solaristors, the two-in-one transistor plus solar cell may be implemented by an oxide *resistive switching* effect in the flow of photo-generated carriers [89], [90], [573], [574], [575]. In computer science, a paradigm shift is taking place in replacing (three-terminals) CMOS transistors by (two-terminals) memristors, which are well-known to closely mimic biological neurons and human learning (see e.g. [576]) in a smaller space and with much less power consumption. In a similar fashion, a paradigm shift from phototransistors to solaristors may enable a more biorealistic and self-powered *photo-neuromorphic engineering*. Besides, the introduction of photovoltaic and/or photonic aspects into arising neuromorphic devices will, not only produce much faster and efficient self-powered adaptive electronics, but may also create new and exciting possibilities in

artificial neuroscience, artificial neural communications, sensing and machine learning as will be surveyed further on.

3. Oxide Thin-films in Neuromorphic Devices

Neuromorphic engineering, artificial neural networks and brain-inspired computing are now receiving renewed attention [577], [578], [579], [580], [20] as a way to surpass the Von-Neumann paradigm [29]. The neuromorphic engineering approach aim is to mimic directly the biophysical processes that underlie neural computation in biological neural systems. The brain's cognitive power is not based in high-performance and fast computing with exact digital precision (as today computers do), but rather is due to an extremely interconnected network of slow, imprecise and, to some extent, untrustable analog components performing a probabilistic form of collective computation at the minimum energy (metabolic) cost [581]. Human's brains are outstanding in learning structure within from sensory data with excellent efficiency in generalization and dimensionality reduction. Neuromorphic computing is therefore especially suited for solving structured data in very high dimensions, such as high-level visual cognition (within supervised or unsupervised learning frameworks), temporal learning, including temporal difference learning and temporal sequence learning, for reward prediction from the perspective of reinforcement learning [582],[583]. The term *neuromorphic*, coined by Carver Mead in 1990 [584], was originally used to describe systems fabricated using standard CMOS processes as Neurogrid [31], TrueNorth [585], SpiNNaker [586] or Loihi [587]. As opposed to the neuro-computing approaches that are mainly concerned with fast and large simulations of spiking neural networks, the *intrinsic* neuromorphic systems are designed to directly emulate the biophysics and the connectivity of cortical neurons [588]. The implementation of intrinsic neuromorphic computing on the hardware level is intensively explored beyond CMOS including resistive switching (e.g oxide-based resistive switching [24], [589]), spintronics (e.g. spin torque devices [590], [28]), nanomagnetism (e.g. superconducting-magnetic [591], [592]) or nanophotonics [593], [594]. As shown in Fig. 8(e),(f), these emerging nanoscale intrinsic synapse technologies have the potential to greatly improve circuit integration densities and to reduce power-dissipation which architecture is (in general) *two-electrodes out-plane* (i.e. vertical - the layout of solar cells and solaristors) and no *three-electrodes in-plane* (i.e. lateral – the layout of silicon CMOS transistors). At the time being, beyond CMOS neuromorphic functionalities are primarily realized by resistive switching

30

phenomena (electro-ionic signaling is what actually happens in biological neurons [595]) and oxide thin-films are one of the most investigated material systems.

3.1. Neuromorphic Devices

3.1.1. Biological Synapses in Short

Emerging *Non-Von-Neuman* systems that emulate biological functionality more directly are composed of various basic building blocks: (1) artificial neurons (*active signaling devices*), (2) axons and dendrites (*connections*), and (3) synapses (*non-volatile transistors*) which mimic the elemental components of the brain circuitry. The nano-technologic replication of these basic elements will produce neuromorphic circuits with *more-human* artificial intelligence (AI) capabilities. The core elements of biological neural networks are spiking neurons which are known to be a major signaling unit of the nervous system (Fig. 9(a)). In biological neurons, the spike transduction is mediated primarily by a series of ion channels (e.g. sodium (Na^+) and potassium (K^+)) that modulates, permit or hinder polarizing signals to charge (or discharge) through the cell membrane (see e.g. [596]). The neuron membrane has therefore the role of a leaky capacitor whose voltage builds-up when an incoming spike (or train of spikes) comes up but slowly discharges over time. The ion channels modify significantly their conductivity when the neuron membrane is sufficiently polarized through its dendritic terminals. Then, a voltage spike (or action potential) is triggered and travels along the axon (Fig. 9(b)). Like electrical cables, neurons have an extended network of input connections (dendrites) and output connections (axons), which transport the electrical signals in neural circuits. In a typical multipolar neuron, each neuron has many dendrites (providing an enlarged surface area to receive signals) but usually has a single axon. A salient example are the Purkinje cells in the cerebellar cortex. These cells exhibit complex dendritic trees of up to ~200,000 connections, but still they have just one axon. Therefore, they process a large quantity of input signals, assimilating large amounts of sensory information but still they only transduce one single output signal [597]. However, the axon also commonly splits at its far end into many branches allowing the action potential signal to pass simultaneously to many other neurons. The synapse is the connection element between axons and dendrites. The adult human brain is estimated to contain ~10^{10} neurons and~10^{14} synapses [598], with a cortex synapse density of ~10^{12} cm^{-3} [599], [600]. As the equivalent of nano-transistors, they regulate the intensity of the axon signal transferred to the dendrite. One neuron releases

31

neurotransmitter molecules (e.g. monoamines, amino acids, peptides, or gasotransmitters enclosed within small sacs called synaptic vesicles) into the inter-neuron synaptic gap (~20 nm). Vesicles then bind to neurotransmitter receptors (a protein that trigger the electrical signal by regulating the activity of the ion channels) on the postsynaptic cell membrane's side of the synaptic gap. At rest, the neuron membrane potential is polarized at ~ tens of mV (Fig. 9(b)). The ionic drift (Na^+, K^+…) through the ion channels during neurotransmission, progressively depolarizes the postsynaptic neuron membrane. Eventually, a threshold is reached and an electrical signal is generated (action potential). The *synaptic weight* is the strength of this interconnection and provides the *memory* capacity of the network. These interconnections are not static but may vary over time or depending of their previous history, i.e. they have a certain degree of plasticity. *Synaptic plasticity* is the ability of synapses to strengthen or weaken over time, in response to increases or decreases in their activity, providing the *learning* capability of the neural network. A model of the correlation of the variation of the inter-neuronal synaptic weight in response to a train of neuronal spikes is commonly known as *spike-timing-dependent plasticity* (STDP) which is in the origin of many *learning algorithms* for spiking neural networks [601]. Plastic change often results from the alteration of the number of neurotransmitter receptors located on a synapse [602] but also dendrites themselves appear to be capable of plastic changes [603]. In oxide based neuromorphic technologies, while axon and dendrites are basically electrical connections (e.g. TCOs), neuronal and synaptic operations are performed by resistive switching solid-state devices (see Fig. 10) also known as *synaptors* and *neuristors* (see Fig. 11).

3.1.2. Resistive Switching

Neuromorphic cortical circuits, which mimic the interconnectivity and many biological aspects of biological neurons, may be achieved in practice by using the oxide's inherent resistive switching features. The resistive switching effect consists of a sudden change of the resistance of a material after applying an electric field (or current), typically in an insulating sandwich-like structure in between two metal electrodes. The possible microscopic origin of RS is diverse and both, volatile and non-volatile RS, are being investigated in a wide range of material systems (not only in oxide thin-films). After the *set* bias, in non-volatile RS, the insulator's resistance does not return over time to its original low-conductive value (or the other way around, after the *reset* voltage bias). In *unipolar* RS, the set and reset may be of the same polarity while in *bipolar* RS, the set and reset are of opposite polarity (Fig. 10 (a),(b)).

Thus, this non-volatile RS is now being widely studied for emerging random-access memories (RAMs) [22],[604],[605]. The most notable non-volatile RS are; (i) *Resistive* (i.e., ReRAM). This RS is due to a permanent change on the electrical resistance of the capacitor through an otherwise insulating thin-film oxide. In general, this RS is due to either (or both), a conductive filament formation (filamentary chain of ionic defects) or a dramatic change in the Schottky barrier height due to the migration of ions in the electrode's vicinity [24]. (ii) *Conductive bridge* (i.e., CBRAM). This RS is based on the electrochemical formation of conductive metallic filaments through an insulating solid electrolyte. This RS is produced by the migration of ions from an electrochemically active electrode into the insulator. (iii) *Phase change materials* (i.e., PCM). This RS is due to a large difference in electrical resistivity between the materiral's amorphous (low-conductance) and crystalline (high-conductance) phases. (iv) *Ferroelectric*. The switching of the ferroelectric polarization is intrinsically non-volatile and there are several architectures of ferroelectric memories. For example, in a sandwich-like ferroelectric tunnel junction the resistance of the structure varies with switching the polarization as the tunnel current depends on the Schottky barrier heights (switching the polarization accumulates or depletes carriers at the interfaces and its band bending also varies). (v) Very recently, purely electronic non-volatile RS (in the form of coherent electronic waves) has been observed in nanoscale a-$SiON_x$ [631]. Some selected material systems for the different RS include the following:

- o ReRAM. Resistive switching is due to chains of defects through an otherwise insulating thin-film oxide. The first report of resistive switching phenomena was arguably the one by Hickmott in 1962 [70]. Materials for non-volatile unipolar and/or bipolar RS include; (1) simple binary metal oxides (usually off-stoichiometry) such as SiO_{2-x} [606] or metal doped SiO_2 ($Ta:SiO_2$, $Cu:SiO_2$, $Pt:SiO_2$, $Sn:SiO_2$, $Zn:SiO_2$) [605], TiO_{2-x} [607],[608],[609], HfO_{2-x} [610], [611], [612], [613], [614], [615], Ta_2O_{5-x} [616], [615],[617],[618], Al_2O_{3-x} [619], [620], ZnO_x [621], [622], [623], [624], ZrO_{2-x} [625], [626], WO_{3-x} [627], NiO_x [628],[629],[630], [631] Co_3O_{4-x} [629], MgO_x [632], Fe_3O_{4-x} [633], [634], [635], MnO_{2-x} [636], Cr_2O_{3-x} [637], $Cu_{2-x}O$ [638], Gd_2O_{3-x} [639], [640], CeO_{2-x} [641], [642], MoO_{3-x} [643], [644], VO_{2-x} [645], Y_2O_{3-x} [646], Nb_2O_5 [647], La_2O_{3-x} [648] or GeO_{2-x} [649] (2) Complex oxides such as $BiFeO_3$ [650], $SrTiO_3$ [651], [652], $LaCrO_3$ [653], $ZnSO_3$ [654], $CoFe_2O_4$ [655], $Pr_xCa_{1-x}MnO_3$ (PCMO) [656], [657], [658], [659], [660], [661], [662], $Na_xK_{1-x}NbO_3$ [42] or $YBa_2Cu_3O_{7-x}$ (YBCO) [663]. (3) Amorphous oxides such as a-Ga_2O_{3-x} [664], a-Lu_2O_{3-x} [665], and In-Ga-Zn-O (IGZO) [666]. (4) Oxy-chalcogenides as ZnO_x/ZnS [667] and chlacogenides as Sn:GeS [668]. (5)

Hybrid organic–inorganic perovskites (HOIPs) (e.g. $CH_3NH_3PbI_{3-x}Cl_x$) [669], [670]). (6) 2D (or quasi 2D) material systems as Ga_2O_3 [671], graphene oxide (GO), $MoS_{2-x}O_x$ [672], MoS_2 [673],[674],[675] or h-BN [676], [677], [678]. (7) Organic semiconductors and biomaterials including small molecule (e.g. BCPO) [679] ionic-electronic conducting polymers (e.g. PEDOT:PSS, PEDOT:PTHF) or biomaterials (chitosan, ferritin, silk fibroin, collagen, DNA) [680], [681].

o CBRAM. Conductive-bridging is based on the electrochemical formation of conductive metallic filaments through an insulating solid electrolyte [682]. The electrochemical materials are generally composed of two different electrodes: one electrochemically active (generally Cu or Ag) and one inert (e.g. Pt, Au, Ru, Pd or W) electrode. These two electrodes are separated by a solid insulator electrolyte thin-film with good ionic conductivity such as amorphous silicon a-Si [683], a-SiC [684], silicon nitride SiN_x, [683], silicon oxynitride $SiON_x$ [685], SiO_2 [683], metal-oxides (e.g. ZrO_2, [686], GeO_2 [687], $ZnFe_2O_4$ [688] or Al_2O_3 [689]), inorganic halide perovskites (e.g. $CsPbBr_3$ [690]), organic semiconductors (e.g. P3HT:PCBM [691]), biopolymers (silk fibroin [692]) or some chalcogenides such as Ag_2S [693], GeS_x and $GeSe_x$, [694].

o PCM. Phase change memory (PCM) depends on the large difference in electrical resistivity between the amorphous (low-conductance) and crystalline (high-conductance) phases of so-called phase change materials. Materials used for phase change memories (PCM) should in general meet two requirements: large crystalline/amorphous resistivity ratios and fast re-crystallization times. A major breakthrough was reached in 1987 by the discovery of fast switching alloys on the pseudobinary line $GeTe$-Sb_2Te_3 which exhibited crystallization times in the 10^{-8} s range and up to 5 orders of magnitude resistivity change [695]. Phase change materials are therefore semiconducting chalcogenides alloys on the $GeTe$-Sb_2Te_3 pseudobinary line (e.g. $Ge_2Sb_2Te_5$, $GeSb_2Te_4$, $GeTe$, or Sb_2Te_3) [696] while another successful alloy is the eutectic composition Sb_2Te [697].

o Ferroelectric/Multiferroics. Oxygen-octahedral perovskites and related materials (e.g. $Pb(Zr,Ti)O_3$, $BaTiO_3$, $KNbO_3$, $BiFeO_3$) are prominent RS ferroelectrics/multiferroics [698] although there are also notable ferroelectric organic polymers such as polyvinylidene fluoride (PVDF) [699], [700], [701], [702]. The $Pb(Zr,Ti)O_3$ (PZT) system is

the most investigated and implemented material in current applications while $BiFeO_3$, $BaTiO_3$-based, $K_{1-x}Na_xNbO_3$ or $(Bi_{0.5}Na_{0.5})TiO_3$ are promising lead-free ferroelectrics [703], [704], [705]. However, their inherent poor CMOS compatibility makes PZT and common lead-free perovskites difficult to be integrated with current industry mainstream. To address the issue, there is a strong interest in nanoscale engineered CMOS compatible oxide ferroelectric thin-films. Recently, ferroelectricity at nanoscale in CMOS compatible high-*k* dielectric $Hf_xZr_{1-x}O_2$ [706] was demonstrated. Following this discovery, thin films based on (doped or undoped) HfO_2 and ZrO_2 have been shown to be ferroelectric as well [707], [708], [709].

In volatile resistive switching, in contrast, the resistance collapse after the *set* voltage (or current) bias is not permanent, but vanishes over time. The insulating material also experiment a sudden drop in its resistivity after applying a set bias larger than a certain threshold, but the material returns to its highly-resistive original value after a characteristic time. A well-known route for volatile resistive switching features is implemented in *Mott insulators* in which a metal-insulator-transition is observed [710]. In a MIT transition, the resistivity drop takes place locally, when a section of the material changes from the insulating to the metallic phase as a result of an applied bias (Fig. 10(c)).

- o Mott insulators. Examples of Mott insulators are NbO_2 [711], [712], vanadium oxides such as VO_2 [713],[714],[715], V_2O_3 [80],[715], Cr-doped V_2O_3 ($V_{2-x}Cr_xO_3$) [716], some nickelates/Ni-compounds (e.g. $SmNiO_3$ [717], $La_{2-x}Sr_xNiO_4$ [718]), Fe_3O_4 [719] and some chalcogenides such as $NiSe_{2-x}S_x$ [716] or $GaTa_4Se_8$ [720].

Therefore, oxide thin-films are a particularly attractive material system for implementing resistive switching since, not only they feature both volatile and non-volatile resistive switching, but also the number of technological options available is huge; there is a lot of room for further research taking into account the number of potential oxide candidates, their various thin-film growth methodologies together with the exploration of their diverse RS microscopic origin (where some of these implementations are, in addition, CMOS compatible). Coming back to biological cortical circuits and with the objective to trace a neuromorphic correspondence, it may be argued that the two basic elements of biological brains, in its simplest view, are spiking neurons and synapses (i.e., the plastic connections in between neurons). The two types of oxide's resistive switching enable the definition of the

two basic hardware elements of oxide-based neuromorphic systems, i.e., artificial synapses and artificial neurons [721]. The artificial analogous of a biological synapse, which emulates their non-volatile memory features, may be referred as a *Synaptor* (Fig. 11(a)). On the other hand, the artificial neuromorphic circuit emulating the volatile action potential behavior of spiking neurons may be referred as a *Neuristor*, (Fig. 11(b)). When these two elements are wired in a network, they form artificial neural networks which emulate biological brain circuits (Fig. 11(c)). One of the key questions associated with neuromorphic computing is which neural network model to use [601]. One popular inclusion for synapse models is a plasticity mechanism which has been found to be related to learning in biological brains. Both, short-term and long-term potentiation (STP/LTP) and depression (STD/LTD) have been extremely common in neuromorphic implementations and are specific forms of spike-timing dependent plasticity (STDP) rules (Fig. 11). Analogously, a variety of biologically-plausible and biologically-inspired neuron models have been implemented in hardware while network models describe how different neurons and synapses are connected and how they interact, as it will be shown in the next sections.

3.2. Synaptors

Interest in nonlinear two-electrode resistive switching devices has been boosted since 2008 when a TiO_2 memristor was "found" [722] and, short after, the early arrays of TiO_2 memristors on CMOS chips were reported by Hewlett-Packard researchers [723], [604]. Memristor is the device component that mimic biological synapses. A resistance switch of a non-volatile RS device replicates the way the cortex synapses are modified when a new memory is acquired. A thin (<100 nm) oxide thin-film layer exhibiting either unipolar or bipolar non-volatile RS sandwiched between two metallic electrodes is the easiest way to implement a synaptor. Unipolar RS (in which the secondary reverse pulse is of any polarity) is typically observed in simple binary oxide thin-films (e.g. NiO, TiO_2, ZrO_2, HfO_2) and with symmetrical inert electrodes [22]. Wide bandgap stoichiometric oxides are very good insulators and the RS is induced by the oxide's soft dielectric breakdown (electroforming) under an applied field in range of few MV/cm. Electroforming results in a collective ion migration (such as oxygen vacancies) that leave behind filamentary conducting structures [24]. Once these filaments are formed, the reversible RS is indeed due to the subsequent filament breaking and reconnection after electric field pulses. In bipolar RS (reverse pulse of opposite polarity), an electric field results in an ionic migration that induces local structural changes in the vicinity of the

36

metal/oxide Schottky barriers. The electrode choice has been demonstrated to be of critical importance, as it leads to a significant modulation in the overall resistance of the device. Reactive oxide capping layers (e.g. CeO_{2-x}) can also be engineered to control the RS effect [724]. A number of investigations have been conducted on double and multiple oxide layers (e.g. $GeO_{2-x}/HfON_x$ [725], MoO_{3-x}/Gd_2O_{3-x} [726], $HfO_{2-x}/TiO_{2-x}/HfO_{2-x}/TiO_{2-x}$ [727]) to reduce the RS variability and to implement multi-level storage functions. This synaptic plasticity plays a crucial role in the way the brain implements learning and memory [728]. In biological neurons, depending on its characteristic timescale, there is short-term synaptic plasticity ($\sim10^{-3}$-10s) and long-term plasticity ($\sim10^2$-10^4 s). Short-term potentiation (STP) - (or short-term depression STD) refers to the transient enhancement (reduction) of the synaptic strength on the timescale of the short-term synaptic plasticity while long-term potentiation (LTP) or depression (LTD) refers to the long-term plasticity. Both could be mimicked in a single synaptor by tuning the voltage bias coding thus resulting in the desired spike-timing-dependent-plasticity (STDP) [729], [730], [731]. The STDP learning rule states that a synapse is strengthened if the presynaptic neuron fires shortly before the postsynaptic neuron, and weakened when the temporal order is reversed. In canonical STDP, LTP occurs when presynaptic spikes (and associated excitatory postsynaptic potentials - EPSPs) lead postsynaptic spikes by up to ~20 ms, and LTD occurs when postsynaptic spikes lead presynaptic spikes and EPSPs by up to 20–100 ms, with a sharp (1–5 ms) transition between LTP and LTD and plasticity requires multiple (typically, 60–100) pre-post spike pairs [732]. It might be mentioned that, more advanced learning rules, other than STDP, are currently being implement with oxide-based memristors. For example, Xiong *et al.* [652] implemented Bienenstock, Cooper, and Munro (BCM) learning rules, arguably the most accurate model of the synaptic plasticity to date, with a tunable sliding biorealistically frequency threshold in $SrTiO_3$ memristors. They adjusted the neuromorphic BCM forgetting rate by engineering the electrode/oxide interface by tuning the electrode composition.

3.3. Neuristors

Neuristors are the active elements of a neuromorphic circuit which mimic the essential features for action-potential (i.e. nerve impulse) computing; (i) threshold-driven spiking (all or nothing response after an electric spike), (ii) lossless spike propagation and (iii) shape and a refractory period (short memory) [601]. *Neuristors* circuits have approximated this spiking behavior by a series models for action potential generation such as the Hodgkin-Huxley (H-H)

[733], leaky-integrate-and-fire (LIF) [734], FitzHugh–Nagumo [735], Morris–Lecar [736] or Hindmarsh–Rose [737]. The threshold-driving spiking may be enabled by a volatile resistive switching phenomenon: the material remains insulating until a threshold field is reached, resulting in a resistance collapse. The device returns to its original insulating state when the field is removed with a characteristic relaxation time (replicating the refractive period of neurons). That required additional short memory may come from the relaxation time of some volatile resistive switching phenomena [738], [739]. Pickett et $al.$ [740] demonstrated that the Na^+ and K^+ ion channels of the Hodgkin-Huxley model are mathematically equivalent to two volatile NbO_2 resistive switches undergoing an insulator to metal transition. The two channels are energized (d.c.-biased) with opposite polarity voltages, similar to the sodium and potassium channels of the Hodgkin-Huxley model, and are coupled to each other through a load resistor. The NbO_2 RS threshold behavior in combination with the RC constant of additional capacitors mimics the key features of biological neurons such as spiking, signal gain, and the refractory period (Fig 11(a)). Tailored neural coding (shape, period or number of spikes) is accomplished by tuning the capacitor's RC constant (Fig. 11(b)). The key feature that leads to LIF or more refined quasi-H-H behaviors is the response of the oxide thin-film metal-insulator-transition RS upon application of a train of voltage pulses [734], [731], [741], [742],[743],[744]. Biological systems are however much more complex than simple integrate-and-fire behavior, where up to twenty-three types of biological neuronal behaviors are experimentally demonstrated. Yi et $al.$ [745] suggested that scalable active MIT VO_2 RS neurons possess all three classes of excitability (Hodgkin's classification) and most of the known biological neuronal dynamics (Fig. 11(c)). The authors also suggested that MIT VO_2 RS neurons may be intrinsically stochastic. The introduction of controlled stochastic properties in neuromorphic artificial neuronal networks is still an open issue but the lack of built-in stochasticity for CMOS neurons has been pointed out to be a handicap for achieving complex computational tasks [746], (e.g, Bayesian inference, that require stochastic neuronal populations) as will be discussed in the last sections. Besides, many cortical neurons are silent; they spike rarely, and some do not spike at all and their roles are still under debate [747], [748], [749]. These kind of silent neurons have also been emulated with functional oxide thin films (e.g. In-Ga-Zn-O [750]).

3.4. Neural Networks

Oxide-based memristors offer excellent size scalability, fast switching, and low energy per conductance update thus allowing computing and memory to be integrated in a highly parallel architecture [576]. Advanced synaptic functionalities (such as spike-timing-dependent plasticity - STDP, pattern recognition, data mining or sparse coding and image processing) were demonstrated recently exploiting the RS features of functional oxide thin-films. Just to name a few examples; Wang et al. [685] obtained the STDP functionality by matching the neuristor electric pulses to TiO_2 synaptors (with a diffuse SiO_x:Ag electrode) with the OTF controling the synaptic weight change by the relative timing between pulses. Alibart et al. [751] first demonstrated pattern classification by a single-layer perception network with a nanoscale-TiO_2 crossbar arrays. Prezioso et al. [752] demonstrated a fully operational TiO_{2-x} neural network to pattern recognition of a 3×3 pixel matrix image with several black/white characters. The neuromorphic circuit was a TiO_{2-x} memristor crossbar and an Al_2O_3/TiO_{2-x} interface to reduce variability able to implement 30 different synaptic weights. In a similar fashion, Sheridan et al. [753] implemented a WO_x-based 32×32 crossbar array for sparse coding implementation where the color code corresponds to different oxide thin-film conductance states. WO_x memristors (with shorter-term memory) were also demonstrated [754] to implement a neural network based computing paradigm called reservoir computing (such systems have been demonstrated for hand-written digit recognition). Other recent implementations of crossbar arrays based on HfO_x are as big as 128×64 cells [755]. Choi et al. [756] implemented a neuromorphic chip using a TaO_x/Ta_2O_5:Si heterostructure for data mining of breast cancer images with unsupervised learning rules competitive with standard covariance matrix approaches. In this work, the silicon doping tunes the RS filament conductance (ion-hopping distance and drift velocity) at the nanoscale. In a similar approach, Wang et al. [757] reported fully RS neural networks for pattern classification with unsupervised learning by silver nanoparticles in an insulator oxide matrix (SiO_xN_y and SiO_{2-x}).

Although these impressive progresses (which have been booming during the last few years), there are, however, a number of open challenges to exploit the full potential of oxide-based artificial neural networks (ANNs) yet. A major basic challenge is still the lack of detailed understanding of brain's operational principles while other specific challenges related to ANNs would be the level of replication required of biological brain functionalities (e.g. biological-inspired or biological-plausible) [601], the number of interconnections (biological neural systems may have more than 100,000 interconnections per neuron) or the practical implementation of new technologies versus the well stablished CMOS technology [758]. For

example, given the level of technology maturity, attempts to implement oxide-based memristive neural networks have struggled with device non-uniformity, resistance level instability, sneak path currents, and wire resistance, which have limited array sizes and system performance [759]. To mitigate the oxide-based RS device integration issues, a number of industries and academics are now working on the optimization of oxide-based crossbar arrays for brain-inspiring computing (see e.g. [760], [761], [762], [576], [763]). For example, very recently, Li *et al.* [764] reported an "on-chip" experimental demonstration of highly efficient in situ learning in a multilayer neural network implemented in a 128×64 Ta/HfO$_2$/Pt memristor array. The network was trained on 80,000 samples from the Modified National Institute of Standards and Technology (MNIST) handwritten digit database with an on-line algorithm, after which it correctly classified 91.71% of 10,000 separate test images. This level of performance was obtained even with a fraction of devices in the crossbar unresponsive (11%) to programming pulses and simulations projected up to 97% accuracy in larger arrays (1024×512). The approach demonstrates the self-adapting capability of the in-situ learning to hardware imperfections and suggests that analog oxide-based RS memristor neural networks can achieve accuracy approaching that of state-of-the-art digital CMOS systems with potentially significant improvements in speed-energy efficiency (Fig. 13).

4. Oxide Thin-films for Future Photo-Neuromorphic Science and Engineering

4.1. Information vs Energy

During many centuries, a key aspect of the human brain evolution was to balance energy consumption with information processing [765]. The human body transmits around 11 million bits of information per second to the brain, but it can only be processed a small portion of this huge amount of information. For example, visual attention can select only ~30–60 bits of information for processing with each glimpse [766]. The energy resources (metabolic costs) are limited; the nervous system still consumes 20% of energy for just 2% of body mass (action potential generation, action potential maintenance and synaptic transmission) [767]. Oxide-based RS possess some additional important advantages for the design of advanced neuromorphic systems with a better information/energy balance to generate adaptive behavior, but at the same time reducing the amount of energy that it consumes [768], [769]. These advantages also include their multi-energy harvesting features, CMOS-like scaling potential and some other unique photonic features.

(1) Energy Harvesting. Functional oxide thin-films have already demonstrated their potential to reduce energy consumption as well as harvest, generate and store energy. Oxides are used in a wide range of applications, such as fuel cells (e.g. CeO_2, Cu_2O, $PrBaCo_2O_5$, ZrO_2, Bi_2O_3) [770], batteries (e.g. $LiCoO_2$, $LiNiO_2$, V_2O_5, MoO_3) [771], supercapacitors (e.g. RuO_2, MnO_2, NiO, Co_3O_4, V_2O_5, TiO_2, Fe_3O_4, SnO_2) [772], hydrogen (e.g. TiO_2, ZrO_2, ZnO, SnO_2, Nb_3O_7F, $Mg(BH_4)_2$-MoO_3, MgH_2-Co_2NiO) and biodiesel production (e.g. MgO, ZnO, $ZnAl_2O_4$) [773]. Metal oxides have also attracted much attention for thermoelectric power generation material (e.g. $SrTiO_3$, ZnO, $CaMnO_3$, Na_xCoO_2, $Ca_3Co_4O_9$)at high temperatures on the basis of their potential advantages over heavy metallic alloys (e.g. Bi_2Te_3, $PbTe$) in chemical and thermal robustness [774],[775],[776],[777]. Some oxides are intensively investigated for piezoelectric energy harvesting (e.g.$Pb(Zr,Ti)O_3$, ZnO) [778],[779], efficient electric energy transportation and conversion (e.g. Ga_2O_3, La-Ba-Cu-O, Y-Ba-Cu-O) [780],[781][782]. Oxides are also used widely to harvest light energy (e.g. solar water splitting [783] or photovoltaics [51]) and they are generally adopted because they deliver performance advantages, a lower cost and larger device stability. The oxide layer is present in several kinds of solar cells (as shown in section 2) and is multifunctional (e.g. as transparent conductive electrodes, as light absorbers or as transport layers) which opens up uncountable possibilities to combine with the RS active layer.

(2) Scaling. Metal-oxide resistive switching devices mostly rely on simple and compact two-electrodes metal-insulator-metal structure that can be scaled aggressively well below conventional RAM cells. The so-called Resistive Random Access Memory (ReRAM) is already regarded as a promising technology for implementing the next-generation of non-volatile memory [784]. Oxide based ReRAMs are attractive due to a relatively lower energy consumption (as compared to the phase change memory), the compatibility with CMOS technology (including binary oxides such as HfO_{2-x},[785], TiO_2[722] or Ta_2O_5[786]) and their potential for 3D integration [604]. ReRAMs are closely Related to oxide-based Ferroelectric Random Access Memory (FRAM) and ferroelectric tunnel junctions (FTJs)[787], [788]. The ReRAM (and FRAM) main advantages are the device simplicity (i.e., two terminals which is the same as a solar cell), its infinitesimal dimensions and its ultra-low power consumption that so far are unmatched by conventional VLSI circuits[21]. The RS action takes place in the insulating material (i.e. the functional oxide thin-film). Scaling down the thickness of such a material will reduce both the required set voltage as well as the read voltage used during operation. In this context, few nanometer-thick (or less) RS synapses with operating voltages

41

below 1V and switching energies of ~fJ have been demonstrated [22] ,[589], [789], [790]. For RS neurons to be biologically competitive, their energy efficiency needs to be $> 10^{13}$ spikes/J (energy use < 0.1 pJ/spike), and their area needs to be < 100 μm^2 [745]. For example, Yi *et al.* [745] showed (by SPICE simulations) that VO_2 neuristors are biologically competitive in terms of energy efficiency/area and can surpass the estimated human brain benchmark of 1.8×10^{14} spikes/J (or 5.6 fJ/spike energy use) at neuron sizes smaller than 3 μm^2. These figures indicate that those RS devices could in principle be powered by a network of equally minute nano-solar cells. The small amount of energy required for powering the neural circuitry makes the hypothesis of a solar brain plausible: a solar cell with 20% efficiency and an area of ~0.05 m^2 (i.e., ~20 cm $\times$ 20 cm) would produce ~10 W.

(3) *Oxide Functionalities*. Oxide thin-films with wurtzite, corundum or zinc-blende structures are good candidates as photo-active semiconductors covering all the range from ultra-wide bandgap (i.e., deep ultraviolet ~ 100 nm) such as BeO (10.6 eV) [791],optical bandgap such as CuO_x (1.4-2.2 eV), β-$AgGaO_2$ (2.2 eV) [792] or $CuGaO_2$ (1.47 eV) [793] to long-wave infrared such as Ti_2O_3 (0.09 eV) which correspond to a cut-off absorption wavelength of 13.3 μm[794]. Besides, the light absorption capability of bulk or thin-film can be improved when they become nanostructured owing to the enhanced light scattering within the oxide nanoparticles which results in improved quantum efficiency. Therefore, optically engineered oxides and their alloys can be tuned to respond to any wavelength in the germicidal UVC to the thermal imaging IRC range (~20 THz) which is a much broader range that the human visual perception range of 400-700 nm. At the time being Ga_2O_3 (5 eV) is the widest band-gap transparent conductive oxide to be used as electrode [130]. Besides its tunable light harvesting features, some non-centrosymetric functional oxide thin-films are among the best(inverse) piezoelectric (i.e., material deformations after an electrical field) and photostrictive (light induced non-thermal deformations) materials and, therefore, very interesting candidates to implement motoractive inference in (photo)-neuromorphic systems [795], [796], [797]. These unique opto-mechanical features are affected by the oxide's singular material properties such as polarization switching and fatigue, ionic defects, depletion layers, depolarization fields or contributions of domain-wall displacement. In this sense, oxide thin-films (e.g. $BiFeO_3$, $SrRuO_3$, $Pb(Zr,Ti)O_3$) and many other piezoelectrics are currently investigated as next-generation optoelectronic devices, such as remote switches, light-controlled elastic micromotors, microactuators and other opto-mechanical systems[798], [799], [800],[801],[802], [803], [804], [805]. In addition, some oxide thin-films are notable photochromic (light induced color

change - e.g. WO_3, MoO_3, and V_2O_5), thermochromic (heat induced color change- e.g. VO_2), and electrochromic (electricity induced color change- e.g. WO_3, TiO_2, MoO_3, Ta_2O_5, Nb_2O_5, NiO, V_2O_5) materials [806],[807].

4.2. New Aspects in Information Processing

The brain is the most powerful and complex known computational system having numerous levels of interaction ranging from gene networks that control cell function to neural circuits that control behavior. Recent works evaluate the memory capacity of the human brain to be in the order of 10^{15} Bytes [808]. Understanding how neural networks integrate, encode, and compute information is central to understanding brain function [809]. Mathematical frameworks such as the graph theory [810] or (Shannon's [811]) information theory [812] are well suited to address some of these issues in a rigorous manner. Because of its general applicability, information theory, in particular, has been widely used in neuroscience [812], [813], [814], [815], [816], [817]. For instance, these sorts of mathematical tools have extensively used for analyzing data from electroencephalography (EEG), magnetoencephalography (MEG), and functional magnetic resonance imaging (fMRI) [818], [819], [820]. These analyses, in turn, quantifies phenomena like encoding (e.g., how much information a neuron provides [821], [822]), complex encoding relationships [823], [824],[825], [817], studies of neural connectivity [826], [827], [828], [829] and sensory encoding [821], [830], [831], [832]. Other important topics include human behavioral (e.g. trial-based data [833], [834], [835] and single-trial time-averaged analyses [836], [837]) and cognitive sciences [838], [839], [840], [841]. When compared with biological brains, these powerful information-theoretic related methodologies have almost not yet been applied to neuromorphic technologies [842], [26], [843], [23]. The brain-inspired solid-state neuristor device was postulated by Hewitt Crane in 1960s as an electronic analog of the Hodgkin-Huxley axon and early implementations required inductors [844]. A memristor (closely) obeys Chua's non-linear equations [845] and examples are any property that changes material resistance: oxygen vacancy concentration in oxides, structural phase (amorphous *vs* crystalline), magnetization or spin state, correlated electron state (Mott insulator *vs* conductor). The NbO_2 memristors in particular exhibit an insulator-to-metal transition that can be considered as an electronic analogous of the Hodgkin–Huxley ion channels [846]. Therefore, the information theory concepts (see Fig. 14 (a),(b),(c)) intensively developed for biological neurons can, in principle, be applied to oxide-based resistive switching (- e.g. of simple devices [847], [848], [849]). These devices feature genuine physical effects that could be sought as non-linearity, plasticity,

43

excitation, and extinction which could be naturally coupled with living biological systems and tracing a cybernetic parallelism [850],[25],[746],[851]. Some of the potential directions of future research in this area are discussed in the following sections.

4.3. Neural Codes

Communication is particularly relevant for networks that are specialized to transmit or distribute information in a coordinated manner. The neuronal response to the inputs is known to be noisy [852] dictating a bound on the amount of information that can be transferred over neurons [853]. A train of neural spikes may contain information based on different coding schemes (typically $\sim 10^{-3}$s temporal resolution scale), each resulting in a different estimate of the capacity of the neuronal channel [854]. The single neuron capacity depends on coding, characteristics of the communication channel, and optimization over input distributions, among other issues [855]. How spike trains encode information is among the most important questions in neuroscience [730]. Both, spike timing and spike frequency have been proposed as modes of information transfer in biological brains [856] and both can codes can be investigated in oxide-based synaptors, neuristors and arrays [857], [858], [859], [860]. Owing to its enhanced energy efficiency, spike timing appears to be a preponderant code in biological brains while frequency codes are believed to be exponentially more costly [861], [862], [863]. For example, Feali *et al.* [864] studied the reliability of spike timing for spike train generated by memristors in which probabilistic and noise features were included. However, where the density of neurons is not as high and the stimulus tends to be slowly varying, a frequency code is a more robust alternative [865], [866], [867], [652]. Feali *et al.* [868] also emulated neuristor adaptive behavior (spike-frequency adaptation) in SPICE environment. Parihar *et al.* [869] experimentally demonstrated spontaneous stochastic spiking along with electrically controllable firing probabilities using VO_2-based metal-insulation-transitions neurons owing two noise sources - thermal noise and threshold fluctuations, which act as precursors of bifurcation. Levi *et al.* [870] further developed the concept by investigating the biomimetic neuronal networks towards brain-morphic artificial intelligence. Implementation of light-stimulated synaptic emulators may greatly enhance computational speed by providing devices with high bandwidth, low power computation requirements, and low crosstalk [871], [872], [873], [874], [875], [876], [877], [878], [675], [879], [880]. Oxides also are an excellent platform for innovative photo-driven learning as several synaptic functionalities, such as tunable photoelectric STP/STD and LTP/LTD, may be emulated taking advantage of the inherent persistent

photoconductivity and volatile resistive switching characteristics of the some oxide-based devices (Fig. 15). While the fastest timescale on which biological neurons operate is in the order of milliseconds, the photonic integrate-and-fire devices operate on picoseconds thus representing a virtually unexplored sensory and cognitive processing paradigm of the radio frequency spectrum [881],[882],[883],[884],[593],[885].

Brain is indeed a large collection of neurons in which any individual neuron response can be highly variable typical of stochastic ensembles. Being in close proximity to each other, the response of neurons to a stimulus has been determined to be highly correlated. The nature and level of this collective interdependence is currently a hot topic in neuroscience [886],[887]. In practice, when dealing with bundles of neurons, the possible numbers of inputs and responses is very high. Ince *et al.* [888] investigated the average mutual information (a Shannon entropy-based measure of the decrease of the uncertainty) of few biological neuron systems and compared to the estimated average mutual information for the whole population. They found that, while the effect of interaction increases significantly with population size, using pairs of neurons provides a reasonable estimate of the information transfer rate. Thus, the population structure can be captured by looking at the pairwise interactions between neurons. Many functional oxide properties (ferroelectricity in particular) depends precisely either in nanoscale correlation and atomic collective behavior which may also be induced by/to adjacent materials and interfaces [889],[890],[891],[892],[893]. In a Hebbian view [894], synaptic efficacy arises from a presynaptic cell's repeated and persistent stimulation of a postsynaptic cell. This pre-conditioning is a well-known behavior of any ferroelectric [895] together with their stochastic multi-step polarization switching [896],[897],[898]. Oxide spin and multiferroic systems are leading candidates for achieving attojoule-class logic gates for computing containing intrinsic stochasticity and complexity [899],[900] where spike-timing-dependent plasticity can be harnessed from inhomogeneous polarization switching [901],[902],[903],[904]. Functional oxides therefore open up new and exciting possibilities for investigating the effect of correlating artificial neurons by examining the interdependence of minute devices at the nanoscale starting from simple systems [905],[906],[907]. For example, Lin *et al.* [908] demonstrated that tuning of the insulating phase resistance in VO_2 correlated threshold switch circuits can enable direct mimicry of neuronal origins of disorders in the central neural system (Fig. 14(e)-(f)). Many research works on molecular neurophysiology have suggested the correlation of pathologically altered action potential excitability [909],[910]. Several neurological disorders including depression or attention deficit hyperactivity disorder

(ADHD) originate in faulty brain signaling frequencies. Therefore, circuits based on functional oxides may be regarded as complementary to model animal studies for neuroscience, especially when precise measurements of local electrical properties or competing parallel paths for conduction in complex neural circuits can be a challenge to identify onset of breakdown or diagnose early symptoms of disease. Complementing this, there are some preliminary indications that information theoretic formulations can help to understand how some of these disruptions take place [911], [912], [913], [914], [915], [916].

4.4. Neural Sensors

The nervous system is under selective pressure to generate adaptive behavior at the minimal energy cost and, thus metabolic energy consumption constrains the design of brains [917], [918], [767]. An strategy for enhancing its energy efficiency can be achieved by the optimal placement of components within nervous systems/sensory systems to minimize energetic costs by *saving wire* [919], [920]. Our perception of the world is indirect and visual perception is well-known to be a primary source of information and it works in a hierarchical manner with increasing abstraction as the signals progressed through the various visual areas in the brain [45], [839]. As the photovoltaic effect is the conversion of a photon into an electronic current, the visual cycle is the biological conversion of a photon into an electrical signal (action potential). In the retina, the photon is absorbed by pigments (e.g. opsin and retinal) via photo-isomerization. Neural signals from the retina photoreceptors undergo processing by other neurons whose axons form the optic nerve [921], [922]. Wavelength tunable oxide photo-neuromorphic systems (Fig. 16) are expected to enable new adaptative optoelectronic concepts [923], [924], [925], [926]. In metal oxides, the construction of special structures (e.g. low dimensional such as quantum dots, 1D wires and 2D sheets), doping, and taking advantages of the surface plasma resonance effect, the hot electron injection effect and the multiple excitons effect are commonly used methods to enhance the light absorption [927], [61]. The conceptual change that may be enabled by oxide thin-films with photoactive and resistive switching functionalities would be that the light sensing capabilities of the synaptic devices could be located in the memory and the information itself (photons) can power the neural circuit. In this sense, for example, Bao *et al.* [928] reported very recently *computing in sensor* artificial shape perception retina network based on tunable RS Neurons by one HfO_x-based memristor and a Si nMOSFET in serial is used to construct photoreceptor cell and ganglion cell. Yu *et al.* [929] engineered an oxide-based stochastic compact RS memory model demonstrating by simulation an artificial visual

(image orientation or edge detection) system tolerant to device variation. Wang *et al.* [930] demonstrated alight triggered ferroelectric/electrochemical neuromorphic artificial visual-perception system which transduces incident light signals with different frequency, intensity, and wavelength into synaptic signals, both volatile and non-volatile. In a similar fashion, Gao *et al.* [931] reported photo-plastcity of a Schottky ITO/Nb:SrTiO$_3$ enabling an optoelectronic analog of the mechanical aperture device showing adaptive and stable optical perception capability under different illuminating conditions suitable for the mimicry of interest-modulated human visual memories.

Other well-known critical energetic cost factors of sensory neural information processing are *noise* (i.e., signal-to-noise ratio (SNR)) and *response speed* (i.e. bandwidth) [932]. Measures for improving SNR include; (i) more receptors and ion channels, (ii) greater number of synaptic vesicles and (iii) averaging outputs in time/space. Measures for improving bandwidth include more ion channels while more receptors and ion channels results in larger refractory period. Numerous examples of energy efficient strategies exist at all levels of neural organization(e.g. combinations of ion channels within single neurons, ion channel size, coding of information within populations of neurons or computational maps [918]. The efficiency with which single neurons code information is critically dependent upon the biophysical properties of their membranes, such as the total surface area or the combinations of ion channels that they express, because the movement of ions across the membrane is the major energetic cost of neurons [45], [933]. Numerous features of neurons such as their conduction velocity, time constants and space constants are dependent upon the combinations and densities of ion channels within the membrane [934]. In a similar fashion, artificial neuromorphic systems should be optimized (in terms of information *vs* energy) by mimicking this wide range of biological solutions although many basic mechanisms are still under intensive investigation [588], [935], [936]. For example, the TaO$_{2-x}$ nanoscale filament in a Ta$_2$O$_5$ system is determined to be crucially affected by the migration dynamics of its oxygen vacancies [937] and is has been reported to be enhanced by the introduction of an ion diffusion limiting layer at the TiN/TaO$_x$ interface [938]. RS may be enhanced by doping as, for example, dilute aliovalent Li^{1+} doping at the Fe^{3+} sites of BiFeO$_3$ [939]. As the size of the conducting filaments is reduced down to atomic scale, the quantum conductance effect has been reported to offering great opportunities for the realization of ultrahigh-density storage, logic-in-memory circuits, atomic scale photodetectors [940].

4.5. Neural Inference

The brain is constantly bombarded with more information from multiple sensory channels than it can process. One of the fundamental insights of Claude Shannon [811] was that information is contained in events that are a departure from the norm; any system that processes information will attempt to optimize the use of its resources by creating a model of the information, and then focus its resources on those aspects of the signal that deviate from this model [941], [942]. In 1953, Hyman [943], already related the brain response times to the average information entropy which is now confirmed by modern methods such as fMRI (see e.g. [944]). Surprises (or wows!) have higher cognitive costs [945]. Itti and Baldi [946], [947], defined surprise (in a Bayesian formulation) as the Kullback–Leibler divergence between the prior probability of a model and its posterior probability given an observation or stimulus and Zenon *et al.* [841] suggested that surprise is a mean of computing the cost for updating the model. The free energy principle [948] states that (biological) systems try to minimize the difference between their model and their sense and associated perception and is minimized by continuous correction of the system's model (i.e., prediction errors.). In recent years, there have been several reports re-interpreting models of natural information processing systems (neural networks, chemical signaling, etc.) in terms of memristors units including the giant axon of squids [733], electrical networks of plants such as *aloe vera* [949] or *mimosa pudica* [950], and microorganism adaptation [951]. For example, the amoeba like cell *physarum polycephalum* when exposed to a pattern of periodic environmental changes learns and adapts its behavior in anticipation of the next stimulus to come and such behavior can be mapped into the response of a simple electronic circuit consisting of a LC contour and a memory-resistor (a memristor) to a train of voltage pulses that mimic environment changes [951]. Associative memory with memristive neural networks was first demonstrated experimentally in simple neural networks consisting of few electronic neurons connected by two memristor–emulator synapses (e.g. [952]). Cognitive tasks rely on the capability to perform inference and do not differentiate between computing and memory. Querlioz *et al.* [953] developed a bioinspired approach for programming memory devices, which naturally gives rise to an inference engine [954]. Bayesian inference can be efficiently performed with stochastic signals [955],[956],[957] which is particularly suited to oxide functional devices that exhibit faults and device variations [958],[959],[960],[728]. Adaptive oxide electronics is then plausible; it has been repeatedly shown that properties, such as resistivity, polarization, and magnetization, of many oxides can be modified electrically in a non-volatile manner, suggesting that these materials

respond to electrical stimulus similarly as a neural synapse [18]. The implementation of oxide-based self-powered photo-sensitive memories would continuously monitor the reality at an additional zero energetic cost which also would result in a minimization of its internal states [961]. It is conceivable that the size (and/or entropy - the long-term average of surprise is entropy) of AI cognitive models can be much reduced with tailored artificial synapses able to monitoring in-situ [962], [963], for example, colors (i.e., light wavelength) and textures (i.e. light irradiance) (see e.g. [964], [929], [930], [931]). In an information theory basis, free energy minimization is equivalent to maximizing the mutual information between sensory states and internal states [965] which is also related to the principle of sensor's minimum redundancy [966], [967]. A similar free-energy approach for the nervous system [767] exists for ferroelectric materials [968]; while in biological brains minimizing surprise enables them to resist a natural tendency to disorder, in ferroelectrics its entropy is minimized by reorganizing internal dipoles which generate a spontaneous polarization at the surfaces [969]. In ferroelectrics, their polarization can be controlled by light and (or light/voltage) [970], [87], [971], [972], [973] thereby potentially enabling photo-inference. In a similar way, some spintronic materials such as (Co,Si)-co-substituted $Lu_3Fe_5O_{12}$ presented spin-current photoinduced magnetic anisotropy and long-term potentiation with a photomemory effect [974].

More generally, *Active inference* is the principle of free energy minimization applied to action in which higher cortical levels send descending proprioceptive predictions (while ascending connections convey prediction errors) minimizing surprise of sensory observations (e.g., [975], [976], [977], [978], [979], [980], [981], [982]). By actively modifying the environment or conform to the expected state, systems can further minimize its free energy [983]. In an active inference framework, action (i.e., policy selection), perception (i.e., state estimation), and learning (i.e., reinforcement learning) all minimize the same quantity: variational free energy - motivated from the need for agents to maintain their exchange with the environment in equilibrium [979]. This is formally consistent with formulations of Markovian problems with Bayesian surprise and optimal decisions based on expected utility and risk-sensitive (Kullback-Leibler) control where softmax parameters become the Bayes-optimal precision of beliefs about policies [977]. While staying fully grounded in an information-theoretic foundation, this emerging neurocomputational framework considers humans as embodied, ecologically embedded, social agents who shape and are shaped by their environment and provides a theoretical basis for a unified treatment of particles, organisms, and interactive machines, spanning from the inorganic to organic, non-life to life, and natural to artificial agents [984] and giving

explanation for many cognitive phenomena, including consciousness [985]. It has been suggested that any optimal control problem (when the environment becomes an integral part of perception and action) can be cast as an active inference problem [986]. Given its simplicity and generality, the predictive coding formulation of generalized filtering may be particularly attractive (e.g. approximate Bayesian inference using variational procedures). Therefore, it may be possible to formulate engineering devices that explicitly encode the generalized motion of analog signals and use the ensuing simplicity of generalized filtering in a control setting of particular interest for neuromorphic engineering [987]. In this sense, Pio-Lopez *et al.* [988] presented a proof-of-concept implementation of robot control using active inference. They argue, that a key generalization will be integrating planning mechanisms allowing the robot to proactively avoid obstacles or to consider future (predicted) and not only currently sensed contingencies [989],[990], [991], [992], [993]. In a scheme of active inference, outputs are coordinated (biological robots send ascending sensory signals and descending motor predictions) so as to selectively sample sensory input in ways that better fulfill predictions, thereby minimizing predictive coding errors [994]. In biological systems, neuromodulators like dopamine are considered to report and modulate encoding prediction error [995], [996]. Some of these neuromodulation features could, in principle, be implemented with some of the unique oxide thin-film functionalities [110], [9] which may be stretchable and conformal on demand [997], [998], [999], [1000], [1001]. For example, Kim *et al.* [1002] demonstrated nociceptor behaviors with Pt/HfO$_2$/TiN memristor electronic receptors which can transfer external stimuli to artificial nerves. The device exhibited up to four specific nociceptive behaviors; threshold, relaxation, allodynia, and hyperalgesia, according to the strength, duration, and repetition rate of the external stimuli. Besides, humans can monitor and memorize various body motions. Motion memory devices are very recently developed to mimic this biological process which will be able to exhibit a series of functions, such as sensing, memory, and feedback (see e.g. [1003]).

4. Conclusion Remarks and Future Outlook

Oxide thin-films are becoming a key enabling technology in many modern energy, information and communication applications. Here, it has been overviewed some of the recent functional oxide-based advances for photovoltaic and neuromorphic engineering towards the envisioned goal of future self-powered photo-neuromorphic systems. Achievements in these merging fields will enable the implementation of *living technologies* with unprecedented

capability of adaptation and learning at zero energy cost. However, oxide photovoltaics as well as oxide resistive switching intrinsic neuromorphic engineering are still under intensive development where some of the recent trends can be summarized as follows:

- Oxides are widely used in solar cells (e.g. as light harvesters, conductors (TCOs), semiconductors (TSOs) and insulators (TIOs)) and are generally adopted because they deliver performance advantages, a lower cost and larger device stability or brings new functionalities into the structure such as ferroelectricity.

- Virtually any light harvesting device in a vertical architecture requires, at least, one transparent conducting electrode for the light to penetrate into the light absorbing core layers. For some consumer electronics applications, these transparent metals should be also flexible which is enabled by amorphous oxide semiconductors such as In-Ga-Zn-O (IGZO). Another key factor in the adoption of oxide semiconductors is that they are compatible with the strict manufacturing requirements of large-scale, large-volume, flexible, low cost and disposable/reusable devices.

- The technology for n-type TCOs can be considered as mature with ITO ($Sn:In_2O_3$), FTO ($F:SnO_2$) and AZO ($Al:ZnO$) being commercial products. Their conductivities lie routinely in the range of 10^3-10^4 $\Omega^{-1}cm^{-1}$ with a good transparency (>80%) in the visible part of the spectrum. Such TCOs are currently the standard choice for use in transparent electrode applications and are also hugely important for information and communication technologies such as displays, touch screens, solar cells or light emitting diodes.

- For many of these applications it is required a transparent low resistant p-type contact as well. However, current p-type TCOs are much less efficient in terms of resistance vs transparency ratio since the top of the valence band of most oxide materials is comprised of strongly localized O $2p$-derived orbitals. At the time being, NiO and SnO are perhaps the most investigated binary oxides for improving p-type TCOs by doping (e.g. Li, Cs) although their sheet resistance is still low (~20 $\Omega^{-1}cm^{-1}$). During the last two decades, it has been a lot of research in cu-based delafossites (e.g. $CuGaO_2$, $CuInO_2$, $CuCrO_2$, $CuBO_2$, $CuScO_2$ or $SrCu_2O_2$) to implement a chemical modulation of the valence band by the hybridization of O $2p$ orbitals with closed-shell Cu d orbitals forming strong covalent bindings. This results in a large dispersion at the top of the valence band and reduction of the localization of holes thus increasing significantly the conductivity (up to ~300 $\Omega^{-1}cm^{-1}$ for doped $CuCrO_2$).

51

- Recent trends for *p*-type TCOs are the identification of a series of new *p*-type TCOs such as ZnM_2O_4 spinels (M=Rh,Ir), Sr-,Ca-,Ba-doped $LaCrO_3$ and $La_xSr_{1-x}VO_3$ with conductivities as high as 872.3 $\Omega^{-1}cm^{-1}$. The concept of chemical modulation was extended to oxychalcogens because of the greater hybridization between the Cu 3*d* orbitals and the chalcogen *p* orbitals as for example $LaCuOSe$ (910 $\Omega^{-1}cm^{-1}$) and there exist the promise to further enhancements for layered quinary oxychalcogenides (e.g. $[Cu_2S_2][Ba_3Sc_2O_5]$).

- Owing to the large (and tunable) bandgap energy range covered by metal oxides, there are many oxides potentially suitable as light harvesters in conventional *p-n* type solar cells (the ideal bandgap according with the *Shockley-Queisser* limit is around ~1.2-1.4 eV). Nevertheless, since silicon and other III-V semiconductors have historically received much more attention (and, more recently, chalcogenides and halides) only a bunch of metal oxides have been seriously investigated as the photon absorber materials; in particular, cupper oxides (Cu_2O, CuO), cobalt oxides (Co_2O_4) and bismuth oxides (Bi_2O_3). All oxide photovoltaics is a field under development with the maximum power conversion efficiency in this kind of cells being around ~8% (Cu_2O).

- Oxides are, in contrast, the most investigated material system for implementing the bulk photovoltaic effect (BPE), particularly on classic wide bandgap (~3-4 eV) ferroelectrics such as $LnNbO_3$, $Pb(Zr,Ti)O_3$ and $BaTiO_3$. This BPE is notable for the achievement of photovoltages much larger than the bandgap and enormous photo-induced fields (of up to several MV/cm). However, it was the multiferroic $BiFeO_3$ oxide the one that has recently reignited the field of ferroelectric photovoltaics owing to its reduced bandgap of 2.2-2.7 eV which holds the promise of harvesting a significant part of the solar spectrum. This interest has resulted in an increasing family of ferroelectric oxides with narrower optical bandgaps such as $[KNbO_3]_{1-x}[BaNi_{1/2}Nb_{1/2}O_{3-\delta}]_x$, Bi_2FeCrO_6, $KBiFe_2O_5$, $Bi_xMn_{1-x}O_{3-\delta}$, $Pb(Zr,Ti)O_3-NiO_\delta$ or $BaTi_{1-x}(Mn_{1/2}Nb_{1/2})_xO_3$. This is a very active field of research with a maximum power conversion efficiency of around ~8% (Bi_2FeCrO_6).

- Transparent semiconducting oxides (TSOs) have widely been used as barrier (or transport) layers in many thin-film photovoltaics solar cells such as organics (OPV), plastic, dye sensitized, halide perovskite, a-Si, CdTe, CZTSSe and $Cu(In,Ga)Se_2$ (CIGS). In these structures, TSO thin-films deliver some critical advantages, including; (i) optical transparency, (ii) tunable conductivity, (iii) tunable band-alignment, (iv) sealing from the environment, and (v) easy and cheap processing.

- As *electron transport materials* (ETM), the most common oxide semiconductor is TiO_2 and other oxides such as ZnO or WO_3 $BaSnO_3$, $SrTiO_3$ and Zn_2SnO_4 are also widely used. As *hole transport materials* (HTM), the most common oxide semiconductor is NiO while other binary oxides such as Cu_2O, MoO_3, V_2O_5 or GeO_2 are also being intensively investigated.

- As transport materials, ferroelectric oxides (such as $Pb(Zr,Ti)O_3$) add new functionalities to the structure (a ferroelectric layer can be seen as a semiconductor with switchable surface charge polarity). Because of its tuneable internal dipole effect, ferroelectrics bend their electronic band structure and offsets with respect to adjacent metals and/or semiconductors when switching the ferroelectric polarization so that the overall solar cell conductivity can be tuned orders of magnitude thus resulting in a transistor effect. A solaristor (a portmanteau of SOLAR cell transISTOR) is a compact two terminal (i.e. neuromorphic) self-powered phototransistor. The two-in-one transistor plus solar cell achieves the high-low current modulation by a memresistive effect in the flow of photogenerated carriers.

- The implementation of intrinsic neuromorphic computing on the hardware level is intensively explored beyond CMOS including resistive switching (e.g oxide-based resistive switching), spintronics (e.g. spin torque devices), nanomagnetism (e.g. superconducting-magnetic) or nanophotonics. These emerging nanoscale intrinsic synapse technologies have the potential to greatly improve circuit integration densities and to reduce power-dissipation which architecture is (in general) *two-electrodes out-plane* (i.e. vertical - the layout of solar cells and solaristors) and no *three-electrodes in-plane* (i.e. lateral – the layout of silicon CMOS transistors). At the time being, beyond CMOS neuromorphic functionalities are primarily realized by resistive switching phenomena.

- Functional oxide thin-films are one the most investigated material system for implementing resistive switching features. Oxide thin-films are important as they feature the two main types of resistive switching: *non-volatile* and *volatile*. These two types of resistive switching allow implementing the basic hardware elements of oxide-based neuromorphic systems; *Synaptors* (which emulate the memory behaviour of synapses) and *Neuristors* (which emulate the leaky, integrate, and fire behaviour of spiking neurons).

- Non-volatile resistive switching is due to chains of defects through an otherwise insulating thin-film oxide. Materials for non-volatile unipolar and/or bipolar RS include; (i) simple binary metal oxides (usually off-stoichiometry) such as SiO_{2-x} or metal doped SiO_2 ($Ta:SiO_2$, $Cu:SiO_2$, $Pt:SiO_2$, $Sn:SiO_2$, $Zn:SiO_2$), TiO_{2-x}, HfO_{2-x}, Ta_2O_{5-x}, Al_2O_{3-x}, ZnO_x, ZrO_{2-x}, WO_{3-x}, NiO_x, Co_3O_{4-x}, MgO_x, Fe_3O_{4-x}, MnO_{2-x}, Cr_2O_{3-x}, $Cu_{2-x}O$, Gd_2O_{3-x}, CeO_{2-x}, MoO_{3-x}, VO_{2-x}, Y_2O_{3-x}, Nb_2O_{5-x}, La_2O_{3-x} or GeO_{2-x}. (ii) Complex oxides such as $BiFeO_3$, $SrTiO_3$, $LaCrO_3$, $ZnSO_3$, $CoFe_2O_4$, $Pr_xCa_{1-x}MnO_3$ (PCMO), $Na_xK_{1-x}NbO_3$ or $YBa_2Cu_3O_{7-x}$ (YBCO). (iii) Amorphous oxides such as a-Ga_2O_{3-x}, a-Lu_2O_{3-x} and In-Ga-Zn-O (IGZO). (iv) 2D (or quasi 2D) oxides as Ga_2O_3, graphene oxide (GO) and $MoS_{2-x}O_x$.

- For synaptors, the most used oxides are PCMO, HfO_{2-x}, Ta_2O_{5-x}, TiO_{2-x}, NiO_x, WO_x and Al_2O_{3-x}. Advanced features as, for example, pattern recognition, human thought patterns, neural fear-conditioning signal recognition or speech recognition have been already reported for neuromorphic systems with these oxides (see e.g. [22], [850])

- Volatile resistive switching is generally achieved in systems where a metal-insulator transition (MIT) is observed (i.e., *Mott insulators*). The resistance collapse occurs when part of the material changes from the insulating to the metallic phase as a result of an applied voltage. Examples of Mott insulators are NbO_2, vanadium oxides such as VO_2, V_2O_3, Cr-doped V_2O_3 ($V_{2-x}Cr_xO_3$), some nickelates/Ni-compounds (e.g. $SmNiO_3$, $La_{2-x}Sr_xNiO_4$) and Fe_3O_4 (magnetite).

- The electrical spiking signals in neurons, so called action potentials, are caused by the change in the ion concentrations (e.g., Na^+ and K^+) within and outside the neuron cell body. The generation and propagation of action potentials relies on the pumping of the ions by voltage-gated ion channel and has been described by a set of nonlinear differential equations or neuron models (e.g. Hodgkin-Huxley (H-H) [733], leaky-integrate-and-fire (LIF) [734], FitzHugh–Nagumo [735], Morris–Lecar [736] or Hindmarsh–Rose [737]). Recently, it has been suggested that the behavior of neurons initiating action potentials can be emulated by a neuristor that is built from two Mott memristors along with resistors and capacitors [740]. Following this work, a series of neuristors have been defined with NbO_2 and VO_2 Mott memristors that possess all three classes of excitability (Hodgkin's classification), most of the known biological neuronal dynamics, and are suggested to be intrinsically stochastic [745].

54

As a future outlook, oxide-based neuromorphic devices feature genuine physical effects that could be sought as non-linearity, plasticity, excitation, and extinction which could be naturally coupled with living biological systems and tracing a cybernetic parallelism. For example, oxide-based VO_2 neuristors have been reported to pave the way to stochastic computation (stochastic computation is what actually happens on the brain and is very difficult to implement with CMOS neurons). In a similar fashion, tuning of the insulating phase resistance in correlated Mott memristor circuits can enable direct mimicry of neuronal origins of disorders in the central neural system and to further study the *neuronal coding*. In such arrangements, the implementation of light-stimulated synaptic emulators may greatly enhance computational speed by providing devices with high bandwidth, low power computation requirements, and low crosstalk. While the fastest timescale on which biological neurons operate is in the order of milliseconds, the photonic integrate-and-fire devices operate on picoseconds thus representing a virtually unexplored sensory and cognitive processing paradigm of the radio frequency spectrum. Further, the nervous system is under selective pressure to generate adaptive behaviour at the minimal energy cost and, thus metabolic energy consumption constrains the design of brains. A strategy for enhancing its energy efficiency can be achieved by the optimal placement of components within nervous systems/sensory systems to minimize energetic costs by saving wire. The conceptual change that may be enabled by oxide thin-films with photoactive and resistive switching functionalities would be that the light sensing capabilities of the synaptic devices could be located in the memory and the information itself (photons) or *computing in sensor*. The implementation of oxide-based self-powered photo-sensitive memories would continuously monitor the reality at an additional zero energetic cost which also would result in a *minimization of its internal states* (free energy). As a summary, it is conceivable that the size of artificial intelligence hardware complexity and its related cognitive models would be much reduced in the future with tailored oxide-based photo-neuromorphic artificial synapses.
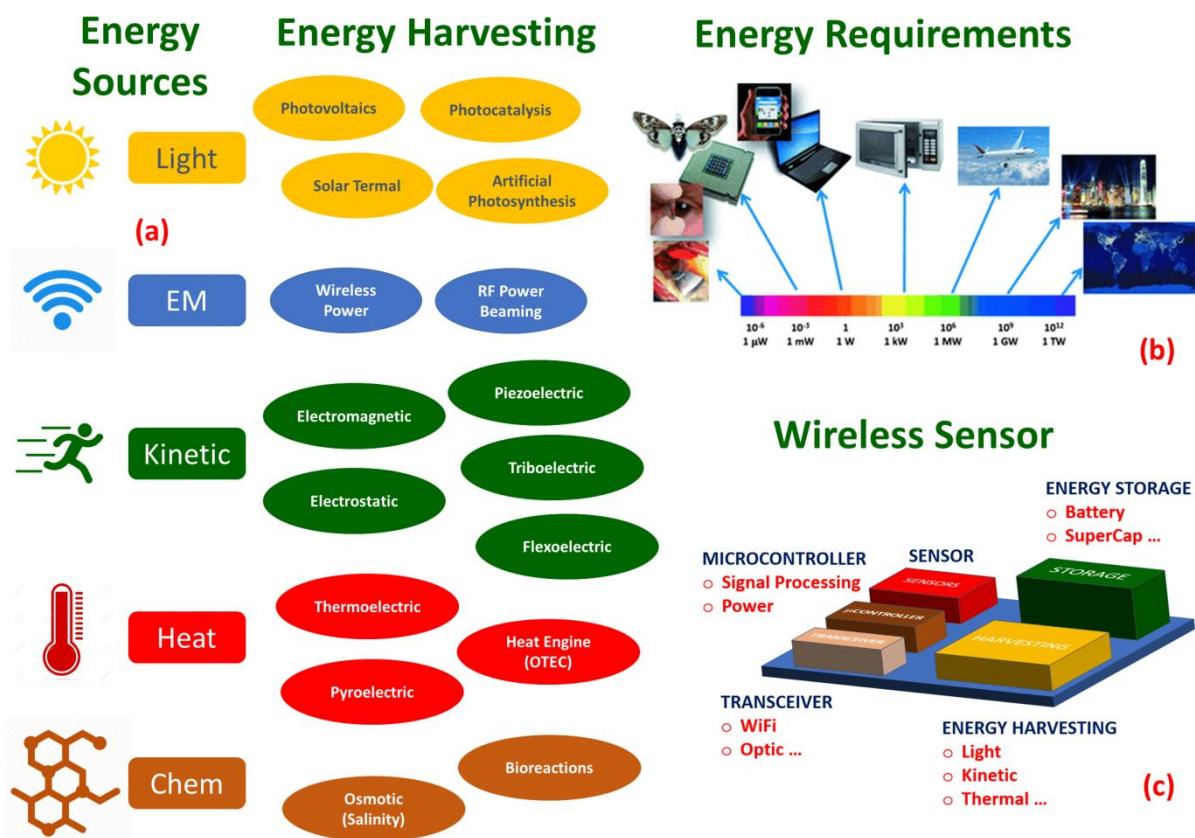
Figure 1. *Energy Harvesting*. (a) Primary energy sources (light, electromagnetic, kinetic, heat and chemical) and their corresponding physical energy harvesting mechanism. (b) The energy requirements for various consumer electronics ranging from 1 µW to 1W. Home appliances typically are in the range of few kW. Transportation and powering large systems require much electrical power (~1MW-1GW). The global energy consumption of the entire world is around 10 TW. Reproduced with permission from [48], © 2012 COPYRIGHT WILEY-VCH Verlag GmbH & Co. KGaA, Weinheim. (c) The diagram of a typical wireless sensor node. Adapted with permission from [39] © 2010 COPYRIGHT Tan YK, Panda SK. Published in DOI: 10.5772/13062 under CC BY-NC-SA 3.0 license. Available from: http://dx.doi.org/10.5772/13062.
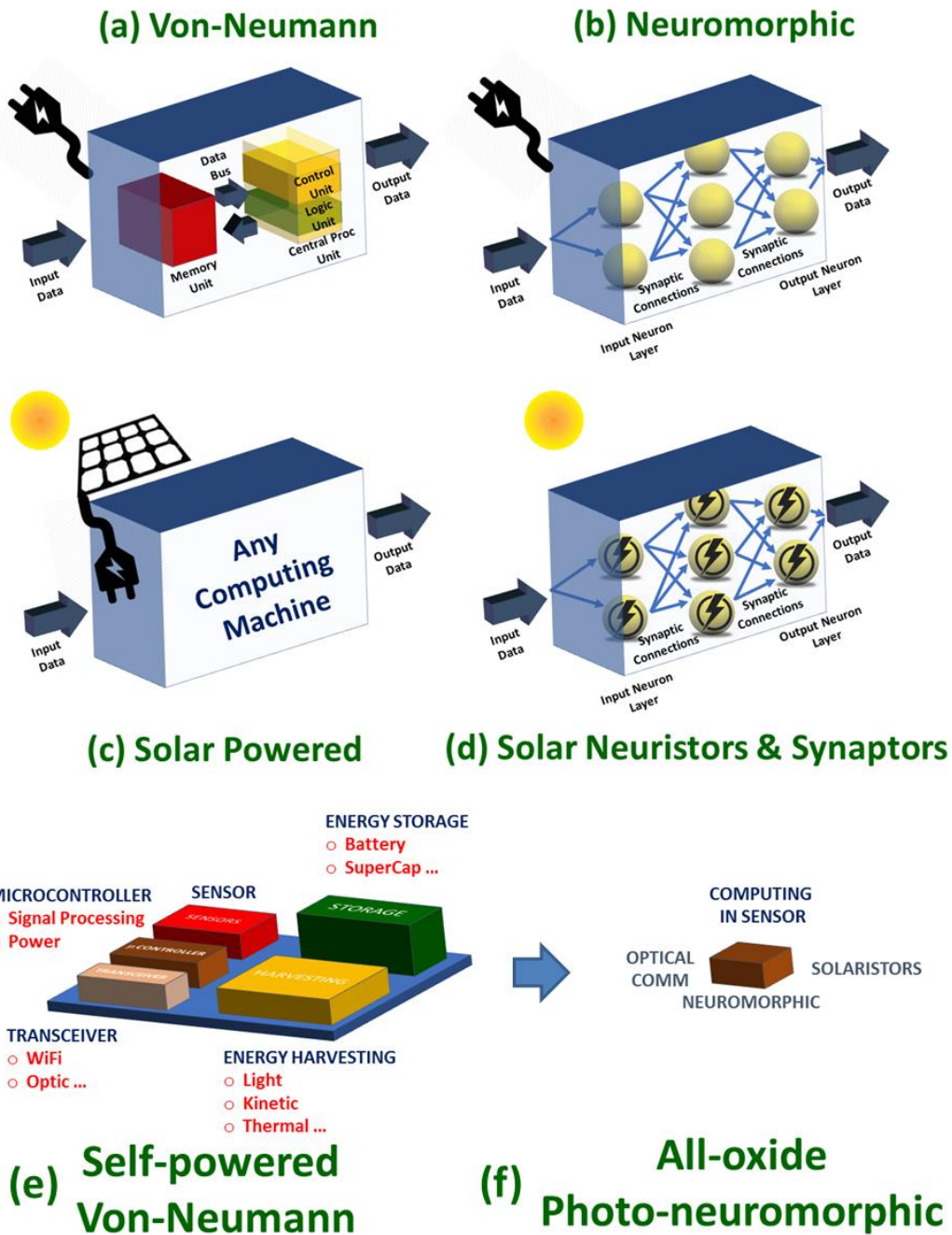
Figure 2. *Von-Neumann vs Neuromorphic Architectures*. Schematic of a serial Von-Neuman machine (a) vs parallel neuromorphic architecture (b). (c) Any computing machine can be powered from a photovoltaic system in a well-known arrangement. (d) In future photovoltaic neuromorphic system any artificial memory (synaptor) and neuron (neuristor) would be (or would be attached) to a minute power station enabling computation and power generation to be in the same place. For example, a typical wireless sensor node (Adapted with permission from [39] © 2010 COPYRIGHT Tan YK, Panda SK. Published in DOI: 10.5772/13062 under CC BY-NC-SA 3.0 license. Available from: http://dx.doi.org/10.5772/13062) can, in principle, be aggressively reduced by removing the storage and harvesting units, implementing computing in sensor and optical communications.
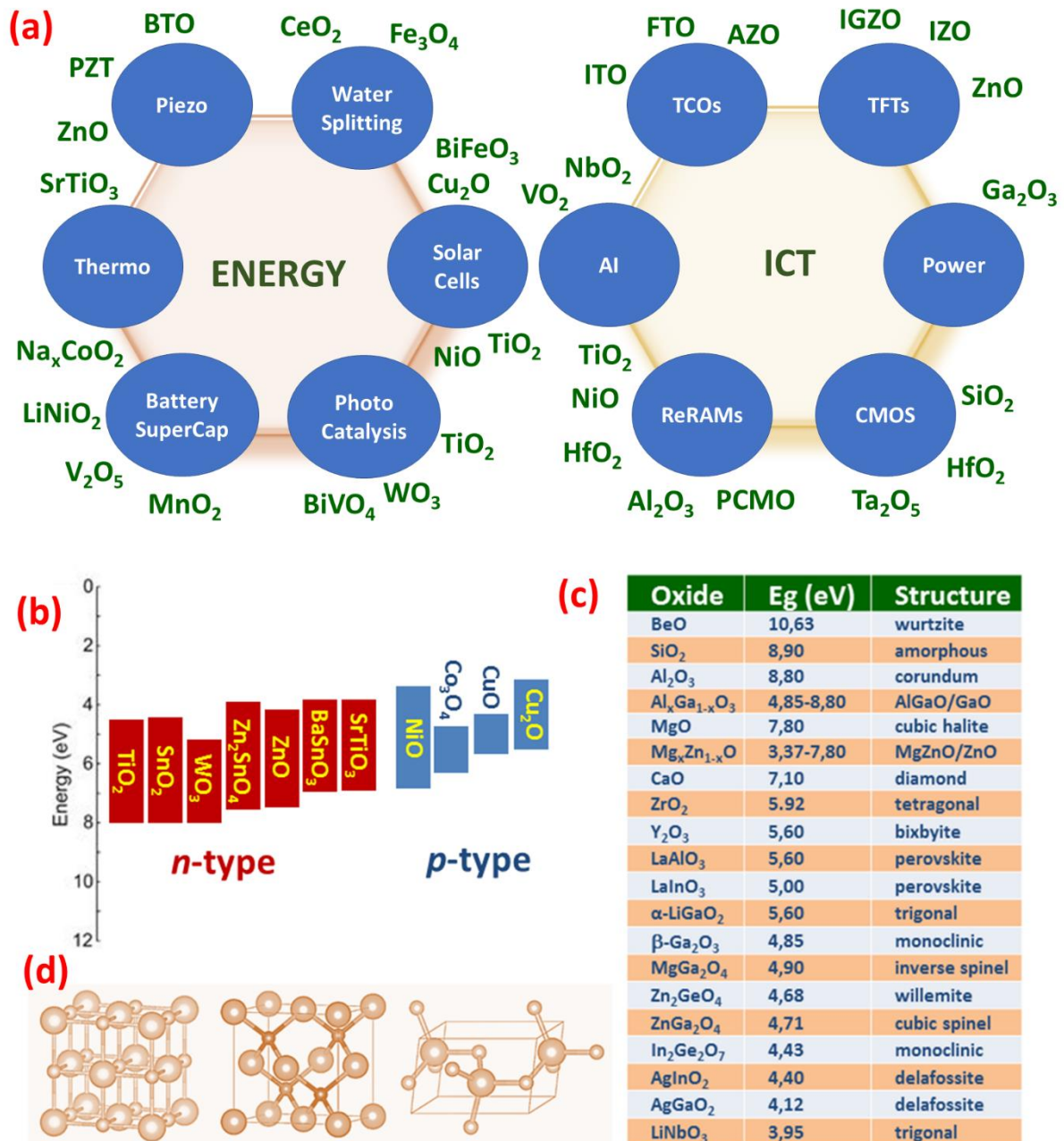
Figure 3. *Oxide Thin-film Applications in Energy and Information and Communication Technologies (ICTs).* (a) Typical energy and ICT technologies where oxides have a role. AI: Artificial Intelligence (neuromorphic computing), TCO: transparent conducting oxide, TFT: thin-film transistor. PZT: $Pb(Zr,Ti)O_3$, BTO $BaTiO_3$, PCMO: $Pr_xCa_{1-x}MnO_3$, ITO: $Sn:In_2O_3$, FTO: $F:SnO_2$, AZO: $Al:ZnO$, IGZO: In-Ga-Zn-O and IZO: In-Zn-O. Energy bandgap and work function of common oxide *n*-type and *p*-type semiconductors. (b) Energy bandgap and crystal structure of some oxide insulators or ultra-wide bandgap semiconductors (in the case of Ga_2O_3) (c). (d) Some of the typical crystal structures of these oxides (wurtzite, cubic, corundum).
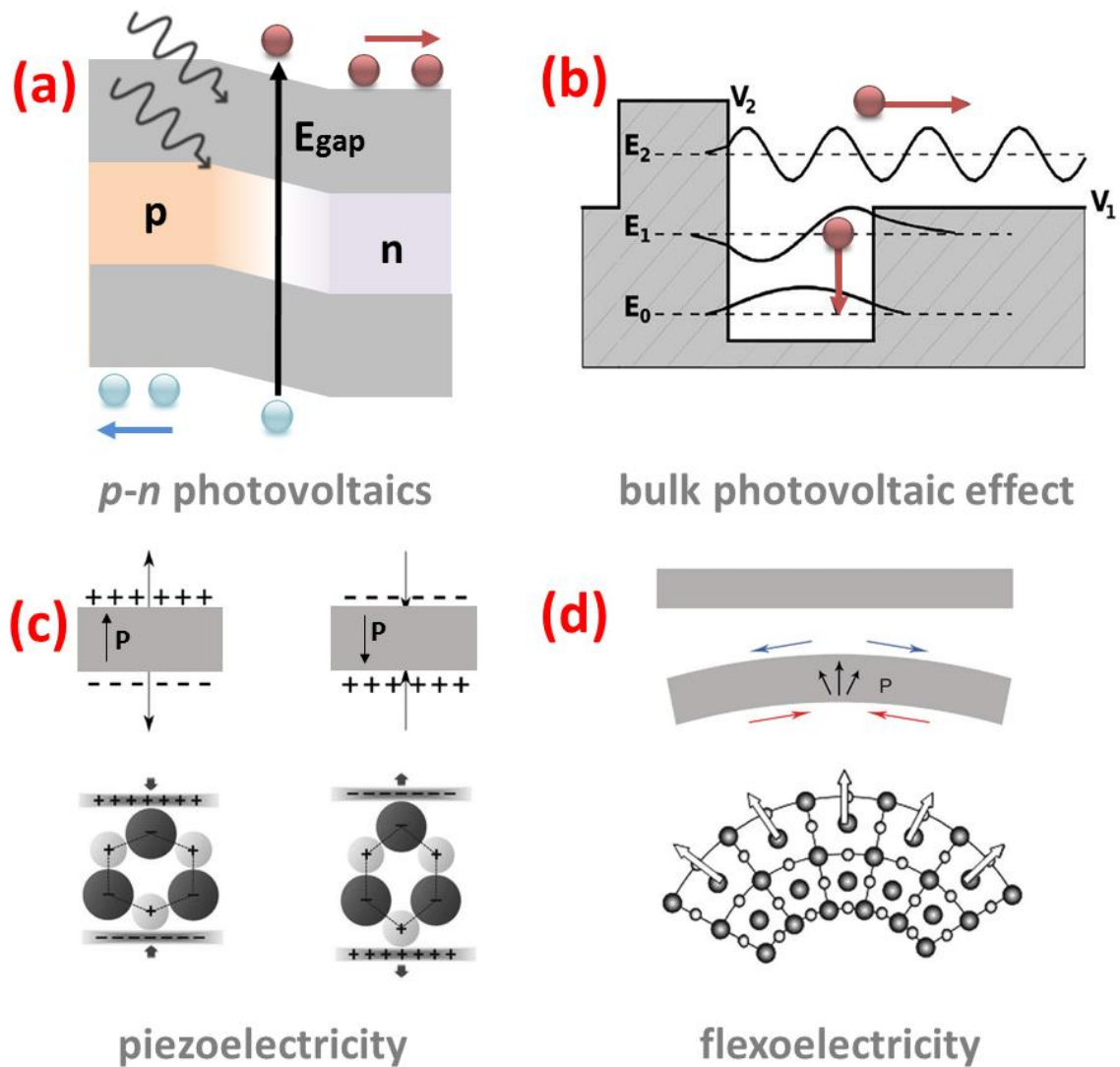
Figure 4. *A Survey of Known Photovoltaic Effects*. Schematic of the conventional (a) *p-n* photovoltaic effect and (b) the bulk photovoltaic effect (BPE). Adapted from [302] with permission from the Royal Society of Chemistry. (c) Mechanical strain has also been studied as a way to enhance photovoltaic conversion in p-n piezoelectric semiconductor junctions (e.g. ZnO) resulting in a piezo-phototronic effect. Adapted with permission from [4], ©2017 COPYRIGHT WILEY-VCH Verlag GmbH & Co. KGaA, Weinheim. (d) Very recently, it has been expanded the class of materials capable of exhibiting the BPE effect by making ordinarily centrosymmetric materials, such as $SrTiO_3$ and TiO_2, lose their inversion symmetry by a strain gradient (i.e, flexoelectricity). Reproduced with permission from [112], ©2013 COPYRIGHT WILEY-VCH Verlag GmbH & Co. KGaA, Weinheim.
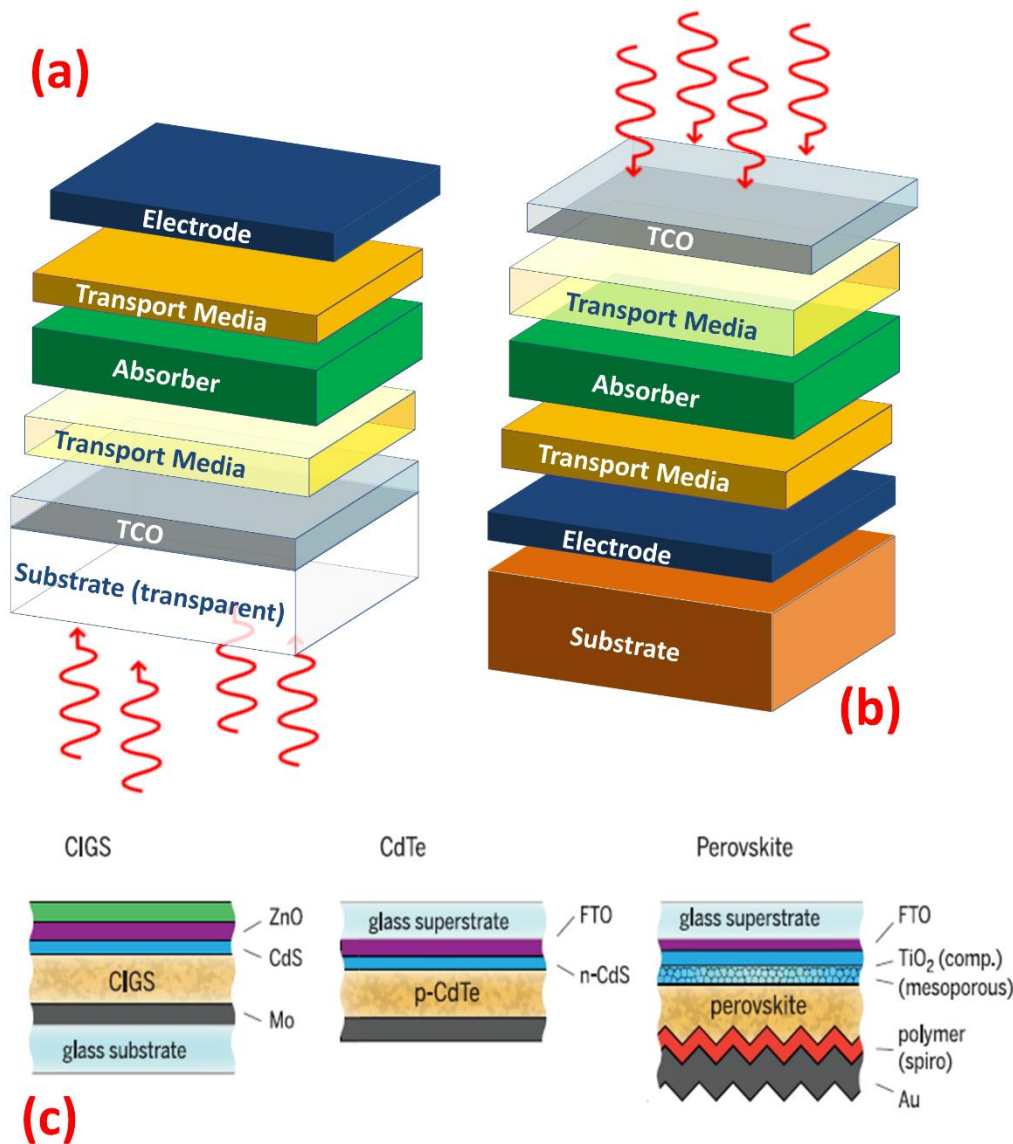
Figure 5. *Schematic of Typical Thin-film Solar Cells*. (a) transparent glass substrate illumination (TGSI) and (b) tranparent conductive electrode illumination (TCEI). Adapted with permission from [62], ©2018 COPYRIGHT Society of Photo-Optical Instrumentation Engineers (SPIE). Source: A. Pérez-Tomás, E. Chikoidze, M. R. Jennings, S. A. O. Russell, F. H. Teherani, P. Bove, E. V. Sandana, and D. J. Rogers "Wide and ultra-wide bandgap oxides: where paradigm-shift photovoltaics meets transparent power electronics", Proc. SPIE 10533, Oxide-based Materials and Devices IX, 105331Q (6 March 2018); doi: 10.1117/12.2302576; https://doi.org/10.1117/12.2302576. Schematic of three different photovoltaic technologies over 20% efficient; CIGS (generally TCEI), CdTe (generally TGSI) and perovskite (generally TGSI). Oxides are present as transparent conductive oxides (FTO) or semiconduct transport media (e.g. ZnO, TiO$_2$). Reproduced with permission from [101], ©2016 COPYRIGHT American Association for the Advancement of Science.
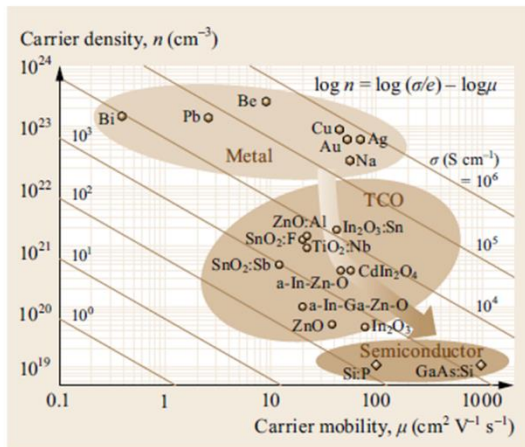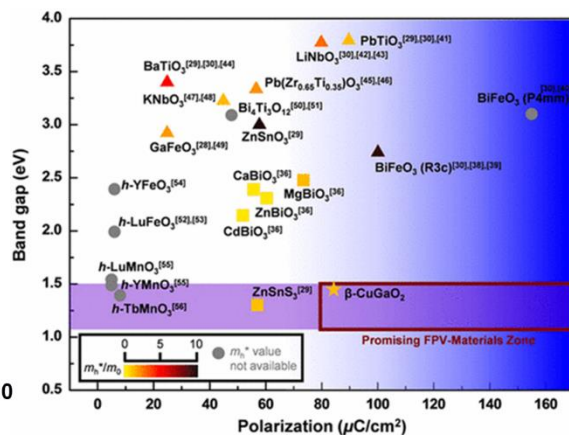
(a) *n*-type TCOs
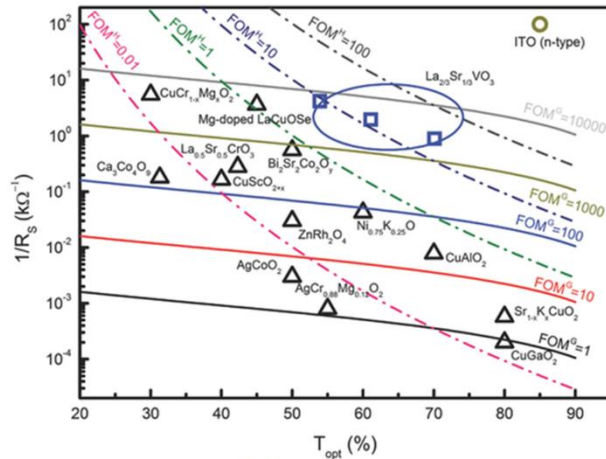
(b) *p*-type TCOs
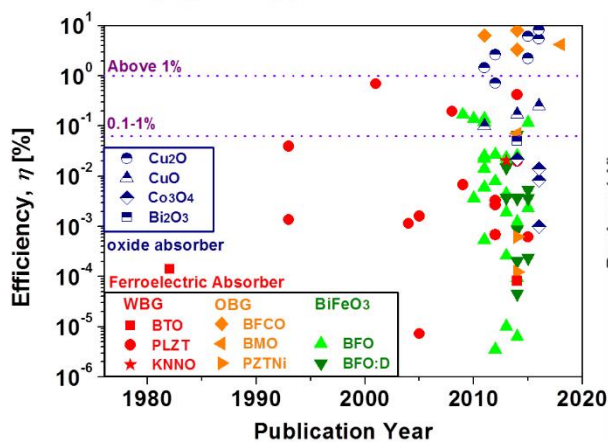
(c) Oxide Solar Cells PCE

(d) Ferroelectric Absorbers

Figure 6. *Performance maps for oxide thin-films for TCOs and light absorbers (p-n and ferroelectric solcar cells).* Performance maps of (a) *n*-type (adapted with permission from [132], ©2017 COPYRIGHT Springer International Publishing AG.) and (b) *p*-type TCOs (adapted with permission from [208], ©2018 COPYRIGHT WILEY-VCH Verlag GmbH & Co. KGaA, Weinheim). (c) Overview of the power conversion efficiency of solar cells based on oxide and ferroelectric oxide absorbers. Adapted with permission from [51], ©2018 COPYRIGHT Elsevier Inc. All rights reserved. (d) Ferroelectric oxide absorber map of bandgap *vs* polarization for some selected oxides. Reproduced with permission from [230], ©2017 COPYRIGHT American Chemical Society.
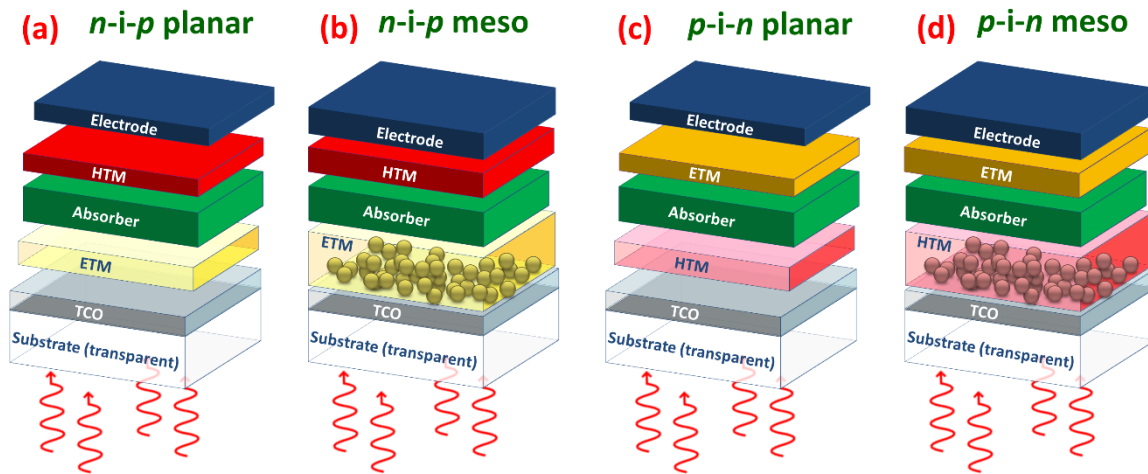
- **TCO: F:SnO$_2$ (FTO), Sn:In$_2$O$_3$ (ITO), Al:ZnO (AZO)**

- **TSO (ETM): e.g. TiO$_2$, ZnO, SnO$_2$, WO$_3$, BaSnO$_3$, SrTiO$_3$, Zn$_2$SnO$_4$, Pb(Zr,Ti)O$_3$**

- **TSO (HTM): e.g. NiO, GO, MoO$_3$, V$_2$O$_5$, GeO$_2$, Cu$_2$O, NiMgLiO**

- **TSI (meso): e.g. SiO$_2$, ZrO$_2$, Al$_2$O$_3$**

Figure 7. *Oxide Layers as Buffer Layers in Thin-film Solar Cells*. Possible configuration of tranport media in thin-film photovoltaics (e.g. organics and halide perovskites). TSO thin-films can be either, *nanostructured* or *planar*. Nanostructured oxide thin-films are made of nanoparticles (e.g. mesoscopic), nanorods, nanoplates, quantum dots or any other nanostructure within the nanoscopic size range (1 to 100 nm) while in the planar configuration they are dense thin-films. The TCO referees to a transparent conductive electrode while ETM and HTM are electron transport media and hole tranport media, respectively. In the mesoscopic structure, the mesoscopic layer can be a transparent semiconductor insulating scaffold.
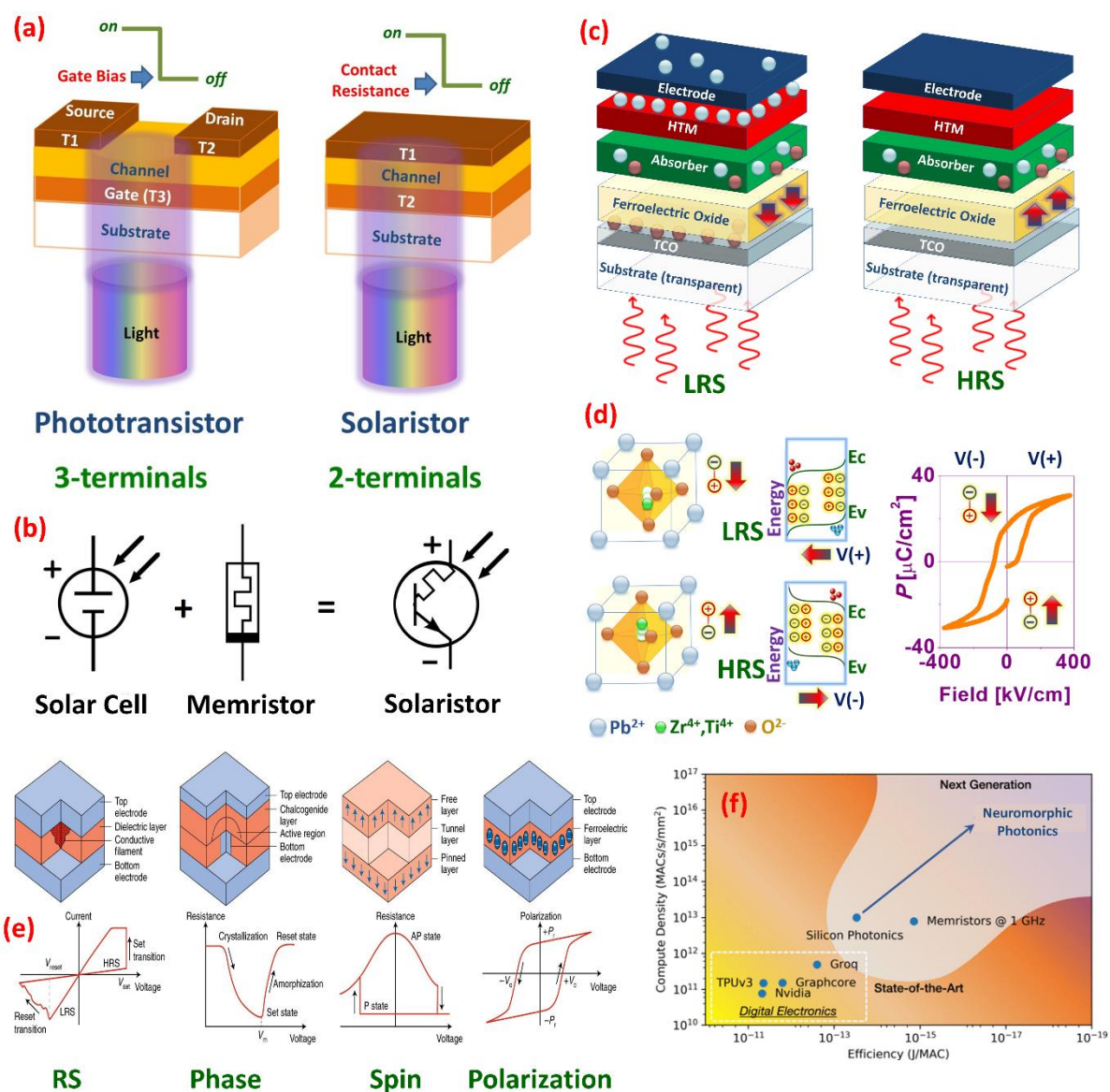
Figure 8. *The Solaristor Concept – A Neuromorphic Self-powered Phototransistor.* (a) A solaristor (from SOLAR cell transISTOR) is a compact two terminal self-powered phototransistor. (b) The two-in-one neuromorphic memristor plus solar cell achieves the high-low current modulation by a resistive switching effect in the flow of photogenerated carriers. (Reproduced from https://en.wikipedia.org/wiki/Solaristor under license CC BY-SA 4.0 (https://creativecommons.org/licenses/by-sa/4.0)). Pannels (c) and (d) show the low resistance state (LRS) and high resistance state (HRS) of a (Pb(Zr,Ti)O$_3$) ferroelectric solaristor depending on the ferroelectric polarization. (e) A solaristor is a compact two terminal photo-transitor and non-volatile memory that possesses a sandwiched neuromorphic architecture. In general, intrinsic neuromorphic functionalities are achieved by filamentary resistive switching (RS), phase changing materials (amorphous *vs* cristalline), spin current or ferroelectric polarization. Reproduced with permission from [16], ©2018 COPYRIGHT Springer Nature. (f) The introduction of photovoltaic and/or photonic aspects into these neuromorphic architectures will produce self-powered adaptive electronics but may also open up new possibilities in artificial neuroscience, artificial neural communications, sensing and machine learning which would enable, in turn, a new era for computational systems owing to the

possibility of attaining high bandwidths with much reduced power consumption. Adapted with permission from [882], ©2018 COPYRIGHT Society of Photo-Optical Instrumentation Engineers (SPIE). Source: B. J. Shastri, M. A. Nahmias, A. N. Tait, T. Ferreira de Lima, H.-T. Peng, and P. R. Prucnal "Integrated neuromorphic photonics", Proc. SPIE 10721, Active Photonic Platforms X, 107211M (19 September 2018); (with permission of authors) doi: 10.1117/12.2322182; https://doi.org/10.1117/12.2322182.
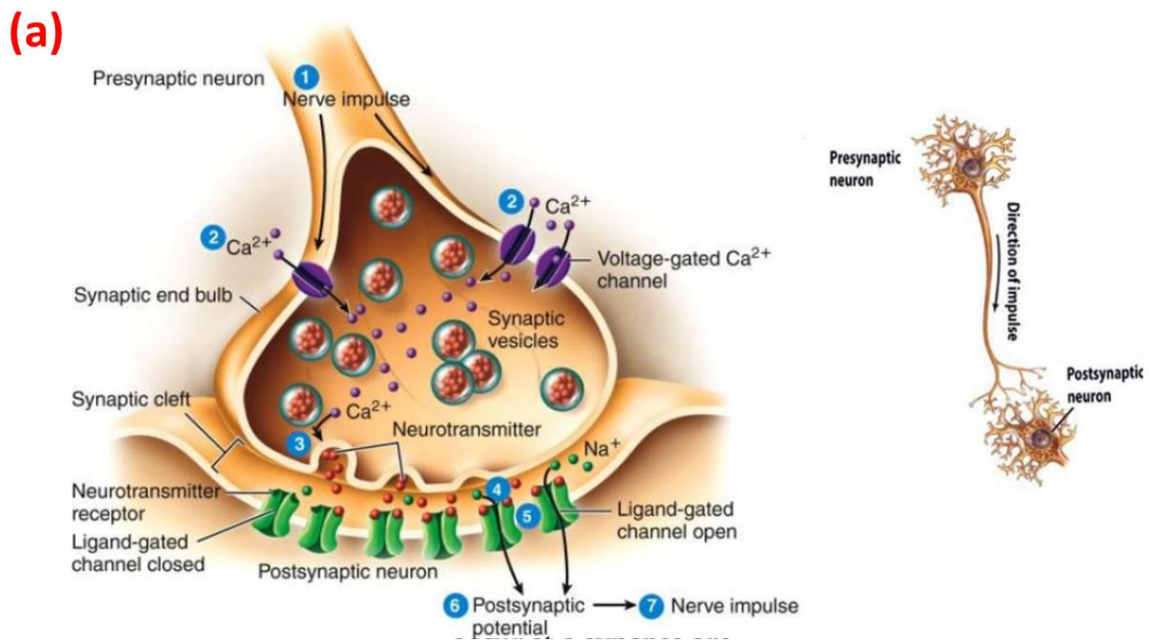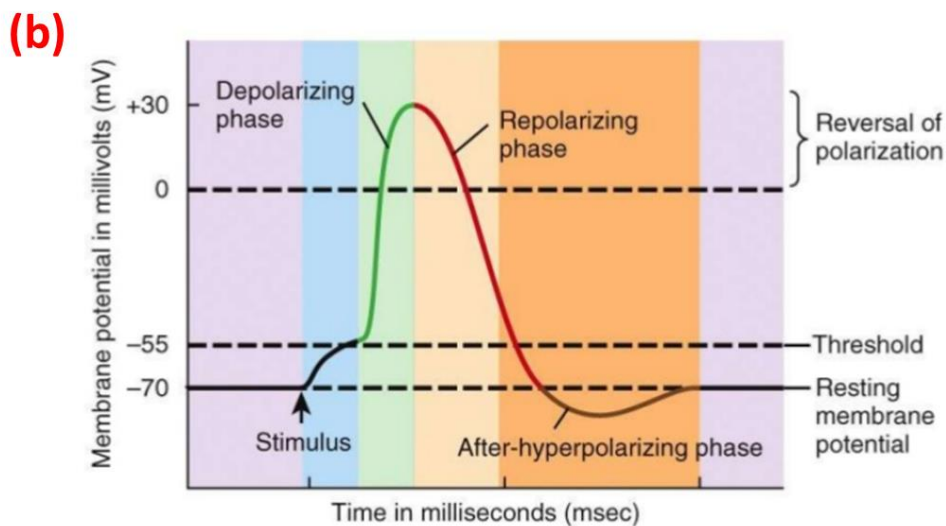
Figure 9. *Biological Synapses*. (a) Overview of the synaptic process showing vesicles neurotranmitters, lipidic membrane and Na^+ and K^+ channels. (b) Action potential voltage *vs* time showing the depolarizion of the neuron membrane and repolarization with a refractory period. Neuromorphic engineering basically is mimicking these basic neuronal process by electronic components. Credits: Images by Curtis DeFriez, Weber State University. ©2013 COPYRIGHT John Willey & Sons. All rights reserved.

66
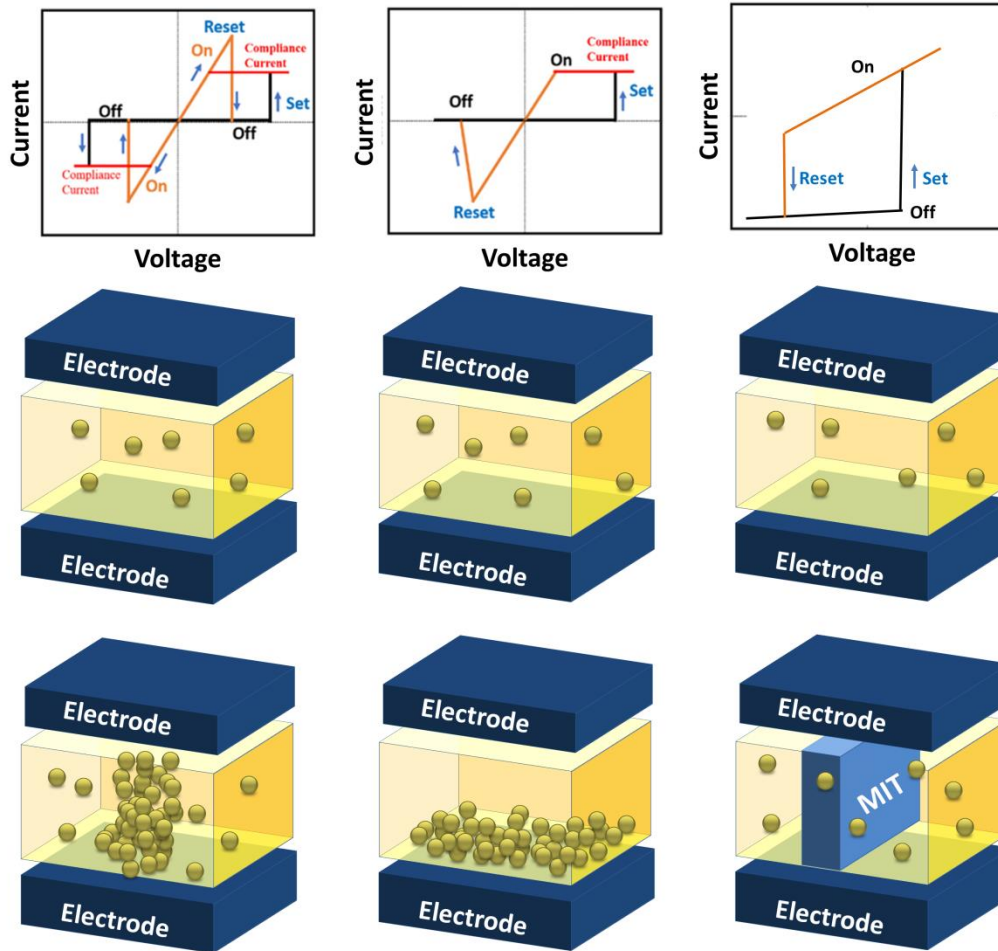
Figure 10. *Artificial Synapses - Resistive Switching in Oxide Thin-Films.* Schematic representation of the three main types of resistive switching: (a) unipolar, (b) bipolar, and (c) volatile (threshold) switching (metal-insulation-transition). Top panels: show the current *vs* voltage characteristics of each resistive switching type. Arrangement adapted with permission from [24] (©2018 COPYRIGHT AIP Publishing) and currrent-voltages curves reproduced with permission from [22] (©2018 COPYRIGHT Springer Science Business Media, LLC, part of Springer Nature) and [714] (©2015 COPYRIGHT Springer Nature Publishing AG Licensed under a Creative Commons Attribution 4.0 International License CC BY 4.0).

Figure 11. *Basic Neuromorphic Devices, Models and Systems*. Neuromorphic devices are electronic components and circuits that mimic basic functionalities of biological brains. Here, we consider two types of neuromorphic devices: (a) synaptors and (b) neuristors, which potentially could implement the core of neuromorphic artificial neural networks (typically in a crossbar array topology (c)). Neuristors are defined as the solid-state intrinsic neuromorphic devices that emulate the action potential behavior of spiking neurons (i.e., neuristors are active signaling 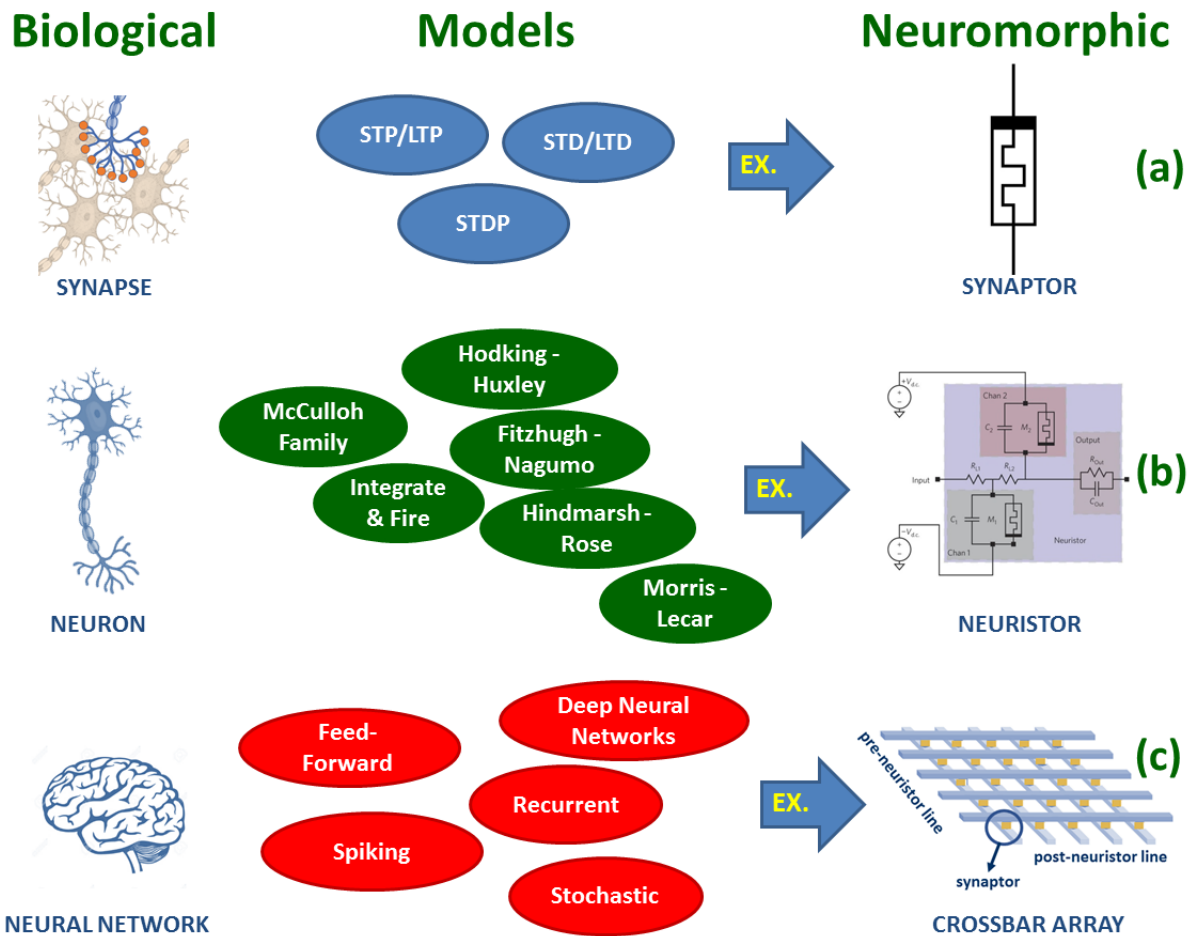circuits) and synaptors emulate the memory behavior of synapses (i.e., synaptors are, in general, simpler two-terminal capacitors -e.g. memristors- exhibiting non-linear plasticity). In practice, a neuristor can be seen as a spiking neuron and a synaptor can be seen as the tunable connection in between two neurons. One of the key questions associated with neuromorphic computing is which neural network model to use [601]. One popular inclusion for synapse models is a plasticity mechanism which has been found to be related to learning in biological brains. Both, short-term and long-term potentiation (STP/LTP) and depression (STD/LTD) have been extremely common in neuromorphic implementations and are specific forms of spike-timing dependent plasticity (STDP) rules. Analogously, a variety of biologically-plausible and biologically-inspired neuron models have been implemented in hardware. Network models describe how different neurons and synapses are connected and how they interact. The Neuristor circuit containing two volatile Mott Memristors (NbO_2) in (b) is reproduced with permission from [740], ©2012 COPYRIGHT Springer Nature.
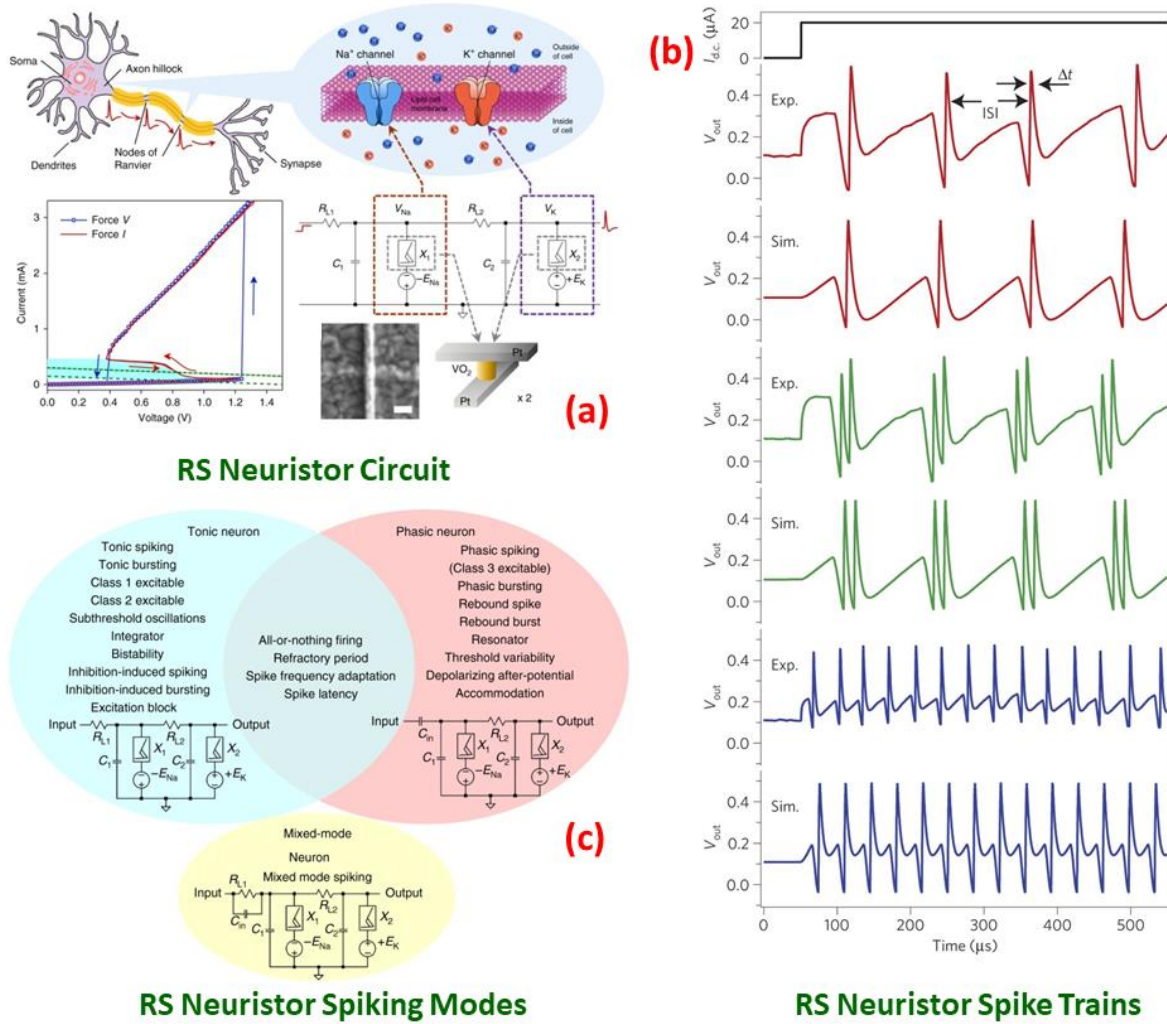
Figure 12. *Oxide-based Biological Plaussible Neuristors.* (a) Basic circuit topology of a two-channel active VO_2 neuristor to mimic the neuronal dynamics [745]. A voltage-gated Na^+ (K^+) channel is emulated by a negatively (positively) d.c. biased active Mott RS memristor device, which is closely coupled with a local membrane capacitor C_1 (C_2) and a series load resistor R_{L1} (R_{L2}). A wide hysteresis loop exists in the voltage-controlled mode due to the Mott transitions. An input current or voltage stimulus can shift the load line into the negative differential resistance regime (green dashed line) and elicit an action potential generation (spiking). (b) Experimental and simulated spike train from a NbO_2 neuristor [740]. As the channel capacitances C_1 and C_2 are adjusted, the inter-spike interval and spike width are modified such that the neuristor exhibits: regular-spiking, chattering and fast-spiking modes of operation. (c) Three active memristor prototype neuron circuits and their experimentally demonstrated spiking behaviors; *tonic excitatory neurons*, with a resistive coupling to dendritic inputs, *phasic excitatory neurons*, with a capacitive coupling to dendritic inputs and *mixed-mode neurons*, with both resistive and capacitive couplings to dendritic inputs. Panels (a) and (c) adapted with permission from [745] ©2018 COPYRIGHT Springer Nature Publishing AG Licensed under a Creative Commons Attribution 4.0 International License CC BY 4.0. Panel (b) adapted with permission from [740] ©2012 COPYRIGHT Springer Nature.

Oxide RS Crossbar Arrays for Brain-inspired Computing

(a)
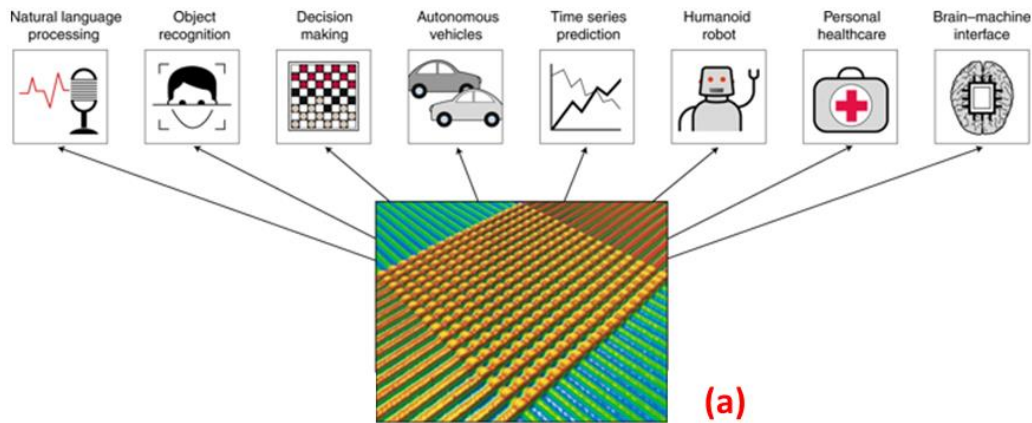
"On the Chip" Oxide RS Artificial Neural Networks

(b)
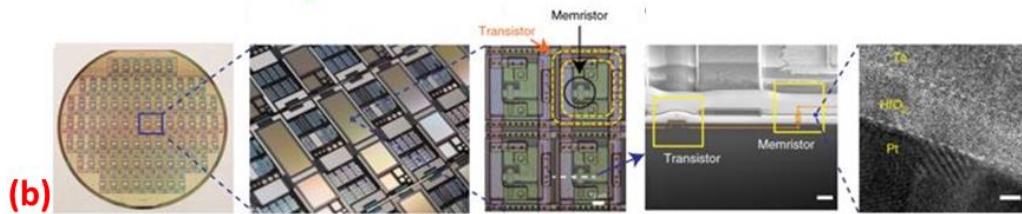
Self-adaptive In-situ Learning

(c) (d) (e) (f) (g)
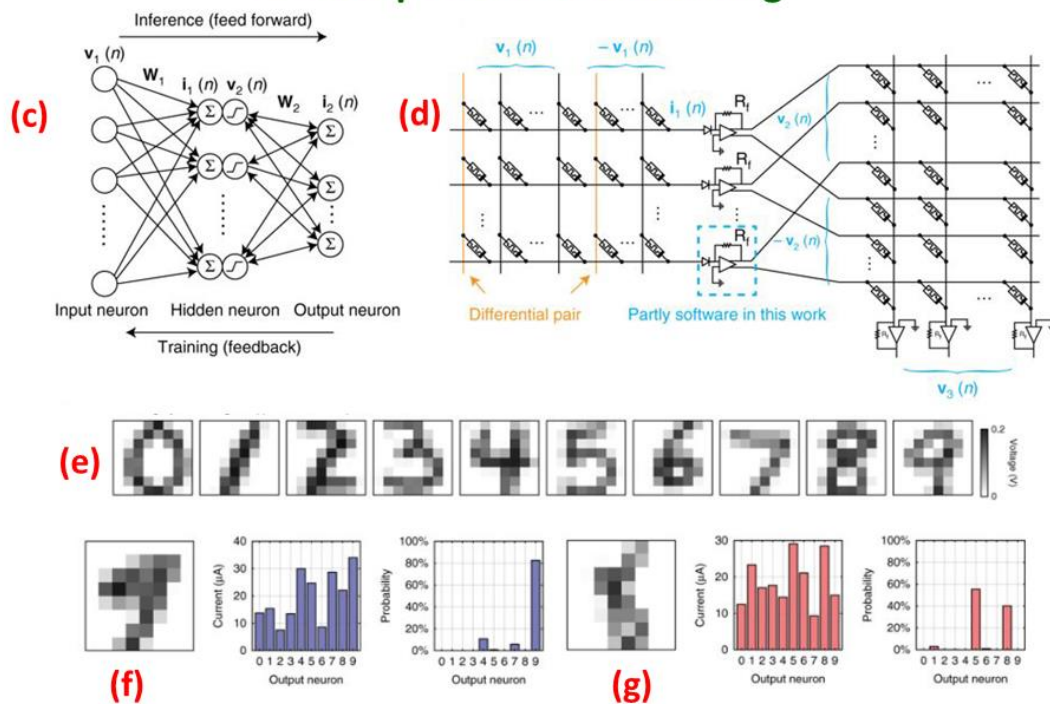
Figure 13. *Oxide-based Neural Networks*. (a) An oxide-based RS crossbar array will carry different and tunable synaptic weights in each cell, forming a computational framework with a broad spectrum of artificial intelligence applications. Adapted with permission from [576] ©2019 COPYRIGHT Springer Nature. (b) „On the chip" integration of oxide-based HfO_2 memristor artificial neural networks [764]. (c) In situ training algorithm showing an schematic diagram of a two-layer neural network where each neuron computes a weighted sum of its

70

inputs and applies a nonlinear activation function. (d) The implementation of the network with a set of memristor crossbars. Each synaptic weight (arrows in c) corresponds to the conductance difference between two oxide-based RS memristors. (e) Typical handwritten digits from the Modified National Institute of Standards and Technology (MNIST) database. In this work, the network was trained using stochastic gradient descent (SGD) to classify handwritten digits in MNIST dataset. (f) and (g) Experimental demonstration of in situ learning capability on a standard machine learning dataset. (f) Typical correctly classified digit "9" and (g) misclassified digit "8" after the in-situ training. The neuron representing the digit "9" has the highest output current, indicating a correct classification while the corresponding Bayesian probability of each digit is calculated by a softmax function. Adapted with permission from [764] ©2018 COPYRIGHT Springer Nature Publishing AG Licensed under a Creative Commons Attribution 4.0 International License CC BY 4.0.

Information Transfer (Mutual Information) in RS Networks
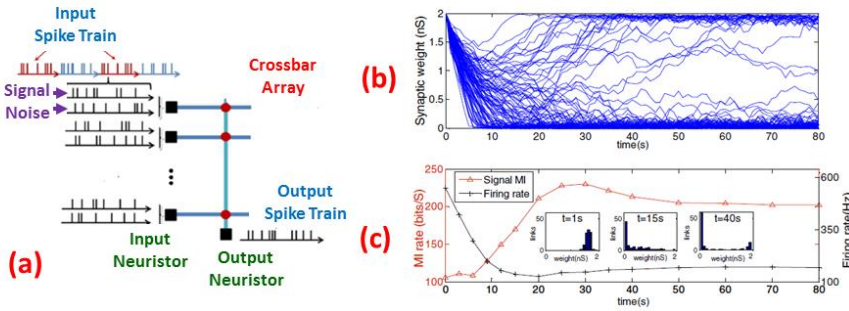
Oxide Based Neuristors Mimicking Neuronal Disorders
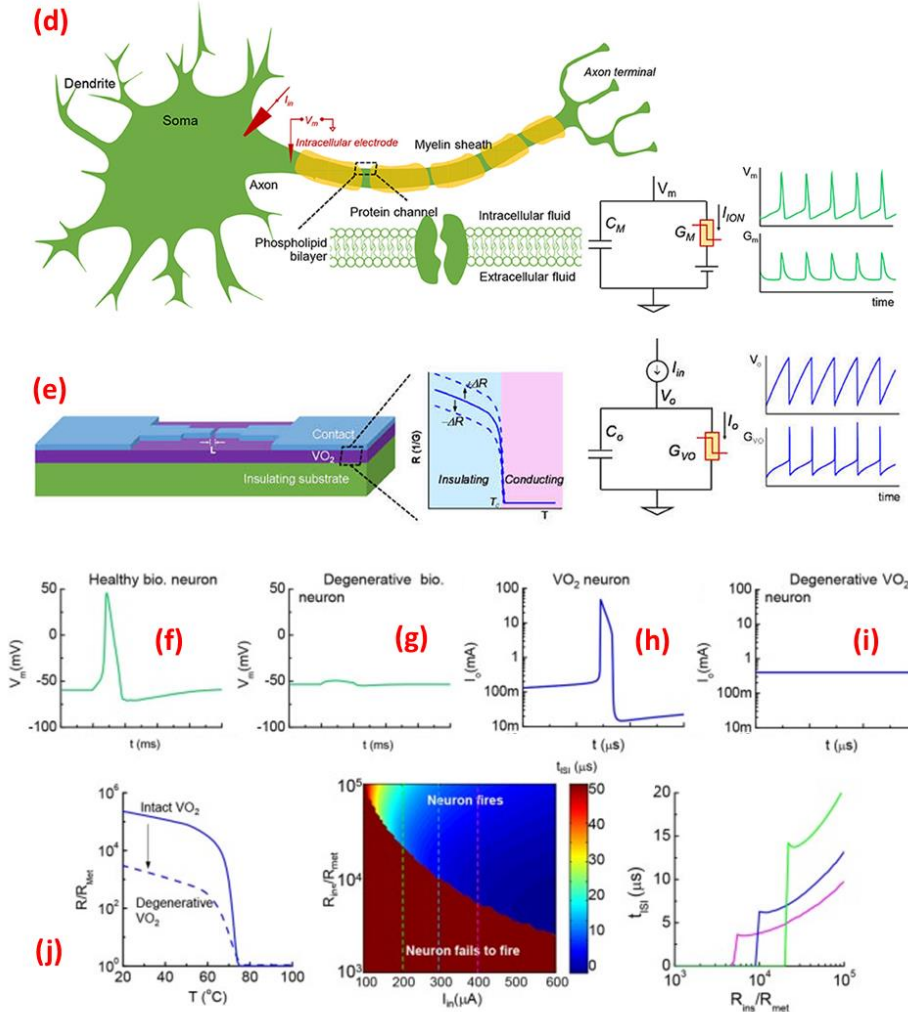
Figure 14. *Neuromorphic Codes Enabled by Oxide Thin-films*. (a) Model of a memristor-based neuromorphic spiking network. The information theory (perhaps the most rigorous way to quantify neural codes) basically is an aspect of probability theory that was developed in the 1940s as a mathematical framework for quantifying information transmission in communication systems. In a spiking neuron, the entropy rate quantifies the amount of uncertainty and translates into the amount of information potentially encoded (intricately linked to the mutual information concept). (b) As an example, a numerical Monte Carlo method with Bayesian estimators of entropy was used in [842] to determine the mutual information between the input and output layers of a memresistive crossbar array neural network based on STDP learning rules. In panel (b) it is shown the changing curves with time

72

of the 100 memristor conductances and, in (c), it is shown the simulated different mutual information rate (MI rate in bits/s) (red triangle line) and mean firing rate (black cross line) of output signals. Simulation results suggest that self-organized refinements would increase the information transfer efficiency of oxide-based RS crossbar networks. Adapted with permission from [842] ©2013 COPYRIGHT Springer-Verlag Berlin Heidelberg. Several neurological disorders including depression or attention deficit hyperactivity disorder (ADHD) originate in faulty brain signaling frequencies. (d) VO_2 MIT neurons can enable direct mimicry of neuronal origins of disorders in the central nervous system [908]. (e) The insulating-state resistance can be changed when VO_2 degrades, and this feature is utilized to model spike-timing related neural disorders. Here, $+\Delta R$ represents an increase of resistance and $-\Delta R$ represents a drop in resistance. (f)-(i) Healthy *vs* degenerative leaky neurons, and VO_2 artificial neurons (f). Healthy biological neuron shows an insulator-to-metal transition during one spike event. (j). Degenerative biological neuron with excess leakage where no action spike is observed (h). In one spike of the VO_2 neuron, the VO_2 device goes through an insulator-to-metal transition (i). Degenerative VO_2 neuron with excess leakage ($-\Delta R$) (j). The resistance as a function of temperature normalized to the metallic state resistance (R_{ins}/R_{met}) illustrates the reduction of resistance of the insulating state by ~100 (F). Contour of inter-spiking-interval shows its dependency on material properties (R_{ins}/R_{met}) and input stimulus. Reduction of insulating-state resistance (R_{ins}) narrows the neuron operating region for a given input stimulus. This example exemplifies the potential use of circuits based on functional oxide neurons as complementary to model animal studies for neuroscience. Reproduced with permission from. Reproduced with permission from [908] ©2018 COPYRIGHT Lin, Guha and Ramanathan under the terms of the Creative Commons Attribution License (CC BY).
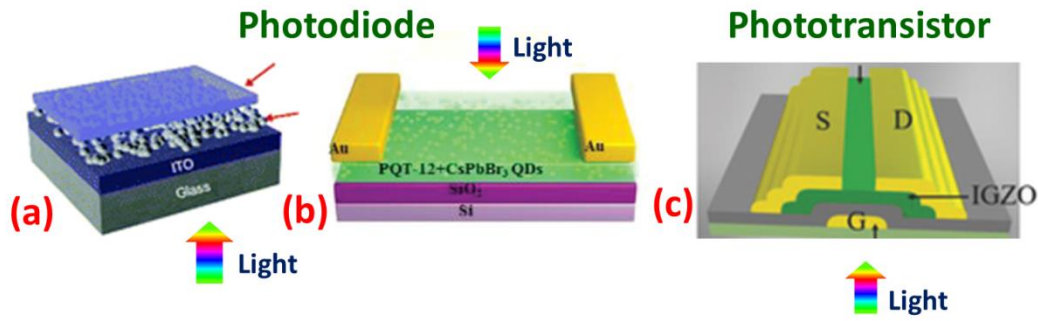
Figure 15. *Light-driven Learning in Neuromorphic Devices.* Examples of "light-driven learning" in various photo-neuromorphic devices which may present one of the following device architectures; two-terminals (a) vertical photodiode, (b) lateral photodiode and (c) three-terminals phototransistor. *Light-driven spike-timing coding* (active layer: In-Ga-Zn-O amorphous oxide) (d) Photon energy and frequency dependence in an IGZO synaptic device. Four different wavelengths were evaluated: red (λ = 620–630 nm), green (λ = 520–530 nm), blue (λ = 460–470 nm), and UV (λ = 380–385 nm) light using light-emitting diodes as light sources. PSC: postsynaptic current. (e) and (f) Emulation of symmetric spike timing dependent plasticity (STDP). (e) A schematic showing two connected IGZO synaptic devices for the emulation of STDP. Here, the left side device is considered as a presynaptic neuron and the right-side device is considered as a postsynaptic neuron. (f) The variation of connection strength between the presynaptic and postsynaptic devices as a function of *Δt*. Here, the *Δt* was varied from −0.5 to +0.5 s. *Light-driven spike-frequency coding* (active layer: inorganic halide perovskite quantum dots CsPbBr$_3$ and organic semiconductor PQT-12)

74

(g) Excitatory post-synaptic current (EPSC), triggered by a presynaptic light spike (500 nm, 0.1 mW/cm^2, 500 ms) with a constant drain voltage of −1 V and gate voltage of −1 V. The inset shows the schematic diagram of the measurement of EPSC. (h) Schematic diagram demonstrating the high-pass temporal filtering function in biological synapses. EPSC of the photo-synaptic transistors by 30 presynaptic light pulses with a constant light intensity of 0.1 mW/cm^2 and light width of 0.5 s. The 30 presynaptic light spikes used for the stimulation of channel conductance are shown in the top half of the figure (in blue). A_1 and A_{30} represent the amplitudes of the first EPSC signal and the 30th EPSC signal, respectively. c) EPSC amplitude ratio (A_{30}/A_1) plotted as a function of the presynaptic light spikes frequency. Panel (a) adapted with permission from [873] ©2019 COPYRIGHT Royal Society of Chemistry. Panels (b), (g) and (h) adapted with permission from [871] ©2019 COPYRIGHT WILEY-VCH Verlag GmbH & Co. KGaA, Weinheim. Panel (c) adapted with permission from [877] ©2018 COPYRIGHT WILEY-VCH Verlag GmbH & Co. KGaA, Weinheim. Panels (d), (e) and (f) adapted with permission from [46] ©2017 COPYRIGHT WILEY-VCH Verlag GmbH & Co. KGaA, Weinheim.

Biological vs Artificial *Living* Forms

Neural Network

(a)

(b)
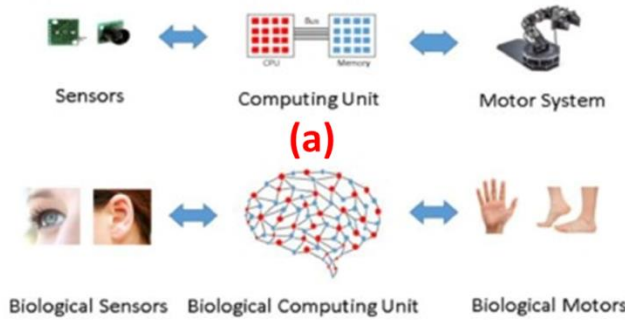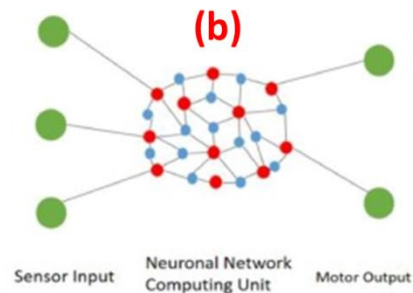
Artificial Visual-Perception Neuromorphic Systems

(c)

(d)

(e)

Ferroelectric

RS (electrochemical)

(f)
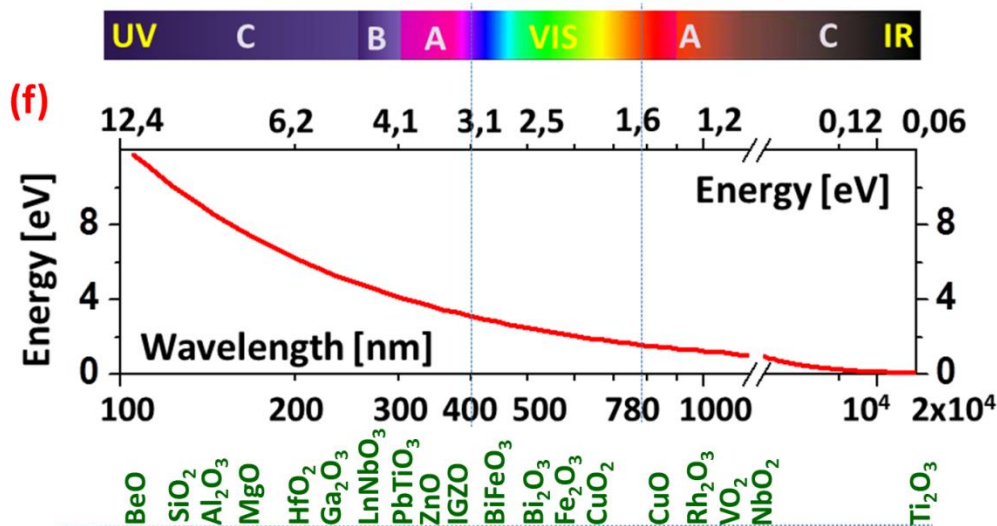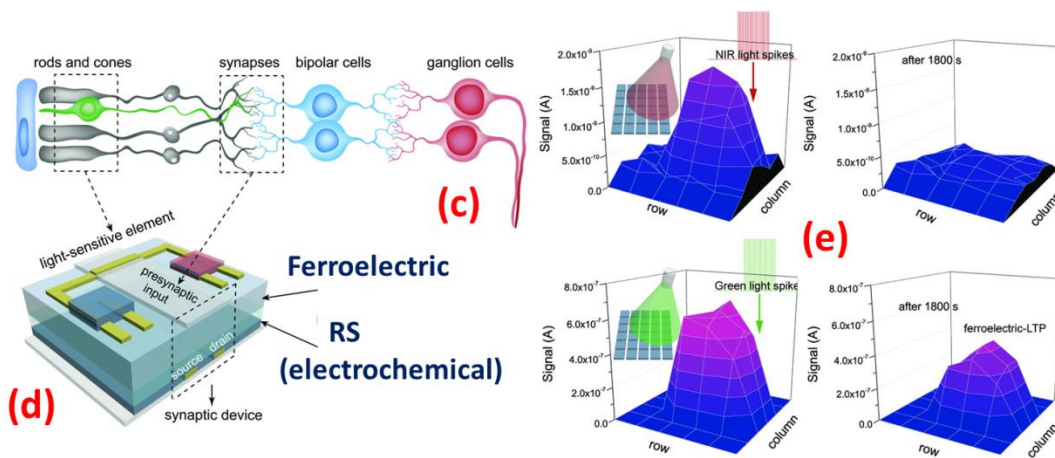
Figure 16. *Neuromorphic Optoelectronic Computing in Sensor.* (a) Conventional (Von Neumann computing system) robot system including sensors, center computing units (CPUs), and motor system *vs* biology body system including biological sensors, biological computing unit and biological motors. The bus in traditional Von Neumann is energetic and speed bottleneck. (b) A *living technology* with a neural network robot control system holds the promise of being more efficient in energy consumption and self-adaptive learning. In a scheme of active inference, outputs are coordinated (biological robots send ascending sensory signals and descending motor predictions) so as to selectively sample sensory input in ways

76

that better fulfill predictions, thereby minimizing predictive coding errors [932]. Panels (a), (b) and (c) reproduced with permission from [851] Human eyes undertake the majority of information assimilation for learning and memory. Transduction of the color and intensity of the incident light into neural signals is the main process for visual perception. However, very few studies integrate light-sensing components with neuromorphic devices to emulate retinal functions at an electronic device level although being essential to acquire advanced imaging functionalities in artificial eyes, such as visual-aided learning and color recognition [930]. (c) Schematic illustration of a retina's multilayer structure. Upon light irradiation, neural signals produced by rods and cones are transmitted through synapses to bipolar and ganglion cell layers to be processed into action potentials. Then action potentials are transferred into the brain via the optic nerve. (d) The synaptic device in this example is electrochemical organic resistive-switching transistor gated by a ferroelectric dielectric. (e) Examples of color-perception functions in the artificial-vision system depending on the wavelength of the illumination and their characteristic retention times. Panels (d), (c), and (e). Adapted with permission from [930] (f) Oxide thin-films are good candidates as photo-active semiconductors covering all the range from ultra-wide bandgap (i.e., deep ultraviolet ~ 100 nm) such as BeO (10.6 eV), UVC (e.g. ~5eV Ga_2O_3), UVA (~3eV ZnO) optical bandgap such as CuO_x (1.4-2.2 eV), to long-wave infrared such as Ti_2O_3 (0.09 eV) which correspond to a cut-off absorption wavelength of 13.3 μm. In addition, some oxide thin-films are among the best photostrictive, photochromic, thermochromic, and electrochromic materials.

Table of contents

Here, it is presented an overview on the implementation of oxide functional thin-films in photovoltaic and neuromorphic technologies with the envisioned goal of producing adaptive autonomous photonic systems in the future. The successful implementation of photo-neuromorphic systems will open up new possibilities in artificial neuroscience, artificial neural communications, sensing and machine learning which would enable, in turn, a new era for computational systems owing to the possibility of attaining high bandwidths with much reduced power consumption.

Keyword

Oxide thin-films, photovoltaics, neuromorphic, ferroelectrics, resistive switching, metal-insulation-transitions, neuroscience, information theory.
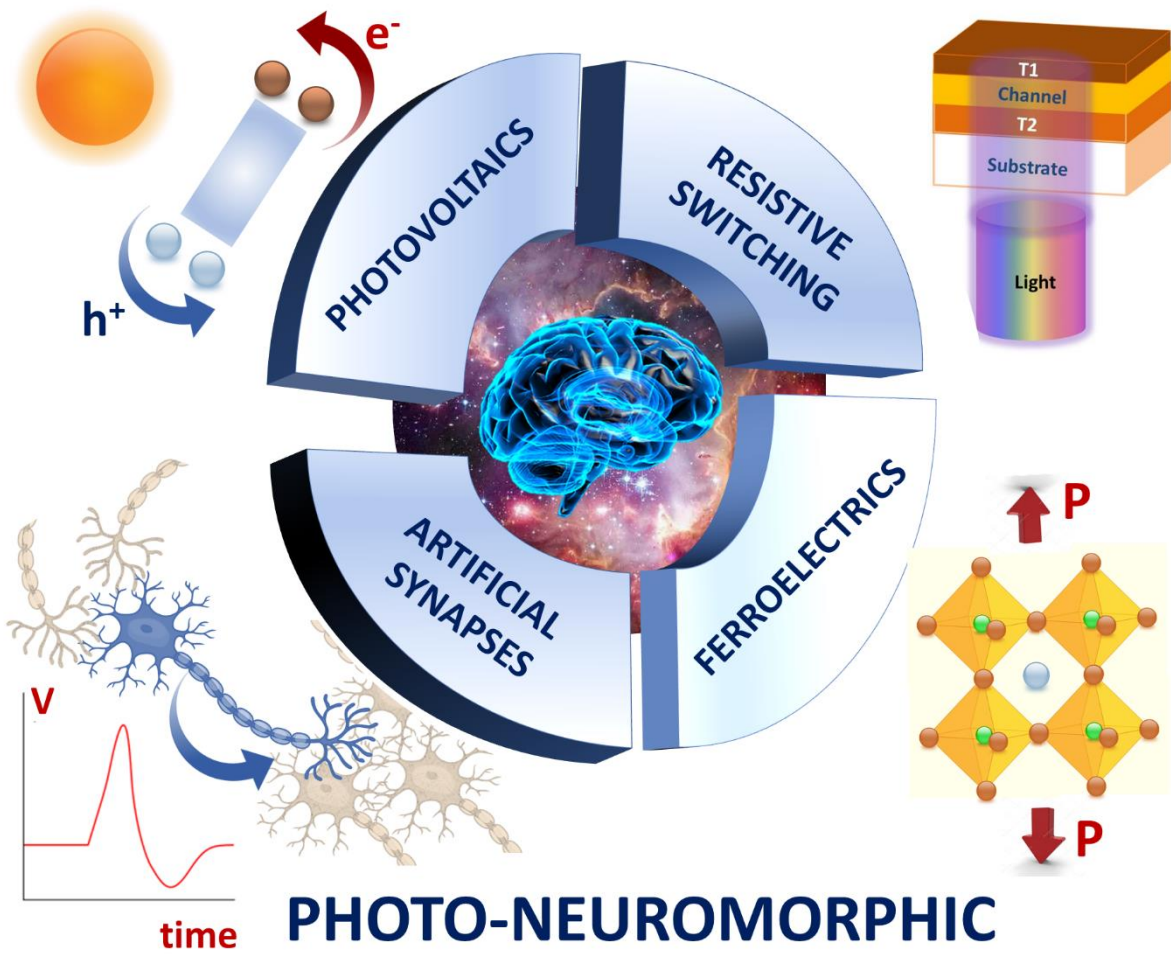
Amador Pérez-Tomás*

Catalan Institute of Nanoscience and Nanotechnology (ICN2), CSIC and the Barcelona Institute of Science and Technology, Barcelona, Spain
E-mail: amador.perez@icn2.cat

Title: Functional Oxides for Photo-Neuromorphic Engineering: towards a Solar Brain.

ToC figure:

FUNCTIONAL OXIDE THIN-FILMS

PHOTO-NEUROMORPHIC

References

[1]   W. Aguilar, G. Santamaría-Bonfil, T. Froese, C. Gershenson, *Frontiers in Robotics and AI* **2014**, *1*, 8. doi: 10.3389/frobt.2014.00008
[2]   Y. Bai, H. Jantunen, J. Juuti, *Advanced Materials* **2018**, *30*, 1707271.
[3]   X. Pu, W. Hu, Z. L. Wang, *Small* **2018**, *14*, 1702817.
[4]   Q. Zheng, B. Shi, Z. Li, Z. L. Wang, *Advanced Science* **2017**, *4*, 1700029.
[5]   A. A. Khan, A. Mahmud, D. Ban, *IEEE Transactions on Nanotechnology* **2019**, *18*, 21-36.
[6]   M. A. Green, *Nature Energy* **2016**, *1*, 15015.
[7]   C. J. Traverse, R. Pandey, M. C. Barr, R. R. Lunt, *Nature Energy* **2017**, *2*, 849-860.
[8]   S. Chandrasekaran, C. Bowen, J. Roscow, Y. Zhang, D. K. Dang, E. J. Kim, R. D. K. Misra, L. Deng, J. S. Chung, S. H. Hur, *Physics Reports* **2019**, *792*, 1-33.
[9]   G. Zhang, M. Li, H. Li, Q. Wang, S. Jiang, *Energy Technology* **2018**, *6*, 791-812.
[10]   X. Zhang, J. Grajal, J. L. Vazquez-Roy, U. Radhakrishna, X. Wang, W. Chern, L. Zhou, Y. Lin, P.-C. Shen, X. Ji, X. Ling, A. Zubair, Y. Zhang, H. Wang, M. Dubey, J. Kong, M. Dresselhaus, T. Palacios, *Nature* **2019**, *566*, 368-372.
[11]   P. Kamalinejad, C. Mahapatra, Z. Sheng, S. Mirabbasi, V. C. M. Leung, Y. L. Guan, *IEEE Communications Magazine* **2015**, *53*, 102-108.
[12]   M. Haras, T. Skotnicki, *Nano Energy* **2018**, *54*, 461-476.
[13]   S. Twaha, J. Zhu, Y. Yan, B. Li, *Renewable and Sustainable Energy Reviews* **2016**, *65*, 698-726.
[14]   Our civilization use secondary forms of energy that derive from the sun, including fossil fuels, which would not be present if the sun could not play a role in photosynthesis to encourage plant growth. The sun light also is the prominent source of renewable energy. The amount of solar energy available (22,000 terawatts (TW) or 350,000,000 TW/h annual) each year dwarfs supplies of any other source of power, including total reserves of all the fossil fuels on Earth and is more than enough, in theory, to cover the planet requirements (~50 TW by 2050). See e.g. http://www.sandia.gov/;   http://www.bp.com/en/global/corporate/energy-economics/statistical-review-of-world-energy.html Solar FAQs, Statistical Review of World Energy (**2017**).
[15]   S. Salahuddin, K. Ni, S. Datta, *Nature Electronics* **2018**, *1*, 442-450.
[16]   D. Ielmini, H. S. P. Wong, *Nature Electronics* **2018**, *1*, 333-343.
[17]   Y. Zi, Z. L. Wang, *APL Materials* **2017**, *5*, 074103.
[18]   S. D. Ha, S. Ramanathan, *Journal of Applied Physics* **2011**, *110*.
[19]   D. Kuzum, S. Yu, H. S. Philip Wong, *Nanotechnology* **2013**, *24*, 382001.
[20]   S. Soman, jayadeva, M. Suri, *Big Data Analytics* **2016**, *1*, 15.
[21]   D. Ielmini, *Microelectronic Engineering* **2018**, *190*, 44-53.
[22]   X. Hong, D. J. Loy, P. A. Dananjaya, F. Tan, C. Ng, W. Lew, *J Mater Sci* **2018**, *53*, 8720-8746.
[23]   M. Pfeiffer, T. Pfeil, *Frontiers in neuroscience* **2018**, *12*, 774-774.
[24]   J. d. Valle, J. G. Ramírez, M. J. Rozenberg, I. K. Schuller, *Journal of Applied Physics* **2018**, *124*, 211101.
[25]   M. Ziegler, C. Wenger, E. Chicca, H. Kohlstedt, *Journal of Applied Physics* **2018**, *124*, 152003.
[26]   D. S. Jeong, *Journal of Applied Physics* **2018**, *124*, 152002.
[27]   S. Pecqueur, D. Vuillaume, F. Alibart, *Journal of Applied Physics* **2018**, *124*, 151902.
[28]   S. Fukami, H. Ohno, *Journal of Applied Physics* **2018**, *124*, 151904.

[29]   J. v. Neumann, *The computer and the brain*, Yale University Press, **1958**.

[30]   S. Yu, B. Gao, Z. Fang, H. Yu, J. Kang, H. S. P. Wong, *Frontiers in neuroscience* **2013**, *7*, 186-186.

[31]   B. V. Benjamin, P. Gao, E. McQuinn, S. Choudhary, A. R. Chandrasekaran, J. Bussat, R. Alvarez-Icaza, J. V. Arthur, P. A. Merolla, K. Boahen, *Proceedings of the IEEE* **2014**, *102*, 699-716.

[32]   T. Ohno, T. Hasegawa, T. Tsuruoka, K. Terabe, J. K. Gimzewski, M. Aono, *Nature Materials* **2011**, *10*, 591.

[33]   J. J. Yang, D. B. Strukov, D. R. Stewart, *Nature Nanotechnology* **2012**, *8*, 13.

[34]   R. Kötter, C. Breslin, A. O'Lenskie, *Philosophical Transactions of the Royal Society of London. Series B: Biological Sciences* **2001**, *356*, 1249-1258.

[35]   F. Pan, S. Gao, C. Chen, C. Song, F. Zeng, *Materials Science and Engineering: R: Reports* **2014**, *83*, 1-59.

[36]   T. Serrano-Gotarredona, T. Masquelier, T. Prodromakis, G. Indiveri, B. Linares-Barranco, *Frontiers in Neuroscience* **2013**, *7*, 2.

[37]   L. M. Krauss, *Edge* **2015**, *https://www.edge.org/response-detail/26163*.

[38]   R. Gray, *http://www.bbc.com/future/story/20170313-the-biggest-energy-challenges-facing-humanity* **2017**.

[39]   Y. K. T. a. S. K. Panda, in *Sustainable Wireless Sensor Networks, Vol. Chapter 2*, IntechOpen, Rijeka, **2010**, pp. 15-43.

[40]   A. Čolaković, M. Hadžialić, *Computer Networks* **2018**, *144*, 17-39.

[41]   K. Qian, V. C. Nguyen, T. Chen, P. S. Lee, *Journal of Materials Chemistry C* **2016**, *4*, 9637-9645.

[42]   B.-Y. Kim, W.-H. Lee, H.-G. Hwang, D.-H. Kim, J.-H. Kim, S.-H. Lee, S. Nahm, *Advanced Functional Materials* **2016**, *26*, 5211-5221.

[43]   B.-Y. Kim, H.-G. Hwang, J.-U. Woo, W.-H. Lee, T.-H. Lee, C.-Y. Kang, S. Nahm, *Npg Asia Materials* **2017**, *9*, e381.

[44]   Y. Sun, X. Zheng, X. Yan, Q. Liao, S. Liu, G. Zhang, Y. Li, Y. Zhang, *ACS Applied Materials & Interfaces* **2017**, *9*, 43822-43829.

[45]   S. B. Laughlin, R. R. de Ruyter van Steveninck, J. C. Anderson, *Nature Neuroscience* **1998**, *1*, 36.

[46]   M. Lee, W. Lee, S. Choi, J.-W. Jo, J. Kim, S. K. Park, Y.-H. Kim, *Advanced Materials* **2017**, *29*, 1700951.

[47]   Z. L. Wang, G. Zhu, Y. Yang, S. Wang, C. Pan, *Materials Today* **2012**, *15*, 532-543.

[48]   Z. L. Wang, W. Wu, *Angewandte Chemie International Edition* **2012**, *51*, 11700-11721.

[49]   J. Briscoe, S. Dunn, *Nano Energy* **2015**, *14*, 15-29.

[50]   F. R. Fan, W. Tang, Z. L. Wang, *Advanced Materials* **2016**, *28*, 4283-4305.

[51]   A. Pérez-Tomás, A. Mingorance, D. Tanenbaum, M. Lira-Cantú, *Chapter 8 - Metal Oxides in Photovoltaics: All-Oxide, Ferroic, and Perovskite Solar Cells* in *The Future of Semiconductor Oxides in Next-Generation Solar Cells* (Ed.: M. Lira-Cantu), Elsevier, **2018**, pp. 267-356.

[52]   Y. Wu, T. van Ree, in *Metal Oxides in Energy Technologies* (Ed.: Y. Wu), Elsevier, **2018**, pp. 1-16.

[53]   N. Tsuda, *Electronic Conduction in Oxides*, Springer, **2000**.

[54]   S. M. Sze, K. K. Ng, *Physics of semiconductor devices*, Wiley-Interscience, Hoboken, N.J., **2007**.

[55]   D. Ginley, H. Hosono, D. C. Paine (Ed.), Handbook of Transparent Conductors., *Springer US* **2011**.

[56]   X. Yu, T. J. Marks, A. Facchetti, *Nat Mater* **2016**, *15*, 383-396.

[57]   A. E. Delahoy, S. Guo, in *Handbook of Photovoltaic Science and Engineering*, John Wiley & Sons, Ltd, **2011**, pp. 716-796.

[58]   R. M. Pasquarelli, D. S. Ginley, R. O'Hayre, *Chemical Society Reviews* **2011**, *40*, 5406-5441.

[59]   S. Rühle, A. Y. Anderson, H.-N. Barad, B. Kupfer, Y. Bouhadana, E. Rosh-Hodesh, A. Zaban, *The Journal of Physical Chemistry Letters* **2012**, *3*, 3755-3764.

[60]   IGZO, *https://www.sharpsma.com/es/igzo* **2019**.

[61]   W. Ouyang, F. Teng, J.-H. He, X. Fang, *Advanced Functional Materials* **2019**, *0*, 1807672.

[62]   A. Pérez-Tomás, E. Chikoidze, M. R. Jennings, S. A. O. Russell, F. H. Teherani, P. Bove, E. V. Sandana, D. J. Rogers, *Wide and ultra-wide bandgap oxides: where paradigm-shift photovoltaics meets transparent power electronics, Vol. 10533*, SPIE, **2018**. Proc. SPIE 10533, Oxide-based Materials and Devices IX, 105331Q (6 March 2018); doi: 10.1117/12.2302576; https://doi.org/10.1117/12.2302576

[63]   A. Pérez-Tomás, M. Lodzinski, O. J. Guy, M. R. Jennings, M. Placidi, J. Llobet, P. M. Gammon, M. C. Davis, J. A. Covington, S. E. Burrows, P. A. Mawby, *Applied Physics Letters* **2009**, *94*, 103510.

[64]   A. Pérez-Tomás, A. Fontserè, M. R. Jennings, P. M. Gammon, *Materials Science in Semiconductor Processing* **2013**, *16*, 1336-1345.

[65]   A. Liu, H. Zhu, H. Sun, Y. Xu, Y.-Y. Noh, *Advanced Materials* **2018**, *30*, 1706364.

[66]   A. Fontserè, A. Pérez-Tomás, V. Banu, P. Godignon, J. Millán, H. D. Vleeschouwer, J. M. Parsey, P. Moens, in *2012 24th International Symposium on Power Semiconductor Devices and ICs*, **2012**, pp. 37-40.

[67]   S. M. Thomas, Y. K. Sharma, M. A. Crouch, C. A. Fisher, A. Perez-Tomas, M. R. Jennings, P. A. Mawby, *IEEE Journal of the Electron Devices Society* **2014**, *2*, 114-117.

[68]   A. Fontserè, A. Pérez-Tomás, M. Placidi, N. Baron, S. Chenot, J. C. Moreno, Y. Cordier, *ECS Solid State Letters* **2013**, *2*, P4-P7.

[69]   S. A. O. Russell, A. Pérez-Tomás, C. F. McConville, C. A. Fisher, D. P. Hamilton, P. A. Mawby, M. R. Jennings, *IEEE Journal of the Electron Devices Society* **2017**, *5*, 256-261.

[70]   T. W. Hickmott, *Journal of Applied Physics* **1962**, *33*, 2669-2682.

[71]   C. An, S. Haddad, W. Yi-Ching, F. Tzu-Ning, L. Zhida, S. Avanzino, S. Pangrle, M. Buynoski, M. Rathor, C. Wei, N. Tripsas, C. Bill, M. V. Buskirk, M. Taguchi, in *IEEE InternationalElectron Devices Meeting, 2005. IEDM Technical Digest.*, **2005**, pp. 746-749.

[72]   E. Janod, J. Tranchant, B. Corraze, M. Querré, P. Stoliar, M. Rozenberg, T. Cren, D. Roditchev, V. T. Phuoc, M.-P. Besland, L. Cario, *Advanced Functional Materials* **2015**, *25*, 6287-6305.

[73]   P. Zubko, S. Gariglio, M. Gabay, P. Ghosez, J.-M. Triscone, *Annual Review of Condensed Matter Physics* **2011**, *2*, 141-165.

[74]   J. M. Rondinelli, N. A. Spaldin, *Advanced Materials* **2011**, *23*, 3363-3381.

[75]   M. Coll, J. Fontcuberta, M. Althammer, M. Bibes, H. Boschker, A. Calleja, G. Cheng, M. Cuoco, R. Dittmann, B. Dkhil, I. El Baggari, M. Fanciulli, I. Fina, E. Fortunato, C. Frontera, S. Fujita, V. Garcia, S. T. B. Goennenwein, C. G. Granqvist, J. Grollier, R. Gross, A. Hagfeldt, G. Herranz, K. Hono, E. Houwman, M. Huijben, A. Kalaboukhov, D. J. Keeble, G. Koster, L. F. Kourkoutis, J. Levy, M. Lira-Cantu, J. L. MacManus-Driscoll, J. Mannhart, R. Martins, S. Menzel, T. Mikolajick, M. Napari, M. D. Nguyen, G. Niklasson, C. Paillard, S. Panigrahi, G. Rijnders, F. Sánchez, P. Sanchis, S. Sanna, D. G. Schlom, U. Schroeder, K. M. Shen, A. Siemon, M. Spreitzer, H. Sukegawa, R.

Tamayo, J. van den Brink, N. Pryds, F. M. Granozio, *Applied Surface Science* **2019**, *482*, 1-93.

[76]   R. Waser, M. Aono, *Nature Materials* **2007**, *6*, 833.

[77]   M. Imada, A. Fujimori, Y. Tokura, *Reviews of Modern Physics* **1998**, *70*, 1039-1263.

[78]   M. Dawber, K. M. Rabe, J. F. Scott, *Reviews of Modern Physics* **2005**, *77*, 1083-1130.

[79]   N. Setter, D. Damjanovic, L. Eng, G. Fox, S. Gevorgian, S. Hong, A. Kingon, H. Kohlstedt, N. Y. Park, G. B. Stephenson, I. Stolitchnov, A. K. Taganstev, D. V. Taylor, T. Yamada, S. Streiffer, *Journal of Applied Physics* **2006**, *100*, 051606.

[80]   J. S. Brockman, L. Gao, B. Hughes, C. T. Rettner, M. G. Samant, K. P. Roche, S. S. P. Parkin, *Nature Nanotechnology* **2014**, *9*, 453.

[81]   W. Shockley, H. J. Queisser, *Journal of Applied Physics* **1961**, *32*, 510-519.

[82]   Y. Xu, T. Gong, J. N. Munday, *Scientific Reports* **2015**, *5*, 13536.

[83]   V. M. Fridkin, A. A. Grekov, A. I. Rodin, *Ferroelectrics* **1982**, *43*, 99-108.

[84]   J. Kreisel, M. Alexe, P. A. Thomas, *Nature Materials* **2012**, *11*, 260.

[85]   J. Seidel, L. M. Eng, *Current Applied Physics* **2014**, *14*, 1083-1091.

[86]   J. E. Spanier, V. M. Fridkin, A. M. Rappe, A. R. Akbashev, A. Polemi, Y. Qi, Z. Gu, S. M. Young, C. J. Hawley, D. Imbrenda, G. Xiao, A. L. Bennett-Jackson, C. L. Johnson, *Nature Photonics* **2016**, *10*, 611.

[87]   A. Pérez-Tomás, M. Lira-Cantú, G. Catalan, *Advanced Materials* **2016**, *28*, 9644-9647.

[88]   L. Z. Tan, F. Zheng, S. M. Young, F. Wang, S. Liu, A. M. Rappe, *Npj Computational Materials* **2016**, *2*, 16026.

[89]   A. Pérez-Tomás, A. Lima, Q. Billon, I. Shirley, G. Catalan, M. Lira-Cantú, *Advanced Functional Materials* **2018**, *28*, 1707099.

[90]   A. Pérez-Tomas, H. Xie, Z. Wang, H.-S. Kim, I. Shirley, S.-H. Turren-Cruz, A. Morales-Melgares, B. Saliba, D. Tanenbaum, M. Saliba, S. M. Zakeeruddin, M. Gratzel, A. Hagfeldt, M. Lira-Cantu, *Sustainable Energy & Fuels* **2019**, *3*, 382-389.

[91]   A. Tebano, E. Fabbri, D. Pergolesi, G. Balestrino, E. Traversa, *ACS Nano* **2012**, *6*, 1278-1283.

[92]   M. C. Tarun, F. A. Selim, M. D. McCluskey, *Physical Review Letters* **2013**, *111*, 187403.

[93]   A. Bera, H. Peng, J. Lourembam, Y. Shen, X. W. Sun, T. Wu, *Advanced Functional Materials* **2013**, *23*, 4977-4984.

[94]   A. Bhatnagar, Y. H. Kim, D. Hesse, M. Alexe, *Nano Letters* **2014**, *14*, 5224-5228.

[95]   F. S. Chen, J. T. LaMacchia, D. B. Fraser, *Applied Physics Letters* **1968**, *13*, 223-225.

[96]   C. E. Land, *IEEE Transactions on Electron Devices* **1979**, *26*, 1143-1147.

[97]   Y. Kong, S. Liu, J. Xu, *Materials* **2012**, *5*, 1954-1971.

[98]   S. Abel, T. Stöferle, C. Marchiori, C. Rossel, M. D. Rossell, R. Erni, D. Caimi, M. Sousa, A. Chelnokov, B. J. Offrein, J. Fompeyrine, *Nature Communications* **2013**, *4*, 1671.

[99]   S. Abel, F. Eltes, J. E. Ortmann, A. Messner, P. Castera, T. Wagner, D. Urbonas, A. Rosa, A. M. Gutierrez, D. Tulli, P. Ma, B. Baeuerle, A. Josten, W. Heni, D. Caimi, L. Czornomaz, A. A. Demkov, J. Leuthold, P. Sanchis, J. Fompeyrine, *Nature Materials* **2019**, *18*, 42-47.

[100]   B. Parida, S. Iniyan, R. Goic, *Renewable and Sustainable Energy Reviews* **2011**, *15*, 1625-1636.

[101]   A. Polman, M. Knight, E. C. Garnett, B. Ehrler, W. C. Sinke, *Science* **2016**, *352*, aad4424.

[102]   S. Rühle, *Solar Energy* **2016**, *130*, 139-147.

[103]   V. M. Fridkin, *Crystallogr. Rep.* **2001**, *46*, 654-658.

[104]   S. M. Young, A. M. Rappe, *Physical Review Letters* **2012**, *109*, 116601.

[105] P. Olbrich, S. A. Tarasenko, C. Reitmaier, J. Karch, D. Plohmann, Z. D. Kvon, S. D. Ganichev, *Physical Review B* **2009**, *79*, 121302.
[106] V. I. Belinicher, B. I. Sturman, *Ferroelectrics* **1988**, *83*, 29-34.
[107] A. M. Burger, R. Agarwal, A. Aprelev, E. Schruba, A. Gutierrez-Perez, V. M. Fridkin, J. E. Spanier, *Science Advances* **2019**, *5*, eaau5588.
[108] R. von Baltz, W. Kraut, *Physical Review B* **1981**, *23*, 5590-5596.
[109] L. Zhu, Z. L. Wang, *Advanced Functional Materials*, *0*, 1808214.
[110] Y. Zhang, W. Jie, P. Chen, W. Liu, J. Hao, *Advanced Materials* **2018**, *30*, 1707007.
[111] M.-M. Yang, D. J. Kim, M. Alexe, *Science* **2018**, *360*, 904-907.
[112] T. D. Nguyen, S. Mao, Y.-W. Yeh, P. K. Purohit, M. C. McAlpine, *Advanced Materials* **2013**, *25*, 946-974.
[113] F. Oba, Y. Kumagai, *Applied Physics Express* **2018**, *11*, 060101.
[114] M. A. Green, *J Mater Sci: Mater Electron* **2007**, *18*, 15-19.
[115] E. Yablonovitch, O. D. Miller, S. R. Kurtz, in *2012 38th IEEE Photovoltaic Specialists Conference*, **2012**, pp. 001556-001559.
[116] https://www.nrel.gov/pv/, **2019**
[117] T. Fujibayashi, T. Matsui, M. Kondo, *Applied Physics Letters* **2006**, *88*.
[118] G. Yue, L. Sivec, J. M. Owens, B. Yan, J. Yang, S. Guha, *Applied Physics Letters* **2009**, *95*, 263501.
[119] M. Morales-Masis, S. De Wolf, R. Woods-Robinson, J. W. Ager, C. Ballif, *Advanced Electronic Materials* **2017**, *3*, 1600529.
[120] C. Guillén, J. Herrero, *Thin Solid Films* **2011**, *520*, 1-17.
[121] D. Wang, Y. Zhang, X. Lu, Z. Ma, C. Xie, Z. Zheng, *Chemical Society Reviews* **2018**, *47*, 4611-4641.
[122] Q. Huang, Y. Zhu, *Advanced Materials Technologies*, **2019**, 4, 1800546.
[123] K. L. Chopra, S. Major, D. K. Pandya, *Thin Solid Films* **1983**, *102*, 1-46.
[124] M. Tadatsugu, *Semiconductor Science and Technology* **2005**, *20*, S35.
[125] K. Ellmer, *Nat Photon* **2012**, *6*, 809-817.
[126] K. S. Kim, Y. Zhao, H. Jang, S. Y. Lee, J. M. Kim, K. S. Kim, J.-H. Ahn, P. Kim, J.-Y. Choi, B. H. Hong, *Nature* **2009**, *457*, 706-710.
[127] S. R. Forrest, *Nature* **2004**, *428*, 911-918.
[128] H. Kang, S. Jung, S. Jeong, G. Kim, K. Lee, *Nature Communications* **2015**, *6*, 6503.
[129] X. Zhang, L. Zhang, J. D. Perkins, A. Zunger, *Physical Review Letters* **2015**, *115*, 176602.
[130] E. Chikoidze, D. J. Rogers, F. H. Teherani, C. Rubio, G. Sauthier, H. J. Von Bardeleben, T. Tchelidze, C. Ton-That, A. Fellous, P. Bove, E. V. Sandana, Y. Dumont, A. Perez-Tomas, *Materials Today Physics* **2019**, *8*, 10-17.
[131] K. Ellmer, R. Mientus, *Thin Solid Films* **2008**, *516*, 4620-4627.
[132] H. Hosono, K. Ueda, in *Springer Handbook of Electronic and Photonic Materials* (Eds.: S. Kasap, P. Capper), Springer International Publishing, Cham, **2017**, pp. 1-1.
[133] Z. Wang, P. K. Nayak, J. A. Caraveo-Frescas, H. N. Alshareef, *Advanced Materials* **2016**, *28*, 3831-3892.
[134] A. Liu, H. Zhu, Y.-Y. Noh, *Materials Science and Engineering: R: Reports* **2019**, *135*, 85-100.
[135] M. Grundmann, F. Klüpfel, R. Karsthof, P. Schlupp, F.-L. Schein, D. Splith, C. Yang, S. Bitter, H. von Wenckstern, *Journal of Physics D: Applied Physics* **2016**, *49*, 213001.
[136] H. Yanagi, K. Ueda, H. Ohta, M. Orita, M. Hirano, H. Hosono, *Solid State Communications* **2001**, *121*, 15-17.
[137] M. Graužinytė, S. Goedecker, J. A. Flores-Livas, *Physical Review Materials* **2018**, *2*, 104604.

[138] E. Chikoidze, A. Fellous, A. Perez-Tomas, G. Sauthier, T. Tchelidze, C. Ton-That, T. T. Huynh, M. Phillips, S. Russell, M. Jennings, B. Berini, F. Jomard, Y. Dumont, *Materials Today Physics* **2017**, *3*, 118-126.

[139] C. P. Liu, K. O. Egbo, C. Y. Ho, J. A. Zapien, W. Walukiewicz, K. M. Yu, *Physical Review Applied* **2019**, *11*, 014019.

[140] A. Samizo, N. Kikuchi, Y. Aiura, K. Nishio, K. Mibu, *Chemistry of Materials* **2018**, *30*, 8221-8225.

[141] T. Arai, S. Iimura, J. Kim, Y. Toda, S. Ueda, H. Hosono, *Journal of the American Chemical Society* **2017**, *139*, 17175-17180.

[142] K. Bädeker, *Annalen der Physik* **1907**, *327*, 749-766.

[143] S. C. Dixon, D. O. Scanlon, C. J. Carmalt, I. P. Parkin, *Journal of Materials Chemistry C* **2016**, *4*, 6946-6961.

[144] I. A. Rauf, *Materials Letters* **1993**, *18*, 123-127.

[145] H. Ohta, M. Orita, M. Hirano, H. Tanji, H. Kawazoe, H. Hosono, *Applied Physics Letters* **2000**, *76*, 2740-2742.

[146] D. S. Bhachu, M. R. Waugh, K. Zeissler, W. R. Branford, I. P. Parkin, *Chemistry – A European Journal* **2011**, *17*, 11613-11621.

[147] K. Ellmer, *Journal of Physics D: Applied Physics* **2001**, *34*, 3097.

[148] H. Agura, A. Suzuki, T. Matsushita, T. Aoki, M. Okuda, *Thin Solid Films* **2003**, *445*, 263-267.

[149] E. L. Papadopoulou, M. Varda, K. Kouroupis-Agalou, M. Androulidaki, E. Chikoidze, P. Galtier, G. Huyberechts, E. Aperathitis, *Thin Solid Films* **2008**, *516*, 8141-8145.

[150] R. S. Ajimsha, A. K. Das, P. Misra, M. P. Joshi, L. M. Kukreja, R. Kumar, T. K. Sharma, S. M. Oak, *Journal of Alloys and Compounds* **2015**, *638*, 55-58.

[151] Y. Furubayashi, T. Hitosugi, Y. Yamamoto, K. Inaba, G. Kinoda, Y. Hirose, T. Shimada, T. Hasegawa, *Applied Physics Letters* **2005**, *86*, 252101.

[152] H. Taro, F. Yutaka, U. Atsuki, I. Kinnosuke, I. Kazuhisa, H. Yasushi, K. Go, Y. Yukio, S. Toshihiro, H. Tetsuya, *Japanese Journal of Applied Physics* **2005**, *44*, L1063.

[153] X. Wu, W. P. Mulligan, T. J. Coutts, *Thin Solid Films* **1996**, *286*, 274-276.

[154] D. M. Meysing, J. M. Burst, W. L. Rance, M. O. Reese, T. M. Barnes, T. A. Gessert, C. A. Wolden, *Solar Energy Materials and Solar Cells* **2013**, *117*, 300-305.

[155] X. Wu, T. J. Coutts, W. P. Mulligan, *Journal of Vacuum Science & Technology A* **1997**, *15*, 1057-1062.

[156] T. J. Coutts, D. L. Young, X. Li, W. P. Mulligan, X. Wu, *Journal of Vacuum Science & Technology A* **2000**, *18*, 2646-2660.

[157] J. H. Ko, I. H. Kim, D. Kim, K. S. Lee, T. S. Lee, J. H. Jeong, B. Cheong, Y. J. Baik, W. M. Kim, *Thin Solid Films* **2006**, *494*, 42-46.

[158] H. Tetsuka, Y. J. Shan, K. Tezuka, H. Imoto, K. Wasa, *Journal of Vacuum Science & Technology A* **2006**, *24*, L4-L6.

[159] H. Tetsuka, Y. J. Shan, K. Tezuka, H. Imoto, K. Wasa, *Journal of Materials Research* **2011**, *20*, 2256-2260.

[160] A. Prakash, P. Xu, A. Faghaninia, S. Shukla, J. W. Ager Iii, C. S. Lo, B. Jalan, *Nature Communications* **2017**, *8*, 15167.

[161] Q. Liu, J. Dai, X. Zhang, G. Zhu, Z. Liu, G. Ding, *Thin Solid Films* **2011**, *519*, 6059-6063.

[162] B. Erina, K. Daisuke, Y. Yasuhiro, H. Mitsutaka, K. Hiroki, K. Yoshihiko, S. Yuichi, *Journal of Physics D: Applied Physics* **2015**, *48*, 455106.

[163] D. Olaya, F. Pan, C. T. Rogers, J. C. Price, *Applied Physics Letters* **2002**, *80*, 2928-2930.

[164] H. H. Wang, F. Chen, S. Y. Dai, T. Zhao, H. B. Lu, D. F. Cui, Y. L. Zhou, Z. H. Chen, G. Z. Yang, *Applied Physics Letters* **2001**, *78*, 1676-1678.

[165] M. Tadatsugu, S. Hideo, T. Shinzo, S. Hirotoshi, *Japanese Journal of Applied Physics* **1994**, *33*, L1693.

[166] M. A. Riza, M. A. Ibrahim, U. C. Ahamefula, M. A. Mat Teridi, N. Ahmad Ludin, S. Sepeai, K. Sopian, *Solar Energy* **2016**, *137*, 371-378.

[167] R. P. Wang, C. J. Tao, *Journal of Crystal Growth* **2002**, *245*, 63-66.

[168] L. Zhang, Y. Zhou, L. Guo, W. Zhao, A. Barnes, H.-T. Zhang, C. Eaton, Y. Zheng, M. Brahlek, H. F. Haneef, N. J. Podraza, M. H. W. Chan, V. Gopalan, K. M. Rabe, R. Engel-Herbert, *Nat Mater* **2016**, *15*, 204-210.

[169] H. Hosono, *Journal of Non-Crystalline Solids* **2006**, *352*, 851-858.

[170] D. Solís-Cortés, E. Navarrete-Astorga, J. L. Costa-Krämer, J. Salguero-Fernandez, R. Schrebler, D. Leinen, E. A. Dalchiele, J. R. Ramos-Barrado, F. Martín, *Ceramics International* **2019**, *45*, 5577-5587.

[171] E. Fortunato, P. Barquinha, R. Martins, *Advanced Materials* **2012**, *24*, 2945-2986.

[172] L. Petti, N. Münzenrieder, C. Vogt, H. Faber, L. Büthe, G. Cantarella, F. Bottacchi, T. D. Anthopoulos, G. Tröster, *Applied Physics Reviews* **2016**, *3*, 021303.

[173] J. Sheng, H.-J. Jeong, K.-L. Han, T. Hong, J.-S. Park, *Journal of Information Display* **2017**, *18*, 159-172.

[174] K. Nomura, H. Ohta, A. Takagi, T. Kamiya, M. Hirano, H. Hosono, *Nature* **2004**, *432*, 488-492.

[175] F. Shao, Q. Wan, *Journal of Physics D: Applied Physics* **2019**, *52*, 143002.

[176] G. Hautier, A. Miglio, G. Ceder, G.-M. Rignanese, X. Gonze, *Nature Communications* **2013**, *4*, 2292.

[177] J. B. Varley, A. Miglio, V.-A. Ha, M. J. van Setten, G.-M. Rignanese, G. Hautier, *Chemistry of Materials* **2017**, *29*, 2568-2573.

[178] H. L. Z. Kelvin, X. Kai, G. B. Mark, G. E. Russell, *Journal of Physics: Condensed Matter* **2016**, *28*, 383002.

[179] B. S. Li, K. Akimoto, A. Shen, *Journal of Crystal Growth* **2009**, *311*, 1102-1105.

[180] E. Ruiz, S. Alvarez, P. Alemany, R. A. Evarestov, *Physical Review B* **1997**, *56*, 7189-7196.

[181] J. M. Zuo, M. Kim, M. O'Keeffe, J. C. H. Spence, *Nature* **1999**, *401*, 49-52.

[182] Y. Ogo, H. Hiramatsu, K. Nomura, H. Yanagi, T. Kamiya, M. Hirano, H. Hosono, *Applied Physics Letters* **2008**, *93*, 032113.

[183] E. Fortunato, R. Barros, P. Barquinha, V. Figueiredo, S.-H. K. Park, C.-S. Hwang, R. Martins, *Applied Physics Letters* **2010**, *97*, 052105.

[184] J. A. Caraveo-Frescas, P. K. Nayak, H. A. Al-Jawhari, D. B. Granato, U. Schwingenschlögl, H. N. Alshareef, *ACS Nano* **2013**, *7*, 5160-5167.

[185] A. Bhatia, G. Hautier, T. Nilgianskul, A. Miglio, J. Sun, H. J. Kim, K. H. Kim, S. Chen, G.-M. Rignanese, X. Gonze, J. Suntivich, *Chemistry of Materials* **2016**, *28*, 30-34.

[186] H. Sato, T. Minami, S. Takata, T. Yamada, *Thin Solid Films* **1993**, *236*, 27-31.

[187] S. C. Chen, C. K. Wen, T. Y. Kuo, W. C. Peng, H. C. Lin, *Thin Solid Films* **2014**, *572*, 51-55.

[188] Y. Huang, Q. Zhang, J. Xi, Z. Ji, *Applied Surface Science* **2012**, *258*, 7435-7439.

[189] J. Y. Zhang, W. W. Li, R. L. Z. Hoye, J. L. MacManus-Driscoll, M. Budde, O. Bierwagen, L. Wang, Y. Du, M. J. Wahila, L. F. J. Piper, T. L. Lee, H. J. Edwards, V. R. Dhanak, K. H. L. Zhang, *Journal of Materials Chemistry C* **2018**, *6*, 2275-2282.

[190] G. Fu, X. Wen, S. Xi, Z. Chen, W. Li, J.-Y. Zhang, A. Tadich, R. Wu, D.-C. Qi, Y. Du, J. Cheng, K. H. L. Zhang, *Chemistry of Materials* **2019**, *31*, 419-428.

[191] W. Chen, F.-Z. Liu, X.-Y. Feng, A. B. Djurišić, W. K. Chan, Z.-B. He, *Advanced Energy Materials* **2017**, *7*, 1700722.

[192] A. Catellani, A. Calzolari, *Materials* **2017**, *10*, 332.

[193] Z. Ye, H. He, L. Jiang, *Nano Energy* **2018**, *52*, 527-540.

[194] H. Kawazoe, M. Yasukawa, H. Hyodo, M. Kurita, H. Yanagi, H. Hosono, *Nature* **1997**, *389*, 939-942.

[195] K. Ueda, T. Hase, H. Yanagi, H. Kawazoe, H. Hosono, H. Ohta, M. Orita, M. Hirano, *Journal of Applied Physics* **2001**, *89*, 1790-1793.

[196] R. Nagarajan, A. D. Draeseke, A. W. Sleight, J. Tate, *Journal of Applied Physics* **2001**, *89*, 8022-8025.

[197] M. Snure, A. Tiwari, *Applied Physics Letters* **2007**, *91*, 092123.

[198] A. Kudo, H. Yanagi, H. Hosono, H. Kawazoe, *Applied Physics Letters* **1998**, *73*, 220-222.

[199] E. Chikoidze, M. Boshta, M. Gomaa, T. Tchelidze, D. Daraselia, D. Japaridze, A. Shengelaya, Y. Dumont, M. Neumann-Spallart, *Journal of Physics D: Applied Physics* **2016**, *49*, 205107.

[200] J. Shook, L. M. Scolfaro, P. D. Borges, W. J. Geerts, *Solid State Sciences* **2019**, *88*, 48-56.

[201] E. Norton, L. Farrell, A. Zhussupbekova, D. Mullarkey, D. Caffrey, D. T. Papanastasiou, D. Oser, D. Bellet, I. V. Shvets, K. Fleischer, *AIP Advances* **2018**, *8*, 085013.

[202] P. Lunca-Popa, J. Afonso, P. Grysan, J. Crêpellière, R. Leturcq, D. Lenoble, *Scientific Reports* **2018**, *8*, 7216.

[203] P. Lunca Popa, J. Crêpellière, P. Nukala, R. Leturcq, D. Lenoble, *Applied Materials Today* **2017**, *9*, 184-191.

[204] M. Ahmadi, M. Asemi, M. Ghanaatshoar, *Applied Physics Letters* **2018**, *113*, 242101.

[205] M. Dekkers, G. Rijnders, D. H. A. Blank, *Applied Physics Letters* **2007**, *90*, 021903.

[206] K. H. L. Zhang, Y. Du, A. Papadogianni, O. Bierwagen, S. Sallis, L. F. J. Piper, M. E. Bowden, V. Shutthanandan, P. V. Sushko, S. A. Chambers, *Advanced Materials* **2015**, *27*, 5191-5195.

[207] S. Dabaghmanesh, N. Sarmadian, E. C. Neyts, B. Partoens, *Physical Chemistry Chemical Physics* **2017**, *19*, 22870-22876.

[208] L. Hu, R. Wei, J. Yan, D. Wang, X. Tang, X. Luo, W. Song, J. Dai, X. Zhu, C. Zhang, Y. Sun, *Advanced Electronic Materials* **2018**, *4*, 1700476.

[209] H. Hiramatsu, K. Ueda, H. Ohta, M. Hirano, T. Kamiya, H. Hosono, *Applied Physics Letters* **2003**, *82*, 1048-1050.

[210] H. Hiramatsu, K. Ueda, H. Ohta, M. Orita, M. Hirano, H. Hosono, *Thin Solid Films* **2002**, *411*, 125-128.

[211] N. Zhang, J. Sun, H. Gong, *Coatings* **2019**, *9*, 137.

[212] C. Guillén, J. Herrero, *Materials Research Bulletin* **2018**, *101*, 116-122.

[213] N. Sarmadian, R. Saniz, B. Partoens, D. Lamoen, *Scientific Reports* **2016**, *6*, 20446.

[214] N. Zhang, X. Liu, D. Shi, B. Tang, A. Annadi, H. Gong, *Materials Today Chemistry* **2018**, *10*, 79-89.

[215] H. Hiramatsu, K. Ueda, H. Ohta, M. Hirano, M. Kikuchi, H. Yanagi, T. Kamiya, H. Hosono, *Applied Physics Letters* **2007**, *91*, 012104.

[216] B. Williamson, G. Limburn, G.W. Watson, G. Hyett, D. Scanlon, *Computationally Driven Discovery of Layered Quinary Oxychalcogenide p-Type Transparent Conductors*, **2018**. ChemRxiv 2018, doi.org/10.26434/chemrxiv.7078205.v2

[217] M.-L. Liu, L.-B. Wu, F.-Q. Huang, L.-D. Chen, I.-W. Chen, *Journal of Applied Physics* **2007**, *102*, 116108.

[218] Z. Ran, X. Wang, Y. Li, D. Yang, X.-G. Zhao, K. Biswas, D. J. Singh, L. Zhang, *npj Computational Materials* **2018**, *4*, 14.

[219] S. Guo, Z. Zhu, X. Hu, W. Zhou, X. Song, S. Zhang, K. Zhang, H. Zeng, *Nanoscale* **2018**, *10*, 8397-8403.

[220] B. K. Meyer, A. Polity, D. Reppin, M. Becker, P. Hering, P. J. Klar, T. Sander, C. Reindl, J. Benz, M. Eickhoff, C. Heiliger, M. Heinemann, J. Bläsing, A. Krost, S. Shokovets, C. Müller, C. Ronning, *physica status solidi (b)* **2012**, *249*, 1487-1509.
[221] A. Živković, A. Roldan, N. H. de Leeuw, *Physical Review B* **2019**, *99*, 035154.
[222] A. Y. Anderson, Y. Bouhadana, H.-N. Barad, B. Kupfer, E. Rosh-Hodesh, H. Aviv, Y. R. Tischler, S. Rühle, A. Zaban, *ACS Combinatorial Science* **2014**, *16*, 53-65.
[223] S. Abbas, M. Kumar, D.-W. Kim, J. Kim, *Small* **2019**, *15*, 1804346.
[224] R. S. Weis, T. K. Gaylord, *Appl. Phys. A* **1985**, *37*, 191-203.
[225] B. Aurivillius, P. H. Fang, *Physical Review* **1962**, *126*, 893-896.
[226] L. E. Cross, *Ferroelectrics* **1987**, *76*, 241-267.
[227] L. B. Elena, *Russian Chemical Reviews* **1994**, *63*, 533.
[228] A. Peláiz-Barranco, Y. González-Abreu, *Journal of Advanced Dielectrics* **2013**, *03*, 1330003.
[229] I. Sullivan, B. Zoellner, P. A. Maggard, *Chemistry of Materials* **2016**, *28*, 5999-6016.
[230] S. Song, D. Kim, H. M. Jang, B. C. Yeo, S. S. Han, C. S. Kim, J. F. Scott, *Chemistry of Materials* **2017**, *29*, 7596-7603.
[231] J. Li, D. Chu, in *Multifunctional Photocatalytic Materials for Energy* (Eds.: Z. Lin, M. Ye, M. Wang), Woodhead Publishing, **2018**, pp. 49-78.
[232] W. H. Brattain, *Reviews of Modern Physics* **1951**, *23*, 203-212.
[233] H. Raebiger, S. Lany, A. Zunger, *Physical Review B* **2007**, *76*, 045209.
[234] G. K. Paul, Y. Nawa, H. Sato, T. Sakurai, K. Akimoto, *Applied Physics Letters* **2006**, *88*, 141901.
[235] A. Paracchino, J. C. Brauer, J.-E. Moser, E. Thimsen, M. Graetzel, *The Journal of Physical Chemistry C* **2012**, *116*, 7341-7350.
[236] Y. Nishi, T. Miyata, T. Minami, *Thin Solid Films* **2013**, *528*, 72-76.
[237] L.O. Grondahl, Unidirectional current-carrying device. **1927**, United States Patent US2017842A.
[238] L. O. Grondahl, P. H. Geiger, *Journal of the A.I.E.E.* **1927**, *46*, 215-222.
[239] L. C. Olsen, F. W. Addis, W. Miller, *Solar Cells* **1982**, *7*, 247-279.
[240] A. Mittiga, E. Salza, F. Sarto, M. Tucci, R. Vasanthi, *Applied Physics Letters* **2006**, *88*, 163502.
[241] M. Tadatsugu, N. Yuki, M. Toshihiro, *Applied Physics Express* **2016**, *9*, 052301.
[242] A. Paracchino, V. Laporte, K. Sivula, M. Grätzel, E. Thimsen, *Nat Mater* **2011**, *10*, 456-461.
[243] J. Li, Z. Mei, L. Liu, H. Liang, A. Azarov, A. Kuznetsov, Y. Liu, A. Ji, Q. Meng, X. Du, *Scientific Reports* **2014**, *4*, 7240.
[244] D. O. Scanlon, G. W. Watson, *The Journal of Physical Chemistry Letters* **2010**, *1*, 2582-2585.
[245] F. Biccari, C. Malerba, A. Mittiga, *Solar Energy Materials and Solar Cells* **2010**, *94*, 1947-1952.
[246] X.-M. Cai, X.-Q. Su, F. Ye, H. Wang, X.-Q. Tian, D.-P. Zhang, P. Fan, J.-T. Luo, Z.-H. Zheng, G.-X. Liang, V. A. L. Roy, *Applied Physics Letters* **2015**, *107*, 083901.
[247] W. Siripala, J. R. P. Jayakody, *Solar Energy Materials* **1986**, *14*, 23-27.
[248] W. Wang, D. Wu, Q. Zhang, L. Wang, M. Tao, *Journal of Applied Physics* **2010**, *107*, 123717.
[249] R. P. Wijesundera, L. K. A. D. D. S. Gunawardhana, W. Siripala, *Solar Energy Materials and Solar Cells* **2016**, *157*, 881-886.
[250] H. M. Wei, H. B. Gong, L. Chen, M. Zi, B. Q. Cao, *The Journal of Physical Chemistry C* **2012**, *116*, 10510-10515.
[251] Y.-K. Hsu, J.-R. Wu, M.-H. Chen, Y.-C. Chen, Y.-G. Lin, *Applied Surface Science* **2015**, *354, Part A*, 8-13.

[252] C. Zhu, M. J. Panzer, *ACS Applied Materials & Interfaces* **2015**, *7*, 5624-5628.

[253] G. E. Nezar, M. R. Hashim, M. C. Khaled, S. A. Mohammed, *Semiconductor Science and Technology* **2016**, *31*, 065001.

[254] C. M. McShane, K.-S. Choi, *Physical Chemistry Chemical Physics* **2012**, *14*, 6112-6118.

[255] F. Kazuya, O. Takeo, A. Tsuyoshi, *Applied Physics Express* **2013**, *6*, 086503.

[256] X. Chen, P. Lin, X. Yan, Z. Bai, H. Yuan, Y. Shen, Y. Liu, G. Zhang, Z. Zhang, Y. Zhang, *ACS Applied Materials & Interfaces* **2015**, *7*, 3216-3223.

[257] I. Masanobu, S. Tsutomu, M. Ko-Taro, I. Yuya, I. Minoru, T. Akimasa, *Journal of Physics D: Applied Physics* **2007**, *40*, 3326.

[258] H.-Y. Shiu, C.-M. Tsai, S.-Y. Chen, T.-R. Yew, *Journal of Materials Chemistry* **2011**, *21*, 17646-17650.

[259] T. Minami, T. Miyata, K. Ihara, Y. Minamino, S. Tsukada, *Thin Solid Films* **2006**, *494*, 47-52.

[260] Y. Ievskaya, R. L. Z. Hoye, A. Sadhanala, K. P. Musselman, J. L. MacManus-Driscoll, *Solar Energy Materials and Solar Cells* **2015**, *135*, 43-48.

[261] T. Minami, T. Miyata, Y. Nishi, *Solar Energy Materials and Solar Cells* **2016**, *147*, 85-93.

[262] Z. Duan, A. Du Pasquier, Y. Lu, Y. Xu, E. Garfunkel, *Solar Energy Materials and Solar Cells* **2012**, *96*, 292-297.

[263] K. P. Musselman, A. Wisnet, D. C. Iza, H. C. Hesse, C. Scheu, J. L. MacManus-Driscoll, L. Schmidt-Mende, *Advanced Materials* **2010**, *22*, E254-E258.

[264] J. Cui, U. J. Gibson, *The Journal of Physical Chemistry C* **2010**, *114*, 6408-6412.

[265] W. Jia, H. Dong, J. Zhao, S. Dang, Z. Zhang, T. Li, X. Liu, B. Xu, *Appl. Phys. A* **2012**, *109*, 751-756.

[266] Y. Luo, L. Wang, Y. Zou, X. Sheng, L. Chang, D. Yang, *Electrochemical and Solid-State Letters* **2011**, *15*, H34-H36.

[267] M. Pavan, S. Rühle, A. Ginsburg, D. A. Keller, H.-N. Barad, P. M. Sberna, D. Nunes, R. Martins, A. Y. Anderson, A. Zaban, E. Fortunato, *Solar Energy Materials and Solar Cells* **2015**, *132*, 549-556.

[268] L. Zhang, H. Sun, L. Xie, J. Lu, L. Zhang, S. Wu, X. Gao, X. Lu, J. Li, J.-M. Liu, *Nanoscale Research Letters* **2015**, *10*, 465.

[269] M. Abd-Ellah, J. P. Thomas, L. Zhang, K. T. Leung, *Solar Energy Materials and Solar Cells* **2016**, *152*, 87-93.

[270] aY. S. Lee, D. Chua, R. E. Brandt, S. C. Siah, J. V. Li, J. P. Mailoa, S. W. Lee, R. G. Gordon, T. Buonassisi, *Advanced Materials* **2014**, *26*, 4704-4710; bT. Minami, Y. Nishi, T. Miyata, *Thin Solid Films* **2013**, *549*, 65-69.

[271] M. Tadatsugu, N. Yuki, M. Toshihiro, *Applied Physics Express* **2015**, *8*, 022301.

[272] M. Tadatsugu, N. Yuki, M. Toshihiro, *Journal of Semiconductors* **2016**, *37*, 014002.

[273] T. Dimopoulos, A. Peić, P. Müllner, M. Neuschitzer, R. Resel, S. Abermann, M. Postl, E. J. W. List, S. Yakunin, W. Heiss, H. Brückl, *Journal of Renewable and Sustainable Energy* **2013**, *5*, 011205.

[274] S. Masudy-Panah, G. K. Dalapati, K. Radhakrishnan, A. Kumar, H. R. Tan, E. Naveen Kumar, C. Vijila, C. C. Tan, D. Chi, *Progress in Photovoltaics: Research and Applications* **2014**.

[275] M.-P. Saeid, K. Radhakrishnan, R. Tan Hui, Y. Ren, W. Ten It, D. Goutam Kumar, *Journal of Physics D: Applied Physics* **2016**, *49*, 375601.

[276] P. Wang, X. Zhao, B. Li, *Opt. Express* **2011**, *19*, 11271-11279.

[277] X. Zhao, P. Wang, Y. Gao, X. Xu, Z. Yan, N. Ren, *Materials Letters* **2014**, *132*, 409-412.

[278] aR. Bhardwaj, R. Barman, D. Kaur, *Materials Letters* **2016**, *185*, 230-234; bJ. Morasch, H. F. Wardenga, W. Jaegermann, A. Klein, *physica status solidi (a)* **2016**, *213*, 1615-1624.

[279] S. Masudy-Panah, K. Radhakrishnan, H. R. Tan, R. Yi, T. I. Wong, G. K. Dalapati, *Solar Energy Materials and Solar Cells* **2015**, *140*, 266-274.

[280] A. Bhaumik, A. Haque, P. Karnati, M. F. N. Taufique, R. Patel, K. Ghosh, *Thin Solid Films* **2014**, *572*, 126-133.

[281] aR. P. Wijesundera, *Semiconductor Science and Technology* **2010**, *25*, 045015; bJ. Charith, K. Vassilios, S. Withana, J. Sumedha, *Applied Physics Express* **2015**, *8*, 065503; cF.-P. Chen, G.-P. Jin, J.-Y. Su, X. Feng, *Journal of Applied Electrochemistry* **2016**, *46*, 379-388.

[282] S. Rühle, A. Y. Anderson, H. N. Barad, B. Kupfer, Y. Bouhadana, E. Rosh-Hodesh, A. Zaban, *Journal of Physical Chemistry Letters* **2012**, *3*, 3755-3764.

[283] B. Kupfer, K. Majhi, D. A. Keller, Y. Bouhadana, S. Rühle, H. N. Barad, A. Y. Anderson, A. Zaban, *Advanced Energy Materials* **2015**, *5*, 1401007-n/a.

[284] B. Wang, Y. Cai, W. Dong, C. Xia, W. Zhang, Y. Liu, M. Afzal, H. Wang, B. Zhu, *Solar Energy Materials and Solar Cells* **2016**, *157*, 126-133.

[285] Z. Yan, D. A. Keller, K. J. Rietwyk, H.-N. Barad, K. Majhi, A. Ginsburg, A. Y. Anderson, A. Zaban, *Energy Technology* **2016**, *4*, 809-815.

[286] H. Behzad, F. E. Ghodsi, E. Peksu, H. Karaagac, *Journal of Alloys and Compounds* **2018**, *744*, 470-480.

[287] M. Patel, S.-H. Park, J. Kim, *physica status solidi (a)* **2018**, *215*, 1800216.

[288] K. Majhi, L. Bertoluzzi, K. J. Rietwyk, A. Ginsburg, D. A. Keller, P. Lopez-Varo, A. Y. Anderson, J. Bisquert, A. Zaban, *Advanced Materials Interfaces* **2016**, *3*, 1500405-n/a.

[289] M. Patel, M. Kumar, H.-S. Kim, W.-H. Park, E. H. Choi, J. Kim, *Materials Science in Semiconductor Processing* **2018**, *74*, 74-79.

[290] P. Lunca Popa, S. Sønderby, S. Kerdsongpanya, J. Lu, H. Arwin, P. Eklund, *Thin Solid Films* **2017**, *624*, 41-48.

[291] A. Iljinas, L. Marcinauskas, *Thin Solid Films* **2015**, *594*, 192-196.

[292] J. Morasch, S. Li, J. Brötz, W. Jaegermann, A. Klein, *physica status solidi (a)* **2014**, *211*, 93-100.

[293] Y. Ling, G. Wang, D. A. Wheeler, J. Z. Zhang, Y. Li, *Nano Letters* **2011**, *11*, 2119-2125.

[294] F. P. Koffyberg, *Journal of Physics and Chemistry of Solids* **1992**, *53*, 1285-1288.

[295] M. Seki, H. Yamahara, H. Tabata, *Applied Physics Express* **2012**, *5*, 115801.

[296] S. K. Suram, P. F. Newhouse, L. Zhou, D. G. Van Campen, A. Mehta, J. M. Gregoire, *ACS Combinatorial Science* **2016**, *18*, 682-688.

[297] H.-N. Barad, D. A. Keller, K. J. Rietwyk, A. Ginsburg, S. Tirosh, S. Meir, A. Y. Anderson, A. Zaban, *ACS Combinatorial Science* **2018**, *20*, 366-376.

[298] S. K. Suram, S. W. Fackler, L. Zhou, A. T. N'Diaye, W. S. Drisdell, J. Yano, J. M. Gregoire, *ACS Combinatorial Science* **2018**, *20*, 26-34.

[299] G. Liu, C. Zhen, Y. Kang, L. Wang, H.-M. Cheng, *Chemical Society Reviews* **2018**, *47*, 6410-6444.

[300] H. Du, S. Liu, G. Li, L. Li, X. Liu, B. Liu, *Chinese Physics B* **2019**, *28*, 016105.

[301] Y. Yuan, Z. Xiao, B. Yang, J. Huang, *Journal of Materials Chemistry A* **2014**, *2*, 6027-6041.

[302] K. T. Butler, J. M. Frost, A. Walsh, *Energy & Environmental Science* **2015**, *8*, 838-848.

[303] A. G. Chynoweth, *Physical Review* **1956**, *102*, 705-714.

[304] J. J. Brady, W. H. Moore, *Physical Review* **1939**, *55*, 308-311.

[305] A. M. Glass, D. von der Linde, T. J. Negran, *Applied Physics Letters* **1974**, *25*, 233-235.

[306] P. S. Brody, *Solid State Communications* **1973**, *12*, 673-676.

[307] P. S. Brody, *Journal of Solid State Chemistry* **1975**, *12*, 193-200.

[308] K. Uchino, M. Aizawa, L. S. Nomura, *Ferroelectrics* **1985**, *64*, 199-208.

[309] P. S. Brody, *Ferroelectrics* **1983**, *50*, 27-32.

[310] S. Y. Yang, J. Seidel, S. J. Byrnes, P. Shafer, C. H. Yang, M. D. Rossell, P. Yu, Y. H. Chu, J. F. Scott, J. W. Ager, L. W. Martin, R. Ramesh, *Nature Nanotechnology* **2010**, *5*, 143-147.

[311] I. Grinberg, D. V. West, M. Torres, G. Gou, D. M. Stein, L. Wu, G. Chen, E. M. Gallo, A. R. Akbashev, P. K. Davies, J. E. Spanier, A. M. Rappe, *Nature* **2013**.

[312] J. W. Bennett, I. Grinberg, A. M. Rappe, *Journal of the American Chemical Society* **2008**, *130*, 17409-17412.

[313] R. Nechache, C. Harnagea, S. Li, L. Cardenas, W. Huang, J. Chakrabartty, F. Rosei, *Nat Photon* **2015**, *9*, 61-67.

[314] V. M. Fridkin, *Ferroelectric Semiconductors*, Published by Springer, **1980**

[315] W. T. H. Koch, R. Munser, W. Ruppel, P. Würfel, *Solid State Communications* **1975**, *17*, 847-850.

[316] G. Zhang, H. Wu, G. Li, Q. Huang, C. Yang, F. Huang, F. Liao, J. Lin, *Scientific Reports* **2013**, *3*.

[317] P. Gunter, *Ferroelectrics* **1978**, *22*, 671-674.

[318] C. L. Diao, H. W. Zheng, *J Mater Sci: Mater Electron* **2015**, *26*, 3108-3111.

[319] C. E. Land, P. S. Peercy, *Ferroelectrics* **1978**, *22*, 677-679.

[320] K. Takagi, S. Kikuchi, J.-F. Li, H. Okamura, R. Watanabe, A. Kawasaki, *Journal of the American Ceramic Society* **2004**, *87*, 1477-1482.

[321] V. S. Dharmadhikari, W. W. Grannemann, *Journal of Applied Physics* **1982**, *53*, 8988-8992.

[322] A. Zenkevich, Y. Matveyev, K. Maksimova, R. Gaynutdinov, A. Tolstikhina, V. Fridkin, *Physical Review B* **2014**, *90*, 161409.

[323] P. S. Brody, B. J. Rod, *Integrated Ferroelectrics* **1993**, *3*, 245-257.

[324] E. Dubovik, V. Fridkin, D. Dimos, *Integrated Ferroelectrics* **1995**, *8*, 285-290.

[325] Y. Watanabe, M. Okano, *Applied Physics Letters* **2001**, *78*, 1906-1908.

[326] M. Ichiki, Y. Morikawa, T. Nakada, R. Maeda, *Ceramics International* **2004**, *30*, 1831-1834.

[327] M. Ichiki, H. Furue, T. Kobayashi, R. Maeda, Y. Morikawa, T. Nakada, K. Nonaka, *Applied Physics Letters* **2005**, *87*, 222903.

[328] M. Qin, K. Yao, Y. C. Liang, *Applied Physics Letters* **2008**, *93*, 122904.

[329] M. Qin, K. Yao, Y. C. Liang, *Journal of Applied Physics* **2009**, *105*.

[330] V. N. Harshan, S. Kotru, *Applied Physics Letters* **2012**, *100*.

[331] B. Chen, Z. Zuo, Y. Liu, Q. F. Zhan, Y. Xie, H. Yang, G. Dai, Z. Li, G. Xu, R. W. Li, *Applied Physics Letters* **2012**, *100*.

[332] P. Zhang, D. Cao, C. Wang, M. Shen, X. Su, L. Fang, W. Dong, F. Zheng, *Materials Chemistry and Physics* **2012**, *135*, 304-308.

[333] V. N. Harshan, S. Kotru, *Ferroelectrics* **2014**, *470*, 99-106.

[334] F. Zheng, P. Zhang, X. Wang, W. Huang, J. Zhang, M. Shen, W. Dong, L. Fang, Y. Bai, X. Shen, H. Sun, J. Hao, *Nanoscale* **2014**, *6*, 2915-2921.

[335] G. Anoop, J. Seo, C. J. Han, H. J. Lee, G. W. Kim, S. S. Lee, E. Y. Park, J. Y. Jo, *Solar Energy* **2015**, *111*, 118-124.

[336] S. Y. Yang, L. W. Martin, S. J. Byrnes, T. E. Conry, S. R. Basu, D. Paran, L. Reichertz, J. Ihlefeld, C. Adamo, A. Melville, Y.-H. Chu, C.-H. Yang, J. L. Musfeldt, D. G. Schlom, J. W. Ager, R. Ramesh, *Applied Physics Letters* **2009**, *95*, 062909.

[337] W. Ji, K. Yao, Y. C. Liang, *Advanced Materials* **2010**, *22*, 1763-1766.

[338] T. L. Qu, Y. G. Zhao, D. Xie, J. P. Shi, Q. P. Chen, T. L. Ren, *Applied Physics Letters* **2011**, *98*, 173507.

[339] R. K. Katiyar, A. Kumar, G. Morell, J. F. Scott, R. S. Katiyar, *Applied Physics Letters* **2011**, *99*.

[340] Y. Zang, D. Xie, X. Wu, Y. Chen, Y. Lin, M. Li, H. Tian, X. Li, Z. Li, H. Zhu, T. Ren, D. Plant, *Applied Physics Letters* **2011**, *99*, 132904.

[341] B. Chen, M. Li, Y. Liu, Z. Zuo, F. Zhuge, Q. F. Zhan, R. W. Li, *Nanotechnology* **2011**, *22*, 195201.

[342] W. Ji, K. Yao, Y. C. Liang, *Physical Review B - Condensed Matter and Materials Physics* **2011**, *84*.

[343] D. Lee, S. H. Baek, T. H. Kim, J. G. Yoon, C. M. Folkman, C. B. Eom, T. W. Noh, *Physical Review B - Condensed Matter and Materials Physics* **2011**, *84*.

[344] J. Seidel, D. Fu, S.-Y. Yang, E. Alarcón-Lladó, J. Wu, R. Ramesh, J. W. Ager, *Physical Review Letters* **2011**, *107*, 126805.

[345] Y. Zang, D. Xie, Y. Chen, X. Wu, T. Ren, H. Zhu, J.-L. Cao, D. Plant, *Journal of Applied Physics* **2012**, *112*, 054103.

[346] W. Dong, Y. Guo, B. Guo, H. Liu, H. Li, H. Liu, *Materials Letters* **2012**, *88*, 140-142.

[347] F. Yan, G. Chen, L. Lu, J. E. Spanier, *ACS Nano* **2012**, *6*, 2353-2360.

[348] W. Dong, Y. Guo, B. Guo, H. Liu, H. Li, *Materials Letters* **2013**, *91*, 359-361.

[349] Z. Lin, W. Cai, W. Jiang, C. Fu, C. Li, Y. Song, *Ceramics International* **2013**, *39*, 8729-8736.

[350] Y. Guo, B. Guo, W. Dong, H. Li, H. Liu, *Nanotechnology* **2013**, *24*, 275201.

[351] Y. Sun, Y. Zhou, H. Liu, Z. Xia, M. Luo, K. Wan, C. Wang, *J Sol-Gel Sci Technol* **2013**, *66*, 429-433.

[352] B. Liu, Z. Peng, J. Ma, J. Wang, Q. Zhao, Y. Wang, *physica status solidi (a)* **2013**, *210*, 819-822.

[353] L. Fang, L. You, Y. Zhou, P. Ren, Z. S. Lim, J. Wang, *Applied Physics Letters* **2014**, *104*.

[354] R. K. Katiyar, P. Misra, S. Sahoo, G. Morell, R. S. Katiyar, *Journal of Alloys and Compounds* **2014**, *609*, 168-172.

[355] Y. e. Zhou, B. Yu, X. Zhu, X. Tan, L. Qian, L. Liu, J. Yu, S. Yuan, *J Sol-Gel Sci Technol* **2014**, *72*, 74-79.

[356] Z. Peng, Y. Wang, B. Liu, *Materials Science in Semiconductor Processing* **2015**, *35*, 115-119.

[357] J. Ding, M. Chen, J. Qiu, N. Yuan, *Sci. China Phys. Mech. Astron.* **2015**, *58*, 1-6.

[358] S. Gupta, M. Tomar, V. Gupta, *Journal of Applied Physics* **2014**, *115*, 014102.

[359] R. K. Katiyar, Y. Sharma, P. Misra, V. S. Puli, S. Sahoo, A. Kumar, J. F. Scott, G. Morell, B. R. Weiner, R. S. Katiyar, *Applied Physics Letters* **2014**, *105*, 172904.

[360] W. Cai, C. Fu, R. Gao, W. Jiang, X. Deng, G. Chen, *Journal of Alloys and Compounds* **2014**, *617*, 240-246.

[361] P. Venkata Sreenivas, P. Dhiren Kumar, K. Rajesh Kumar, C. Indrani, P. Neeraj, M. Pankaj, B. C. Douglas, J. F. Scott, S. K. Ram, *Journal of Physics D: Applied Physics* **2014**, *47*, 075502.

[362] W. Chengyan, L. Xingyun, S. Su, Z. Yong, L. Hongri, S. Yuxia, *Journal of Physics D: Applied Physics* **2014**, *47*, 355104.

[363] Y. Kenji, S. Wataru, M. Makoto, Y. Toshinobu, *Japanese Journal of Applied Physics* **2014**, *53*, 09PA17.

[364] R. K. Katiyar, Y. Sharma, D. Barrionuevo, S. Kooriyattil, S. P. Pavunny, J. S. Young, G. Morell, B. R. Weiner, R. S. Katiyar, J. F. Scott, *Applied Physics Letters* **2015**, *106*, 082903.

[365] R. L. Gao, H. W. Yang, C. L. Fu, W. Cai, G. Chen, X. L. Deng, J. R. Sun, Y. G. Zhao, B. G. Shen, *Journal of Alloys and Compounds* **2015**, *624*, 1-8.

[366] Y. Li, X. Liu, Y. Sun, S. Sheng, H. Liu, P. Yang, S. Yang, *Journal of Alloys and Compounds* **2015**, *644*, 602-606.

[367] L. Zhang, J. Chen, J. Cao, D. He, X. Xing, *Journal of Materials Chemistry C* **2015**, *3*, 4706-4712.

[368] R. Nechache, C. Harnagea, S. Licoccia, E. Traversa, A. Ruediger, A. Pignolet, F. Rosei, *Applied Physics Letters* **2011**, *98*, 202902.

[369] J. Park, S. S. Won, C. W. Ahn, I. W. Kim, *Journal of the American Ceramic Society* **2013**, *96*, 146-150.

[370] C.-S. Tu, F.-T. Wang, R. R. Chien, V. H. Schmidt, C.-M. Hung, C.-T. Tseng, *Applied Physics Letters* **2006**, *88*, 032902.

[371] Z. Wu, Y. Zhang, K. Ma, Y. Cao, H. Lin, Y. Jia, J. Chen, H. Li, *physica status solidi (RRL) – Rapid Research Letters* **2014**, *8*, 36-39.

[372] W. Wei, Y. Dai, B. Huang, *The Journal of Physical Chemistry C* **2009**, *113*, 5658-5663.

[373] L. Pintilie, M. Alexe, A. Pignolet, D. Hesse, *Applied Physics Letters* **1998**, *73*, 342-344.

[374] W. C. Wang, H. W. Zheng, X. Y. Liu, X. S. Liu, Y. Z. Gu, H. R. Zhang, W. F. Zhang, *Chemical Physics Letters* **2010**, *488*, 50-53.

[375] Y. G. Zhang, H. W. Zheng, J. X. Zhang, G. L. Yuan, W. X. Gao, Y. Z. Gu, C. L. Diao, Y. F. Liu, W. F. Zhang, *Materials Letters* **2014**, *125*, 25-27.

[376] S. Kooriyattil, R. K. Katiyar, S. P. Pavunny, G. Morell, R. S. Katiyar, *Applied Physics Letters* **2014**, *105*, 072908.

[377] W. Seok Woo, S. Sik Won, C. Won Ahn, S. A. Chae, A. Ullah, I. Won Kim, *Journal of Applied Physics* **2014**, *115*.

[378] L. Pintilie, M. Alexe, *Journal of the European Ceramic Society* **1999**, *19*, 1485-1488.

[379] K. Kubota, S. Kuroda, *Journal of Physics and Chemistry of Solids* **1981**, *42*, 715-718.

[380] K. Bormanis, A. I. Burkhanov, N. Luu Thi, S. V. Mednikov, M. Antonova, *IOP Conference Series: Materials Science and Engineering* **2013**, *49*, 012027.

[381] T. Batirov, E. Doubovik, R. Djalalov, V. M. Fridkin, *Ferroelectrics Letters Section* **1997**, *23*, 95-98.

[382] T. M. Batirov, K. A. Verkhovskaya, R. K. Dzhalalov, E. V. Dubovik, B. V. Mill, V. M. Fridkin, *Crystallogr. Rep.* **2000**, *45*, 154-156.

[383] S. K. Bsayan, V. V. Lewov, A. Y. Maksimov, *Ferroelectrics Letters Section* **1984**, *2*, 93-96.

[384] H.-Y. Ye, Y. Zhang, D.-W. Fu, R.-G. Xiong, *Angewandte Chemie* **2014**, *126*, 11424-11429.

[385] W.-Q. Liao, Y. Zhang, C.-L. Hu, J.-G. Mao, H.-Y. Ye, P.-F. Li, S. D. Huang, R.-G. Xiong, *Nat Commun* **2015**, *6*.

[386] K. Matsushige, N. Kato, T. Horiuchi, in *Applications of Ferroelectrics, 1990., IEEE 7th International Symposium on*, **1990**, pp. 647-649.

[387] Y. Yuan, T. J. Reece, P. Sharma, S. Poddar, S. Ducharme, A. Gruverman, Y. Yang, J. Huang, *Nature Materials* **2011**, *10*, 296-302.

[388] M. Ichiki, H. Furue, T. Kobayashi, Y. Morikawa, T. Nakada, C. Endo, K. Nonaka, R. Maeda, *Vol. 6035* (Ed.: A. J. Hariz), Brisbane, **2006**.

[389] M. Qin, K. Yao, Y. C. Liang, S. Shannigrahi, *Journal of Applied Physics* **2007**, *101*.

[390] L. Pintilie, C. Dragoi, I. Pintilie, *Journal of Applied Physics* **2011**, *110*.

[391] S. Y. Yang, J. Seidel, S. J. Byrnes, P. Shafer, C. H. Yang, M. D. Rossell, P. Yu, Y. H. Chu, J. F. Scott, J. W. Ager, L. W. Martin, R. Ramesh, *Nat Nano* **2010**, *5*, 143-147.

[392]   K. Yao, B. K. Gan, M. Chen, S. Shannigrahi, *Applied Physics Letters* **2005**, *87*, 212903 212901-212903.

[393]   A. Bhatnagar, A. Roy Chaudhuri, Y. Heon Kim, D. Hesse, M. Alexe, *Nat Commun* **2013**, *4*.

[394]   N. Seiji, U. Tomohisa, N. Daichi, F. Hironori, K. Masafumi, S. Masaru, *Japanese Journal of Applied Physics* **2014**, *53*, 09PA16.

[395]   J. Park, C. Won Ahn, I. Won Kim, *Journal of Applied Physics* **2012**, *112*, 014312.

[396]   T. Choi, S. Lee, Y. J. Choi, V. Kiryukhin, S. W. Cheong, *Science* **2009**, *324*, 63-66.

[397]   H. T. Yi, T. Choi, S. G. Choi, Y. S. Oh, S. W. Cheong, *Advanced Materials* **2011**, *23*, 3403-3407.

[398]   G. Chen, J. Chen, W. Pei, Y. Lu, Q. Zhang, Q. Zhang, Y. He, *Materials Research Bulletin* **2019**, *110*, 39-49.

[399]   J. P. Chakrabartty, R. Nechache, C. Harnagea, F. Rosei, *Opt. Express* **2014**, *22*, A80-A89.

[400]   S. Kumari, N. Ortega, A. Kumar, J. F. Scott, R. S. Katiyar, *AIP Advances* **2014**, *4*, 037101.

[401]   C. W. Zhao, B. C. Luo, S. J. Guo, C. L. Chen, *Ceramics International* **2017**, *43*, 7861-7865.

[402]   S. Das, S. Ghara, P. Mahadevan, A. Sundaresan, J. Gopalakrishnan, D. D. Sarma, *ACS Energy Letters* **2018**, *3*, 1176-1182.

[403]   W. Huang, C. Harnagea, D. Benetti, M. Chaker, F. Rosei, R. Nechache, *Journal of Materials Chemistry A* **2017**, *5*, 10355-10364.

[404]   J. Chakrabartty, C. Harnagea, M. Celikin, F. Rosei, R. Nechache, *Nature Photonics* **2018**, *12*, 271-276.

[405]   A. Kojima, K. Teshima, Y. Shirai, T. Miyasaka, *Journal of the American Chemical Society* **2009**, *131*, 6050-6051.

[406]   J.-H. Im, C.-R. Lee, J.-W. Lee, S.-W. Park, N.-G. Park, *Nanoscale* **2011**, *3*, 4088-4093.

[407]   M. M. Lee, J. Teuscher, T. Miyasaka, T. N. Murakami, H. J. Snaith, *Science* **2012**, *338*, 643-647.

[408]   X. Xu, Z. Liu, Z. Zuo, M. Zhang, Z. Zhao, Y. Shen, H. Zhou, Q. Chen, Y. Yang, M. Wang, *Nano Letters* **2015**, *15*, 2402-2408.

[409]   J. You, L. Meng, T.-B. Song, T.-F. Guo, Y. Yang, W.-H. Chang, Z. Hong, H. Chen, H. Zhou, Q. Chen, Y. Liu, N. De Marco, Y. Yang, *Nat Nano* **2015**, *advance online publication*.

[410]   S. I. Park, S. J. Baik, J.-S. Im, L. Fang, J.-W. Jeon, K. S. Lim, *Applied Physics Letters* **2011**, *99*, 063504.

[411]   F. Meillaud, M. Boccard, G. Bugnon, M. Despeisse, S. Hänni, F. J. Haug, J. Persoz, J. W. Schüttauf, M. Stuckelberger, C. Ballif, *Materials Today* **2015**, *18*, 378-384.

[412]   M. Zhang, L. Qiu, W. Li, J. Zhang, L. Wu, L. Feng, *Materials Science in Semiconductor Processing* **2018**, *86*, 49-57.

[413]   G. Zeng, X. Hao, S. Ren, L. Feng, Q. Wang, *Energies* **2019**, *12*, 1123.

[414]   S. López-Marino, M. Placidi, A. Pérez-Tomás, J. Llobet, V. Izquierdo-Roca, X. Fontané, A. Fairbrother, M. Espíndola-Rodríguez, D. Sylla, A. Pérez-Rodríguez, E. Saucedo, *Journal of Materials Chemistry A* **2013**, *1*, 8338-8343.

[415]   J. K. Larsen, F. Larsson, T. Törndahl, N. Saini, L. Riekehr, Y. Ren, A. Biswal, D. Hauschild, L. Weinhardt, C. Heske, C. Platzer-Björkman, *Advanced Energy Materials*, *0*, 1900439.

[416]   W. Hsu, C. M. Sutter-Fella, M. Hettick, L. Cheng, S. Chan, Y. Chen, Y. Zeng, M. Zheng, H.-P. Wang, C.-C. Chiang, A. Javey, *Scientific Reports* **2015**, *5*, 16028.

[417]   Y. Wang, R. Wenisch, R. Schlatmann, I. Lauermann, *Advanced Energy Materials* **2018**, *8*, 1801692.

[418] T. G. Allen, J. Bullock, Q. Jeangros, C. Samundsett, Y. Wan, J. Cui, A. Hessler-Wyser, S. De Wolf, A. Javey, A. Cuevas, *Advanced Energy Materials* **2017**, *7*, 1602606.

[419] W. Wu, W. Lin, J. Bao, Z. Liu, B. Liu, K. Qiu, Y. Chen, H. Shen, *RSC Advances* **2017**, *7*, 23851-23858.

[420] J. Bullock, Y. Wan, Z. Xu, S. Essig, M. Hettick, H. Wang, W. Ji, M. Boccard, A. Cuevas, C. Ballif, A. Javey, *ACS Energy Letters* **2018**, *3*, 508-513.

[421] W. Lin, W. Wu, J. Bao, Z. Liu, K. Qiu, L. Cai, Z. Yao, Y. Deng, Z. Liang, H. Shen, *Materials Research Bulletin* **2018**, *103*, 77-82.

[422] K. Mallem, Y. J. Kim, S. Q. Hussain, S. Dutta, A. H. T. Le, M. Ju, J. Park, Y. H. Cho, Y. Kim, E.-C. Cho, J. Yi, *Materials Research Bulletin* **2019**, *110*, 90-96.

[423] J. Bullock, Y. Wan, M. Hettick, X. Zhaoran, S. P. Phang, D. Yan, H. Wang, W. Ji, C. Samundsett, Z. Hameiri, D. Macdonald, A. Cuevas, A. Javey, *Advanced Energy Materials* **2019**, *9*, 1803367.

[424] A. Alcañiz, G. López, I. Martín, A. Jiménez, A. Datas, E. Calle, E. Ros, L. G. Gerling, C. Voz, C. del Cañizo, R. Alcubilla, *Solar Energy* **2019**, *181*, 357-360.

[425] P. R. Narangari, S. K. Karuturi, Y. Wu, J. Wong-Leung, K. Vora, M. Lysevych, Y. Wan, H. H. Tan, C. Jagadish, S. Mokkapati, *Nanoscale* **2019**, *11*, 7497-7505.

[426] J. Nowotny, *Oxide Semiconductors for Solar Energy Conversion: Titanium Dioxide*, CRC Press, Taylor & Francis, **2017**.

[427] S. Sajid, A. M. Elseman, H. Huang, J. Ji, S. Dou, H. Jiang, X. Liu, D. Wei, P. Cui, M. Li, *Nano Energy* **2018**, *51*, 408-424.

[428] T. Leijtens, S. D. Stranks, G. E. Eperon, R. Lindblad, E. M. J. Johansson, I. J. McPherson, H. Rensmo, J. M. Ball, M. M. Lee, H. J. Snaith, *ACS Nano* **2014**, *8*, 7147-7155.

[429] B. O'Regan, M. Gratzel, *Nature* **1991**, *353*, 737-740.

[430] D.-K. Hwang, J.-H. Kim, K.-P. Kim, S.-J. Sung, *RSC Advances* **2017**, *7*, 49057-49065.

[431] Z. Shi, A. H. Jayatissa, *Materials (Basel, Switzerland)* **2018**, *11*, 729.

[432] L. K. Ono, E. J. Juarez-Perez, Y. Qi, *ACS Applied Materials & Interfaces* **2017**, *9*, 30197-30246.

[433] F. Gao, Y. Wang, J. Zhang, D. Shi, M. Wang, R. Humphry-Baker, P. Wang, S. M. Zakeeruddin, M. Grätzel, *Chemical Communications* **2008**, 2635-2637.

[434] Z. Li, T. R. Klein, D. H. Kim, M. Yang, J. J. Berry, M. F. A. M. van Hest, K. Zhu, *Nature Reviews Materials* **2018**, *3*, 18017.

[435] H.-S. Kim, C.-R. Lee, J.-H. Im, K.-B. Lee, T. Moehl, A. Marchioro, S.-J. Moon, R. Humphry-Baker, J.-H. Yum, J. E. Moser, M. Grätzel, N.-G. Park, *Scientific Reports* **2012**, *2*, 591.

[436] J. H. Heo, S. H. Im, J. H. Noh, T. N. Mandal, C.-S. Lim, J. A. Chang, Y. H. Lee, H.-j. Kim, A. Sarkar, K. NazeeruddinMd, M. Gratzel, S. I. Seok, *Nat Photon* **2013**, *7*, 486-491.

[437] J. Burschka, N. Pellet, S. J. Moon, R. Humphry-Baker, P. Gao, M. K. Nazeeruddin, M. Grätzel, *Nature* **2013**, *499*, 316-319.

[438] J.-H. Im, I.-H. Jang, N. Pellet, M. Grätzel, N.-G. Park, *Nat Nano* **2014**, *9*, 927-932.

[439] N. J. Jeon, J. H. Noh, Y. C. Kim, W. S. Yang, S. Ryu, S. I. Seok, *Nat Mater* **2014**, *13*, 897-903.

[440] L. Qiu, J. Deng, X. Lu, Z. Yang, H. Peng, *Angewandte Chemie International Edition* **2014**, *53*, 10425-10428.

[441] M. Lee, Y. Jo, D. S. Kim, Y. Jun, *Journal of Materials Chemistry A* **2015**, *3*, 4129-4133.

[442] T. M. Koh, K. Fu, Y. Fang, S. Chen, T. C. Sum, N. Mathews, S. G. Mhaisalkar, P. P. Boix, T. Baikie, *The Journal of Physical Chemistry C* **2014**, *118*, 16458-16462.

[443] S. Pang, H. Hu, J. Zhang, S. Lv, Y. Yu, F. Wei, T. Qin, H. Xu, Z. Liu, G. Cui, *Chemistry of Materials* **2014**, *26*, 1485-1491.

[444] N. Pellet, P. Gao, G. Gregori, T.-Y. Yang, M. K. Nazeeruddin, J. Maier, M. Grätzel, *Angewandte Chemie International Edition* **2014**, *53*, 3151-3157.

[445] J.-W. Lee, D.-J. Seol, A.-N. Cho, N.-G. Park, *Advanced Materials* **2014**, *26*, 4991-4998.

[446] N. J. Jeon, J. H. Noh, W. S. Yang, Y. C. Kim, S. Ryu, J. Seo, S. I. Seok, *Nature* **2015**, *517*, 476-480.

[447] Y. Reyna, M. Salado, S. Kazim, A. Pérez-Tomas, S. Ahmad, M. Lira-Cantu, *Nano Energy* **2016**, *30*, 570-579.

[448] A. Abate, M. Saliba, D. J. Hollman, S. D. Stranks, K. Wojciechowski, R. Avolio, G. Grancini, A. Petrozza, H. J. Snaith, *Nano Letters* **2014**, *14*, 3247-3254.

[449] S. N. Habisreutinger, T. Leijtens, G. E. Eperon, S. D. Stranks, R. J. Nicholas, H. J. Snaith, *Nano Letters* **2014**, *14*, 5561-5568.

[450] K. Cao, Z. Zuo, J. Cui, Y. Shen, T. Moehl, S. M. Zakeeruddin, M. Grätzel, M. Wang, *Nano Energy* **2015**, *17*, 171-179.

[451] Z. Liu, M. Zhang, X. Xu, L. Bu, W. Zhang, W. Li, Z. Zhao, M. Wang, Y.-B. Cheng, H. He, *Dalton Transactions* **2015**, *44*, 3967-3973.

[452] A. Kogo, Y. Sanehira, M. Ikegami, T. Miyasaka, *Journal of Materials Chemistry A* **2015**, *3*, 20952-20957.

[453] A. Abrusci, S. D. Stranks, P. Docampo, H.-L. Yip, A. K. Y. Jen, H. J. Snaith, *Nano Letters* **2013**, *13*, 3124-3128.

[454] X. Yin, Y. Guo, Z. Xue, P. Xu, M. He, B. Liu, *Nano Res.* **2015**, *8*, 1997-2003.

[455] R. Jose, V. Thavasi, S. Ramakrishna, *Journal of the American Ceramic Society* **2009**, *92*, 289-301.

[456] A. Bera, K. Wu, A. Sheikh, E. Alarousu, O. F. Mohammed, T. Wu, *The Journal of Physical Chemistry C* **2014**, *118*, 28494-28501.

[457] C. Wang, Y. Tang, Y. Hu, L. Huang, J. Fu, J. Jin, W. Shi, L. Wang, W. Yang, *RSC Advances* **2015**, *5*, 52041-52047.

[458] K. Mahmood, B. S. Swain, H. S. Jung, *Nanoscale* **2014**, *6*, 9127-9138.

[459] F. J. Ramos, M. C. López-Santos, E. Guillén, M. K. Nazeeruddin, M. Grätzel, A. R. Gonzalez-Elipe, S. Ahmad, *ChemPhysChem* **2014**, *15*, 1148-1153.

[460] L. Liang, Z. Huang, L. Cai, W. Chen, B. Wang, K. Chen, H. Bai, Q. Tian, B. Fan, *ACS Applied Materials & Interfaces* **2014**, *6*, 20585-20589.

[461] D. Bi, G. Boschloo, S. Schwarzmuller, L. Yang, E. M. J. Johansson, A. Hagfeldt, *Nanoscale* **2013**, *5*, 11686-11691.

[462] M. H. Kumar, N. Yantara, S. Dharani, M. Graetzel, S. Mhaisalkar, P. P. Boix, N. Mathews, *Chemical Communications* **2013**, *49*, 11089-11091.

[463] D.-Y. Son, J.-H. Im, H.-S. Kim, N.-G. Park, *The Journal of Physical Chemistry C* **2014**, *118*, 16567-16573.

[464] J. Dong, Y. Zhao, J. Shi, H. Wei, J. Xiao, X. Xu, J. Luo, J. Xu, D. Li, Y. Luo, Q. Meng, *Chemical Communications* **2014**, *50*, 13381-13384.

[465] T. Hu, S. Xiao, H. Yang, L. Chen, Y. Chen, *Chemical Communications* **2018**, *54*, 471-474.

[466] L. Calió, S. Kazim, M. Grätzel, S. Ahmad, *Angewandte Chemie International Edition* **2016**, *55*, 14522-14545.

[467] K.-C. Wang, J.-Y. Jeng, P.-S. Shen, Y.-C. Chang, E. W.-G. Diau, C.-H. Tsai, T.-Y. Chao, H.-C. Hsu, P.-Y. Lin, P. Chen, T.-F. Guo, T.-C. Wen, *Sci. Rep.* **2014**, *4*, 4756.

[468] K.-C. Wang, P.-S. Shen, M.-H. Li, S. Chen, M.-W. Lin, P. Chen, T.-F. Guo, *ACS Applied Materials & Interfaces* **2014**, *6*, 11851-11858.

[469] V. Trifiletti, V. Roiati, S. Colella, R. Giannuzzi, L. De Marco, A. Rizzo, M. Manca, A. Listorti, G. Gigli, *ACS Applied Materials & Interfaces* **2015**, *7*, 4283-4289.

[470] W. Chen, Y. Wu, J. Liu, C. Qin, X. Yang, A. Islam, Y.-B. Cheng, L. Han, *Energy & Environmental Science* **2015**, *8*, 629-640.

[471] J. H. Park, J. Seo, S. Park, S. S. Shin, Y. C. Kim, N. J. Jeon, H.-W. Shin, T. K. Ahn, J. H. Noh, S. C. Yoon, C. S. Hwang, S. I. Seok, *Advanced Materials* **2015**, *27*, 4013-4019.

[472] A. Corani, M.-H. Li, P.-S. Shen, P. Chen, T.-F. Guo, A. El Nahhas, K. Zheng, A. Yartsev, V. Sundström, C. S. Ponseca, *The Journal of Physical Chemistry Letters* **2016**, *7*, 1096-1101.

[473] A. Fakharuddin, L. Schmidt-Mende, G. Garcia-Belmonte, R. Jose, I. Mora-Sero, *Advanced Energy Materials* **2017**, *7*, 1700623.

[474] M. Liu, M. B. Johnston, H. J. Snaith, *Nature* **2013**, *501*, 395-398.

[475] G. E. Eperon, V. M. Burlakov, P. Docampo, A. Goriely, H. J. Snaith, *Advanced Functional Materials* **2014**, *24*, 151-157.

[476] B. Conings, L. Baeten, C. De Dobbelaere, J. D'Haen, J. Manca, H.-G. Boyen, *Advanced Materials* **2014**, *26*, 2041-2046.

[477] G. E. Eperon, S. D. Stranks, C. Menelaou, M. B. Johnston, L. M. Herz, H. J. Snaith, *Energy & Environmental Science* **2014**, *7*, 982-988.

[478] Q. Chen, H. Zhou, Z. Hong, S. Luo, H.-S. Duan, H.-H. Wang, Y. Liu, G. Li, Y. Yang, *Journal of the American Chemical Society* **2014**, *136*, 622-625.

[479] A. Yella, L.-P. Heiniger, P. Gao, M. K. Nazeeruddin, M. Grätzel, *Nano Letters* **2014**, *14*, 2591-2596.

[480] S. Chavhan, O. Miguel, H.-J. Grande, V. Gonzalez-Pedro, R. S. Sanchez, E. M. Barea, I. Mora-Sero, R. Tena-Zaera, *Journal of Materials Chemistry A* **2014**, *2*, 12754-12760.

[481] Y. Zhao, K. Zhu, *The Journal of Physical Chemistry C* **2014**, *118*, 9412-9418.

[482] H. Zhou, Q. Chen, G. Li, S. Luo, T.-b. Song, H.-S. Duan, Z. Hong, J. You, Y. Liu, Y. Yang, *Science* **2014**, *345*, 542-546.

[483] B. Conings, L. Baeten, T. Jacobs, R. Dera, J. D'Haen, J. Manca, H.-G. Boyen, *APL Mater.* **2014**, *2*, 081505.

[484] M. Xiao, F. Huang, W. Huang, Y. Dkhissi, Y. Zhu, J. Etheridge, A. Gray-Weale, U. Bach, Y.-B. Cheng, L. Spiccia, *Angewandte Chemie* **2014**, *126*, 10056-10061.

[485] Y. Wu, A. Islam, X. Yang, C. Qin, J. Liu, K. Zhang, W. Peng, L. Han, *Energy & Environmental Science* **2014**, *7*, 2934-2938.

[486] P. Docampo, F. C. Hanusch, N. Giesbrecht, P. Angloher, A. Ivanova, T. Bein, *APL Mater.* **2014**, *2*, 081508.

[487] Y. Guo, C. Liu, K. Inoue, K. Harano, H. Tanaka, E. Nakamura, *Journal of Materials Chemistry A* **2014**, *2*, 13827-13830.

[488] F. C. Hanusch, E. Wiesenmayer, E. Mankel, A. Binek, P. Angloher, C. Fraunhofer, N. Giesbrecht, J. M. Feckl, W. Jaegermann, D. Johrendt, T. Bein, P. Docampo, *The Journal of Physical Chemistry Letters* **2014**, *5*, 2791-2795.

[489] L. Zheng, Y.-H. Chung, Y. Ma, L. Zhang, L. Xiao, Z. Chen, S. Wang, B. Qu, Q. Gong, *Chemical Communications* **2014**, *50*, 11196-11199.

[490] N. K. Noel, A. Abate, S. D. Stranks, E. S. Parrott, V. M. Burlakov, A. Goriely, H. J. Snaith, *ACS Nano* **2014**, *8*, 9815-9821.

[491] J. H. Heo, D. H. Song, S. H. Im, *Advanced Materials* **2014**, *26*, 8179-8183.

[492] B. J. Kim, D. H. Kim, Y.-Y. Lee, H.-W. Shin, G. S. Han, J. S. Hong, K. Mahmood, T. K. Ahn, Y.-C. Joo, K. S. Hong, N.-G. Park, S. Lee, H. S. Jung, *Energy & Environmental Science* **2015**, *8*, 916-921.

[493] F. Huang, Y. Dkhissi, W. Huang, M. Xiao, I. Benesperi, S. Rubanov, Y. Zhu, X. Lin, L. Jiang, Y. Zhou, A. Gray-Weale, J. Etheridge, C. R. McNeill, R. A. Caruso, U. Bach, L. Spiccia, Y.-B. Cheng, *Nano Energy* **2014**, *10*, 10-18.

[494] H.-H. Wang, Q. Chen, H. Zhou, L. Song, Z. S. Louis, N. D. Marco, Y. Fang, P. Sun, T.-B. Song, H. Chen, Y. Yang, *Journal of Materials Chemistry A* **2015**, *3*, 9108-9115.

[495] H. Nagaoka, F. Ma, D. W. deQuilettes, S. M. Vorpahl, M. S. Glaz, A. E. Colbert, M. E. Ziffer, D. S. Ginger, *The Journal of Physical Chemistry Letters* **2015**, *6*, 669-675.

[496] C.-Y. Chang, C.-Y. Chu, Y.-C. Huang, C.-W. Huang, S.-Y. Chang, C.-A. Chen, C.-Y. Chao, W.-F. Su, *ACS Applied Materials & Interfaces* **2015**, *7*, 4955-4961.

[497] Y. Liu, S. Ji, S. Li, W. He, K. Wang, H. Hu, C. Ye, *Journal of Materials Chemistry A* **2015**, *3*, 14902-14909.

[498] D. Yang, R. Yang, J. Zhang, Z. Yang, S. Liu, C. Li, *Energy & Environmental Science* **2015**, *8*, 3208-3214.

[499] D. Liu, T. L. Kelly, *Nat Photon* **2014**, *8*, 133-138.

[500] X. Dong, H. Hu, B. Lin, J. Ding, N. Yuan, *Chemical Communications* **2014**, *50*, 14405-14408.

[501] D. Liu, M. K. Gangishetty, T. L. Kelly, *Journal of Materials Chemistry A* **2014**, *2*, 19873-19881.

[502] J. Kim, G. Kim, T. K. Kim, S. Kwon, H. Back, J. Lee, S. H. Lee, H. Kang, K. Lee, *Journal of Materials Chemistry A* **2014**, *2*, 17291-17296.

[503] H. Zhou, Y. Shi, K. Wang, Q. Dong, X. Bai, Y. Xing, Y. Du, T. Ma, *The Journal of Physical Chemistry C* **2015**, *119*, 4600-4605.

[504] L. Zuo, Z. Gu, T. Ye, W. Fu, G. Wu, H. Li, H. Chen, *Journal of the American Chemical Society* **2015**, *137*, 2674-2679.

[505] J. Zhang, T. Pauporté, *The Journal of Physical Chemistry C* **2015**, *119*, 14919-14928.

[506] X. Xu, H. Zhang, J. Shi, J. Dong, Y. Luo, D. Li, Q. Meng, *Journal of Materials Chemistry A* **2015**, *3*, 19288-19293.

[507] K. Wang, Y. Shi, Q. Dong, Y. Li, S. Wang, X. Yu, M. Wu, T. Ma, *The Journal of Physical Chemistry Letters* **2015**, *6*, 755-759.

[508] S. S. Shin, W. S. Yang, J. H. Noh, J. H. Suk, N. J. Jeon, J. H. Park, J. S. Kim, W. M. Seong, S. I. Seok, *Nat Commun* **2015**, *6*, 7410.

[509] J.-Y. Jeng, K.-C. Chen, T.-Y. Chiang, P.-Y. Lin, T.-D. Tsai, Y.-C. Chang, T.-F. Guo, P. Chen, T.-C. Wen, Y.-J. Hsu, *Advanced Materials* **2014**, *26*, 4107-4113.

[510] L. Hu, J. Peng, W. Wang, Z. Xia, J. Yuan, J. Lu, X. Huang, W. Ma, H. Song, W. Chen, Y.-B. Cheng, J. Tang, *ACS Photonics* **2014**, *1*, 547-553.

[511] A. S. Subbiah, A. Halder, S. Ghosh, N. Mahuli, G. Hodes, S. K. Sarkar, *The Journal of Physical Chemistry Letters* **2014**, *5*, 1748-1753.

[512] Z. Zhu, Y. Bai, T. Zhang, Z. Liu, X. Long, Z. Wei, Z. Wang, L. Zhang, J. Wang, F. Yan, S. Yang, *Angewandte Chemie International Edition* **2014**, *53*, 12571-12575.

[513] J. Cui, F. Meng, H. Zhang, K. Cao, H. Yuan, Y. Cheng, F. Huang, M. Wang, *ACS Applied Materials & Interfaces* **2014**, *6*, 22862-22870.

[514] Y. Li, S. Ye, W. Sun, W. Yan, Y. Li, Z. Bian, Z. Liu, S. Wang, C. Huang, *Journal of Materials Chemistry A* **2015**, *3*, 18389-18394.

[515] J. H. Kim, P.-W. Liang, S. T. Williams, N. Cho, C.-C. Chueh, M. S. Glaz, D. S. Ginger, A. K. Y. Jen, *Advanced Materials* **2015**, *27*, 695-701.

[516] P.-K. Kung, M.-H. Li, P.-Y. Lin, Y.-H. Chiang, C.-R. Chan, T.-F. Guo, P. Chen, *Advanced Materials Interfaces* **2018**, *5*, 1800882.

[517] J. H. Lee, Y. W. Noh, I. S. Jin, S. H. Park, J. W. Jung, *Journal of Power Sources* **2019**, *412*, 425-432.

[518] J. Zhang, W. Mao, X. Hou, J. Duan, J. Zhou, S. Huang, W. Ou-Yang, X. Zhang, Z. Sun, X. Chen, *Solar Energy* **2018**, *174*, 1133-1141.

[519] W. Chen, Y. Wu, Y. Yue, J. Liu, W. Zhang, X. Yang, H. Chen, E. Bi, I. Ashraful, M. Grätzel, L. Han, *Science* **2015**, *350*, 944-948.

[520] Z. Wu, S. Bai, J. Xiang, Z. Yuan, Y. Yang, W. Cui, X. Gao, Z. Liu, Y. Jin, B. Sun, *Nanoscale* **2014**, *6*, 10505-10510.

[521] F. Hou, Z. Su, F. Jin, X. Yan, L. Wang, H. Zhao, J. Zhu, B. Chu, W. Li, *Nanoscale* **2015**, *7*, 9427-9432.

[522] C. Zuo, L. Ding, *Small* **2015**, *11*, 5528-5532.

[523] L. Meng, Y. Zhang, X. Wan, C. Li, X. Zhang, Y. Wang, X. Ke, Z. Xiao, L. Ding, R. Xia, H.-L. Yip, Y. Cao, Y. Chen, *Science* **2018**, *361*, 1094-1098.

[524] S. Q. Hussain, K. Mallem, M. A. Khan, M. Q. Khokhar, Y. Lee, J. Park, K. S. Lee, Y. Kim, E. C. Cho, Y. H. Cho, J. Yi, *Transactions on Electrical and Electronic Materials* **2019**, *20*, 1-6.

[525] R. S. Bonilla, B. Hoex, P. Hamer, P. R. Wilshaw, *physica status solidi (a)* **2017**, *214*, 1700293.

[526] B. Macco, L. E. Black, J. Melskens, B. W. H. van de Loo, W.-J. H. Berghuis, M. A. Verheijen, W. M. M. Kessels, *Solar Energy Materials and Solar Cells* **2018**, *184*, 98-104.

[527] S. Choi, K. H. Min, M. S. Jeong, J. I. Lee, M. G. Kang, H.-E. Song, Y. Kang, H.-S. Lee, D. Kim, K.-H. Kim, *Scientific Reports* **2017**, *7*, 12853.

[528] H. Tong, M. Liao, Z. Zhang, Y. Wan, D. Wang, C. Quan, L. Cai, P. Gao, W. Guo, H. Lin, C. Shou, Y. Zeng, B. Yan, J. Ye, *Solar Energy Materials and Solar Cells* **2018**, *188*, 149-155.

[529] J. M. Ball, M. M. Lee, A. Hey, H. J. Snaith, *Energy & Environmental Science* **2013**, *6*, 1739-1743.

[530] M. J. Carnie, C. Charbonneau, M. L. Davies, J. Troughton, T. M. Watson, K. Wojciechowski, H. Snaith, D. A. Worsley, *Chemical Communications* **2013**, *49*, 7893-7895.

[531] W. Zhang, M. Saliba, S. D. Stranks, Y. Sun, X. Shi, U. Wiesner, H. J. Snaith, *Nano Letters* **2013**, *13*, 4505-4510.

[532] J. T.-W. Wang, J. M. Ball, E. M. Barea, A. Abate, J. A. Alexander-Webber, J. Huang, M. Saliba, I. Mora-Sero, J. Bisquert, H. J. Snaith, R. J. Nicholas, *Nano Letters* **2013**, *14*, 724-730.

[533] K. Wojciechowski, M. Saliba, T. Leijtens, A. Abate, H. J. Snaith, *Energy & Environmental Science* **2014**, *7*, 1142-1147.

[534] S. K. Pathak, A. Abate, P. Ruckdeschel, B. Roose, K. C. Gödel, Y. Vaynzof, A. Santhala, S.-I. Watanabe, D. J. Hollman, N. Noel, A. Sepe, U. Wiesner, R. Friend, H. J. Snaith, U. Steiner, *Advanced Functional Materials* **2014**, *24*, 6046-6055.

[535] J. Troughton, D. Bryant, K. Wojciechowski, M. J. Carnie, H. Snaith, D. A. Worsley, T. M. Watson, *Journal of Materials Chemistry A* **2015**, *3*, 9141-9145.

[536] E. Edri, S. Kirmayer, M. Kulbak, G. Hodes, D. Cahen, *The Journal of Physical Chemistry Letters* **2014**, *5*, 429-433.

[537] D. Bi, S.-J. Moon, L. Haggman, G. Boschloo, L. Yang, E. M. J. Johansson, M. K. Nazeeruddin, M. Gratzel, A. Hagfeldt, *RSC Advances* **2013**, *3*, 18762-18766.

[538] Z. Ku, Y. Rong, M. Xu, T. Liu, H. Han, *Scientific Reports* **2013**, *3*, 3132.

[539] A. Mei, X. Li, L. Liu, Z. Ku, T. Liu, Y. Rong, M. Xu, M. Hu, J. Chen, Y. Yang, M. Grätzel, H. Han, *Science* **2014**, *345*, 295-298.

[540] M. Hu, L. Liu, A. Mei, Y. Yang, T. Liu, H. Han, *Journal of Materials Chemistry A* **2014**, *2*, 17115-17121.

[541] Y. Yang, K. Ri, A. Mei, L. Liu, M. Hu, T. Liu, X. Li, H. Han, *Journal of Materials Chemistry A* **2015**, *3*, 9103-9107.

[542] S. H. Hwang, J. Roh, J. Lee, J. Ryu, J. Yun, J. Jang, *Journal of Materials Chemistry A* **2014**, *2*, 16429-16433.

[543] X. Yu, S. Chen, K. Yan, X. Cai, H. Hu, M. Peng, B. Chen, B. Dong, X. Gao, D. Zou, *Journal of Power Sources* **2016**, *325*, 534-540.

[544] N. Aeineh, A.-F. Castro-Méndez, P. J. Rodriguez-Cantó, R. Abargues, E. Hassanabadi, I. Suarez, A. Behjat, P. Ortiz, J. P. Martínez-Pastor, I. Mora-Seró, *ACS Omega* **2018**, *3*, 9798-9804.

[545] M. Anaya, W. Zhang, B. C. Hames, Y. Li, F. Fabregat-Santiago, M. E. Calvo, H. J. Snaith, H. Míguez, I. Mora-Seró, *Journal of Materials Chemistry C* **2017**, *5*, 634-644.

[546] Y. Zhao, K. Zhu, *Chemical Society Reviews* **2016**, *45*, 655-689.

[547] S. M. P. Meroni, Y. Mouhamad, F. De Rossi, A. Pockett, J. Baker, R. Escalante, J. Searle, M. J. Carnie, E. Jewell, G. Oskam, T. M. Watson, *Science and Technology of Advanced Materials* **2018**, *19*, 1-9.

[548] L. Liang, Y. Cai, X. Li, M. K. Nazeeruddin, P. Gao, *Nano Energy* **2018**, *52*, 211-238.

[549] M. Duan, Y. Hu, A. Mei, Y. Rong, H. Han, *Materials Today Energy* **2018**, *7*, 221-231.

[550] H. Li, K. Cao, J. Cui, S. Liu, X. Qiao, Y. Shen, M. Wang, *Nanoscale* **2016**, *8*, 6379-6385.

[551] Z. Meng, D. Guo, J. Yu, K. Fan, *Applied Surface Science* **2018**, *430*, 632-638.

[552] Y. Xiong, X. Zhu, A. Mei, F. Qin, S. Liu, S. Zhang, Y. Jiang, Y. Zhou, H. Han, *Solar RRL* **2018**, *2*, 1800002.

[553] M. Stengel, P. Aguado-Puente, N. A. Spaldin, J. Junquera, *Physical Review B* **2011**, *83*, 235112.

[554] F. Chen, A. Klein, *Physical Review B* **2012**, *86*, 094105.

[555] J. E. Rault, G. Agnus, T. Maroutian, V. Pillard, P. Lecoeur, G. Niu, B. Vilquin, M. G. Silly, A. Bendounan, F. Sirotti, N. Barrett, *Physical Review B* **2013**, *87*, 155146.

[556] D. Cao, C. Wang, F. Zheng, W. Dong, L. Fang, M. Shen, *Nano Letters* **2012**, *12*, 2803-2809.

[557] F. Zheng, Y. Xin, W. Huang, J. Zhang, X. Wang, M. Shen, W. Dong, L. Fang, Y. Bai, X. Shen, J. Hao, *Journal of Materials Chemistry A* **2014**, *2*, 1363-1368.

[558] Z. Fan, K. Yao, J. Wang, *Applied Physics Letters* **2014**, *105*, 162903.

[559] K.-J. Baeg, M. Binda, D. Natali, M. Caironi, Y.-Y. Noh, *Advanced Materials* **2013**, *25*, 4267-4295.

[560] D. Kufer, G. Konstantatos, *ACS Photonics* **2016**, *3*, 2197-2210.

[561] F. P. García de Arquer, A. Armin, P. Meredith, E. H. Sargent, *Nature Reviews Materials* **2017**, *2*, 16100.

[562] H. Wang, D. H. Kim, *Chemical Society Reviews* **2017**, *46*, 5204-5236.

[563] T. Nakada, T. Shimizu, H. Nakamura, in *2015 International SoC Design Conference (ISOCC)*, **2015**, 147-148.

[564] Z. Xiao, Y. Yuan, Y. Shao, Q. Wang, Q. Dong, C. Bi, P. Sharma, A. Gruverman, J. Huang, *Nat Mater* **2015**, *14*, 193-198.

[565] Y. Yuan, J. Chae, Y. Shao, Q. Wang, Z. Xiao, A. Centrone, J. Huang, *Advanced Energy Materials* **2015**, *5*, 1500615.

[566] C. Ge, K.-j. Jin, Q.-h. Zhang, J.-y. Du, L. Gu, H.-z. Guo, J.-t. Yang, J.-x. Gu, M. He, J. Xing, C. Wang, H.-b. Lu, G.-z. Yang, *ACS Applied Materials & Interfaces* **2016**, *8*, 34590-34597.

[567] S. Nau, C. Wolf, S. Sax, E. J. W. List-Kratochvil, *Advanced Materials* **2015**, *27*, 1048-1052.

[568] M. E. Gemayel, K. Börjesson, M. Herder, D. T. Duong, J. A. Hutchison, C. Ruzié, G. Schweicher, A. Salleo, Y. Geerts, S. Hecht, E. Orgiu, P. Samorì, *Nature Communications* **2015**, *6*, 6330.

[569]   S. Imura, K. Kikuchi, K. Miyakawa, H. Ohtake, M. Kubota, *Applied Physics Letters* **2014**, *104*, 242101.

[570]   L. Shi, Q. Liang, W. Wang, Y. Zhang, G. Li, T. Ji, Y. Hao, Y. Cui, *Nanomaterials* **2018**, *8*, 713.

[571]   A. Pierre, A. Gaikwad, A. C. Arias, *Nature Photonics* **2017**, *11*, 193.

[572]   P. C. Y. Chow, N. Matsuhisa, P. Zalar, M. Koizumi, T. Yokota, T. Someya, *Nature Communications* **2018**, *9*, 4546.

[573]   M. Kumar, M. Patel, D. Y. Park, H.-S. Kim, M. S. Jeong, J. Kim, *Advanced Electronic Materials* **2019**, *5*, 1800662.

[574]   S.-Y. Cai, C.-Y. Tzou, Y.-R. Liou, D.-R. Chen, C.-Y. Jiang, J.-M. Ma, C.-Y. Chang, C.-Y. Tseng, Y.-M. Liao, Y.-P. Hsieh, M. Hofmann, Y.-F. Chen, *ACS Applied Materials & Interfaces* **2019**, *11*, 4649-4653.

[575]   D. Li, D. Zheng, C. Jin, W. Zheng, H. Bai, *ACS Applied Materials & Interfaces* **2018**, *10*, 19836-19843.

[576]   Q. Xia, J. J. Yang, *Nature Materials* **2019**, *18*, 309-323.

[577]   K. K. Likharev, *Science of Advanced Materials* **2011**, *3*, 322-331.

[578]   D. S. Jeong, C. S. Hwang, *Advanced Materials* **2018**, *30*, 1704729.

[579]   Z. Sun, E. Ambrosi, A. Bricalli, D. Ielmini, *Advanced Materials* **2018**, *30*, 1802554.

[580]   D. Silver, J. Schrittwieser, K. Simonyan, I. Antonoglou, A. Huang, A. Guez, T. Hubert, L. Baker, M. Lai, A. Bolton, Y. Chen, T. Lillicrap, F. Hui, L. Sifre, G. van den Driessche, T. Graepel, D. Hassabis, *Nature* **2017**, *550*, 354.

[581]   G. Cauwenberghs, *Proceedings of the National Academy of Sciences* **2013**, *110*, 15512-15513.

[582]   E. O. Neftci, *iScience* **2018**, *5*, 52-68.

[583]   H. Mostafa, *IEEE Transactions on Neural Networks and Learning Systems* **2018**, *29*, 3227-3235.

[584]   C. Mead, *Proceedings of the IEEE* **1990**, *78*, 1629-1636.

[585]   P. A. Merolla, J. V. Arthur, R. Alvarez-Icaza, A. S. Cassidy, J. Sawada, F. Akopyan, B. L. Jackson, N. Imam, C. Guo, Y. Nakamura, B. Brezzo, I. Vo, S. K. Esser, R. Appuswamy, B. Taba, A. Amir, M. D. Flickner, W. P. Risk, R. Manohar, D. S. Modha, *Science* **2014**, *345*, 668-673.

[586]   E. Painkras, L. A. Plana, J. Garside, S. Temple, F. Galluppi, C. Patterson, D. R. Lester, A. D. Brown, S. B. Furber, *IEEE Journal of Solid-State Circuits* **2013**, *48*, 1943-1953.

[587]   M. Davies, N. Srinivasa, T. Lin, G. Chinya, Y. Cao, S. H. Choday, G. Dimou, P. Joshi, N. Imam, S. Jain, Y. Liao, C. Lin, A. Lines, R. Liu, D. Mathaikutty, S. McCoy, A. Paul, J. Tse, G. Venkataramanan, Y. Weng, A. Wild, Y. Yang, H. Wang, *IEEE Micro* **2018**, *38*, 82-99.

[588]   Y. Yang, W. Lu, *Nanoscale* **2013**, *5*, 10076-10092.

[589]   G. Indiveri, B. Linares-Barranco, R. Legenstein, G. Deligeorgis, T. Prodromakis, *Nanotechnology* **2013**, *24*, 384010.

[590]   M. Romera, P. Talatchian, S. Tsunegi, F. Abreu Araujo, V. Cros, P. Bortolotti, J. Trastoy, K. Yakushiji, A. Fukushima, H. Kubota, S. Yuasa, M. Ernoult, D. Vodenicarevic, T. Hirtzlin, N. Locatelli, D. Querlioz, J. Grollier, *Nature* **2018**, *563*, 230-234.

[591]   M. L. Schneider, C. A. Donnelly, S. E. Russek, B. Baek, M. R. Pufall, P. F. Hopkins, P. D. Dresselhaus, S. P. Benz, W. H. Rippard, *Science Advances* **2018**, *4*, e1701329.

[592]   M. L. Schneider, C. A. Donnelly, S. E. Russek, *Journal of Applied Physics* **2018**, *124*, 161102.

[593]   Z. Cheng, C. Ríos, W. H. P. Pernice, C. D. Wright, H. Bhaskaran, *Science Advances* **2017**, *3*, e1700160.

[594] T. Leydecker, M. Herder, E. Pavlica, G. Bratina, S. Hecht, E. Orgiu, P. Samorì, *Nature Nanotechnology* **2016**, *11*, 769.

[595] Y. M. Fu, C. J. Wan, L. Q. Zhu, H. Xiao, X. D. Chen, Q. Wan, *Advanced Biosystems* **2018**, *2*, 1700198.

[596] G. Voglis, N. Tavernarakis, *EMBO reports* **2006**, *7*, 1104-1110.

[597] S. Masoli, E. D'Angelo, *Frontiers in cellular neuroscience* **2017**, *11*, 278-278.

[598] V. B. Mountcastle, *Perceptual Neuroscience: The Cerebral Cortex*, Harvard University Press, **1998**.

[599] L. Alonso-Nanclares, J. Gonzalez-Soriano, J. R. Rodriguez, J. DeFelipe, *Proceedings of the National Academy of Sciences* **2008**, *105*, 14615-14619.

[600] D. A. Drachman, *Neurology* **2005**, *64*, 2004-2005.

[601] C. D. Schuman, T. E. Potok, R. M. Patton, J. D. Birdwell, M. E. Dean, G. S. Rose, J. S. Plank, in *arXiv e-prints*, **2017**.

[602] K. Gerrow, A. Triller, *Current Opinion in Neurobiology* **2010**, *20*, 631-639.

[603] G. Tavosanis, *Developmental Neurobiology* **2012**, *72*, 73-86.

[604] H. P. Wong, H. Lee, S. Yu, Y. Chen, Y. Wu, P. Chen, B. Lee, F. T. Chen, M. Tsai, *Proceedings of the IEEE* **2012**, *100*, 1951-1970.

[605] T.-C. Chang, K.-C. Chang, T.-M. Tsai, T.-J. Chu, S. M. Sze, *Materials Today* **2016**, *19*, 254-264.

[606] J. Yao, Z. Sun, L. Zhong, D. Natelson, J. M. Tour, *Nano Letters* **2010**, *10*, 4105-4110.

[607] B. J. Choi, D. S. Jeong, S. K. Kim, C. Rohde, S. Choi, J. H. Oh, H. J. Kim, C. S. Hwang, K. Szot, R. Waser, B. Reichenberg, S. Tiedke, *Journal of Applied Physics* **2005**, *98*, 033715.

[608] H. Wang, Y. Zhu, D. Fu, *Journal of Alloys and Compounds* **2017**, *695*, 2669-2671.

[609] D.-H. Kwon, K. M. Kim, J. H. Jang, J. M. Jeon, M. H. Lee, G. H. Kim, X.-S. Li, G.-S. Park, B. Lee, S. Han, M. Kim, C. S. Hwang, *Nature Nanotechnology* **2010**, *5*, 148.

[610] L. Goux, P. Czarnecki, Y. Y. Chen, L. Pantisano, X. P. Wang, R. Degraeve, B. Govoreanu, M. Jurczak, D. J. Wouters, L. Altimime, *Applied Physics Letters* **2010**, *97*, 243509.

[611] Z. Wang, W. G. Zhu, A. Y. Du, L. Wu, Z. Fang, X. A. Tran, W. J. Liu, K. L. Zhang, H. Yu, *IEEE Transactions on Electron Devices* **2012**, *59*, 1203-1208.

[612] S. Yu, H.-Y. Chen, B. Gao, J. Kang, H. S. P. Wong, *ACS Nano* **2013**, *7*, 2320-2325.

[613] S. Long, X. Lian, T. Ye, C. Cagli, L. Perniola, E. Miranda, M. Liu, J. Suñé, *IEEE Electron Device Letters* **2013**, *34*, 623-625.

[614] S. Mandal, A. El-Amin, K. Alexander, B. Rajendran, R. Jha, *Scientific Reports* **2014**, *4*, 5333.

[615] M. R. Park, Y. Abbas, H. Abbas, Q. Hu, T. S. Lee, Y. J. Choi, T.-S. Yoon, H.-H. Lee, C. J. Kang, *Microelectronic Engineering* **2016**, *159*, 190-197.

[616] J. J. Yang, M.-X. Zhang, J. P. Strachan, F. Miao, M. D. Pickett, R. D. Kelley, G. Medeiros-Ribeiro, R. S. Williams, *Applied Physics Letters* **2010**, *97*, 232102.

[617] M. Kyu Yang, H. Ju, G. Hwan Kim, J.-K. Lee, H.-C. Ryu, *Scientific Reports* **2015**, *5*, 14053.

[618] P. W. C. Ho, F. O. Hatem, H. A. F. Almurib, T. N. Kumar, *Journal of Semiconductors* **2016**, *37*, 064001.

[619] C.-Y. Lin, C.-Y. Wu, C.-Y. Wu, C. Hu, T.-Y. Tseng, *Journal of The Electrochemical Society* **2007**, *154*, G189-G192.

[620] C. Xie, B. Nie, L. Zhu, L.-H. Zeng, Y.-Q. Yu, X.-H. Wang, Q.-L. Fang, L.-B. Luo, Y.-C. Wu, *Nanotechnology* **2013**, *24*, 355203.

[621] N. Xu, L. Liu, X. Sun, X. Liu, D. Han, Y. Wang, R. Han, J. Kang, B. Yu, *Applied Physics Letters* **2008**, *92*, 232112.

[622] N. Xu, L. F. Liu, X. Sun, C. Chen, Y. Wang, D. D. Han, X. Y. Liu, R. Q. Han, J. F. Kang, B. Yu, *Semiconductor Science and Technology* **2008**, *23*, 075019.

[623] F. M. Simanjuntak, D. Panda, T.-L. Tsai, C.-A. Lin, K.-H. Wei, T.-Y. Tseng, *J Mater Sci* **2015**, *50*, 6961-6969.

[624] M. Laurenti, S. Porro, C. F. Pirri, C. Ricciardi, A. Chiolerio, *Critical Reviews in Solid State and Materials Sciences* **2017**, *42*, 153-172.

[625] L. Dongsoo, C. Hyejung, S. Hyunjun, C. Dooho, H. Hyunsang, L. Myoung-Jae, S. Sun-Ae, I. K. Yoo, *IEEE Electron Device Letters* **2005**, *26*, 719-721.

[626] X.-Y. Lei, H.-X. Liu, H.-X. Gao, H.-N. Yang, G.-M. Wang, S.-B. Long, X.-H. Ma, M. Liu, *Chinese Physics B* **2014**, *23*, 117305.

[627] W. C. Chien, Y. C. Chen, E. K. Lai, Y. D. Yao, P. Lin, S. F. Horng, J. Gong, T. H. Chou, H. M. Lin, M. N. Chang, Y. H. Shih, K. Y. Hsieh, R. Liu, C. Lu, *IEEE Electron Device Letters* **2010**, *31*, 126-128.

[628] S. Seo, M. J. Lee, D. H. Seo, E. J. Jeoung, D.-S. Suh, Y. S. Joung, I. K. Yoo, I. R. Hwang, S. H. Kim, I. S. Byun, J.-S. Kim, J. S. Choi, B. H. Park, *Applied Physics Letters* **2004**, *85*, 5655-5657.

[629] H. Shima, F. Takano, H. Akinaga, Y. Tamai, I. H. Inoue, H. Takagi, *Applied Physics Letters* **2007**, *91*, 012901.

[630] M. Lee, Y. Park, B. Kang, S. Ahn, C. Lee, K. Kim, W. Xianyu, G. Stefanovich, J. Lee, S. Chung, Y. Kim, C. Lee, J. Park, I. Baek, I. Yoo, in *2007 IEEE International Electron Devices Meeting*, **2007**, 771-774.

[631] G. Ma, X. Tang, H. Zhang, Z. Zhong, X. Li, J. Li, H. Su, *J Mater Sci* **2017**, *52*, 238-246.

[632] H.-H. Huang, W.-C. Shih, C.-H. Lai, *Applied Physics Letters* **2010**, *96*, 193505.

[633] A. Odagawa, Y. Katoh, Y. Kanzawa, Z. Wei, T. Mikawa, S. Muraoka, T. Takagi, *Applied Physics Letters* **2007**, *91*, 133503.

[634] Y. S. Chen, B. Chen, B. Gao, F. F. Zhang, Y. J. Qiu, G. J. Lian, L. F. Liu, X. Y. Liu, R. Q. Han, J. F. Kang, *Applied Physics Letters* **2010**, *97*, 262112.

[635] L. Deng, G. Li, N. Deng, D. Wang, Z. Zhang, W. He, H. Li, J. Pei, L. Shi, *Scientific Reports* **2015**, *5*, 10684.

[636] M. K. Yang, J.-W. Park, T. K. Ko, J.-K. Lee, *Applied Physics Letters* **2009**, *95*, 042105.

[637] S.-C. Chen, T.-C. Chang, S.-Y. Chen, C.-W. Chen, S.-C. Chen, S. M. Sze, M.-J. Tsai, M.-J. Kao, F.-S. Yeh, *Solid-State Electronics* **2011**, *62*, 40-43.

[638] W.-Y. Yang, S.-W. Rhee, *Applied Physics Letters* **2007**, *91*, 232907.

[639] L. Kou-Chen, T. Wen-Hsien, C. Kow-Ming, C. Yi-Chun, K. Chun-Chih, C. Chun-Wen, in *2010 3rd International Nanoelectronics Conference (INEC)*, **2010**, 898-899.

[640] X. Cao, X. Li, X. Gao, W. Yu, X. Liu, Y. Zhang, L. Chen, X. Cheng, *Journal of Applied Physics* **2009**, *106*, 073723.

[641] X. Sun, B. Sun, L. Liu, N. Xu, X. Liu, R. Han, J. Kang, G. Xiong, T. P. Ma, *IEEE Electron Device Letters* **2009**, *30*, 334-336.

[642] H. J. Kim, H. Zheng, J.-S. Park, D. Hun Kim, C. Jung Kang, J. Tae Jang, D. Hwan Kim, T.-S. Yoon, *Nanotechnology* **2017**, *28*, 285203.

[643] D. Lee, D.-j. Seong, I. Jo, F. Xiang, R. Dong, S. Oh, H. Hwang, *Applied Physics Letters* **2007**, *90*, 122104.

[644] M. Arita, H. Kaji, T. Fujii, Y. Takahashi, *Thin Solid Films* **2012**, *520*, 4762-4767.

[645] M. Son, J. Lee, J. Park, J. Shin, G. Choi, S. Jung, W. Lee, S. Kim, S. Park, H. Hwang, *IEEE Electron Device Letters* **2011**, *32*, 1579-1581.

[646] H.-C. Tseng, T.-C. Chang, J.-J. Huang, Y.-T. Chen, P.-C. Yang, H.-C. Huang, D.-S. Gan, N.-J. Ho, S. M. Sze, M.-J. Tsai, *Thin Solid Films* **2011**, *520*, 1656-1659.

[647] H. Sim, D. Choi, D. Lee, M. Hasan, C. B. Samantaray, H. Hwang, *Microelectronic Engineering* **2005**, *80*, 260-263.

[648] P. K. Sarkar, M. Prajapat, A. Barman, S. Bhattacharjee, A. Roy, *J Mater Sci* **2016**, *51*, 4411-4418.

[649] S. Maikap, S. Z. Rahaman, *ECS Transactions* **2012**, *45*, 257-261.

[650] K. Yin, M. Li, Y. Liu, C. He, F. Zhuge, B. Chen, W. Lu, X. Pan, R.-W. Li, *Applied Physics Letters* **2010**, *97*, 042101.

[651] K. Szot, W. Speier, G. Bihlmayer, R. Waser, *Nature Materials* **2006**, *5*, 312.

[652] J. Xiong, R. Yang, J. Shaibo, H.-M. Huang, H.-K. He, W. Zhou, X. Guo, *Advanced Functional Materials* **2019**, *29*, 1807316.

[653] W.-J. Hu, L. Hu, R.-H. Wei, X.-W. Tang, W.-H. Song, J.-M. Dai, X.-B. Zhu, Y.-P. Sun, *Chinese Physics Letters* **2018**, *35*, 047301.

[654] G.-u.-d. Siddiqui, J. Ali, Y.-H. Doh, K. H. Choi, *Materials Letters* **2016**, *166*, 311-316.

[655] M. Mustaqima, P. Yoo, W. Huang, B. W. Lee, C. Liu, *Nanoscale Research Letters* **2015**, *10*, 168.

[656] A. Asamitsu, Y. Tomioka, H. Kuwahara, Y. Tokura, *Nature* **1997**, *388*, 50.

[657] S. Q. Liu, N. J. Wu, A. Ignatiev, *Applied Physics Letters* **2000**, *76*, 2749-2751.

[658] C. Xin, W. Naijuan, A. Ignatiev, in *Symposium Non-Volatile Memory Technology 2005.*, **2005**, pp. 4 pp.-128.

[659] M. Quintero, P. Levy, A. G. Leyva, M. J. Rozenberg, *Physical Review Letters* **2007**, *98*, 116601.

[660] S. Park, J. Noh, M.-l. Choo, A. M. Sheri, M. Chang, Y.-B. Kim, C. J. Kim, M. Jeon, B.-G. Lee, B. H. Lee, H. Hwang, *Nanotechnology* **2013**, *24*, 384009.

[661] D. Lee, J. Park, K. Moon, J. Jang, S. Park, M. Chu, J. Kim, J. Noh, M. Jeon, B. H. Lee, B. Lee, B. Lee, H. Hwang, in *2015 IEEE International Electron Devices Meeting (IEDM)*, **2015**, 4.7.1-4.7.4.

[662] K. Moon, E. Cha, J. Park, S. Gi, M. Chu, K. Baek, B. Lee, S. H. Oh, H. Hwang, *IEEE Electron Device Letters* **2016**, *37*, 1067-1070.

[663] C. Acha, M. J. Rozenberg, *Journal of Physics: Condensed Matter* **2008**, *21*, 045702.

[664] D. Y. Guo, Z. P. Wu, Y. H. An, P. G. Li, P. C. Wang, X. L. Chu, X. C. Guo, Y. S. Zhi, M. Lei, L. H. Li, W. H. Tang, *Applied Physics Letters* **2015**, *106*, 042105.

[665] X. Gao, Y. Xia, B. Xu, J. Kong, H. Guo, K. Li, H. Li, H. Xu, K. Chen, J. Yin, Z. Liu, *Journal of Applied Physics* **2010**, *108*, 074506.

[666] Z. Q. Wang, H. Y. Xu, X. H. Li, H. Yu, Y. C. Liu, X. J. Zhu, *Advanced Functional Materials* **2012**, *22*, 2759-2765.

[667] L. Hu, S. Fu, Y. Chen, H. Cao, L. Liang, H. Zhang, J. Gao, J. Wang, F. Zhuge, *Advanced Materials* **2017**, *29*, 1606927.

[668] R. Rodriguez, B. Poulter, M. Gonzalez, F. Ali, L. D. Lau, M. Mangun, *Materials Sciences and Applications* **2017**, *8*, 9.

[669] E. J. Yoo, M. Lyu, J.-H. Yun, C. J. Kang, Y. J. Choi, L. Wang, *Advanced Materials* **2015**, *27*, 6170-6175.

[670] M. Kumar, H.-S. Kim, D. Y. Park, M. S. Jeong, J. Kim, *ACS Applied Materials & Interfaces* **2018**, *10*, 12768-12772.

[671] S. Wang, C. He, J. Tang, R. Yang, D. Shi, G. Zhang, *Chinese Physics B* **2019**, *28*, 017304.

[672] M. Wang, S. Cai, C. Pan, C. Wang, X. Lian, Y. Zhuo, K. Xu, T. Cao, X. Pan, B. Wang, S.-J. Liang, J. J. Yang, P. Wang, F. Miao, *Nature Electronics* **2018**, *1*, 130-136.

[673] C. Tan, Z. Liu, W. Huang, H. Zhang, *Chemical Society Reviews* **2015**, *44*, 2615-2628.

[674] R. Ge, X. Wu, M. Kim, J. Shi, S. Sonde, L. Tao, Y. Zhang, J. C. Lee, D. Akinwande, *Nano Letters* **2018**, *18*, 434-441.

[675] H.-K. He, R. Yang, W. Zhou, H.-M. Huang, J. Xiong, L. Gan, T.-Y. Zhai, X. Guo, *Small* **2018**, *14*, 1800079.

[676] A. Ranjan, N. Raghavan, S. J. O'Shea, S. Mei, M. Bosman, K. Shubhakar, K. L. Pey, *Scientific Reports* **2018**, *8*, 2854.

[677] C. Pan, Y. Ji, N. Xiao, F. Hui, K. Tang, Y. Guo, X. Xie, F. M. Puglisi, L. Larcher, E. Miranda, L. Jiang, Y. Shi, I. Valov, P. C. McIntyre, R. Waser, M. Lanza, *Advanced Functional Materials* **2017**, *27*, 1604811.

[678] Y. Shi, X. Liang, B. Yuan, V. Chen, H. Li, F. Hui, Z. Yu, F. Yuan, E. Pop, H. S. P. Wong, M. Lanza, *Nature Electronics* **2018**, *1*, 458-465.

[679] J.-Y. Mao, L. Zhou, Y. Ren, J.-Q. Yang, C.-L. Chang, H.-C. Lin, H.-H. Chou, S.-R. Zhang, Y. Zhou, S.-T. Han, *Journal of Materials Chemistry C* **2019**, *7*, 1491-1501.

[680] Z. Lv, Y. Zhou, S.-T. Han, V. A. L. Roy, *Materials Today* **2018**, *21*, 537-552.

[681] N. Raeis-Hosseini, Y. Park, J.-S. Lee, *Advanced Functional Materials* **2018**, *28*, 1800553.

[682] D. Jana, S. Roy, R. Panja, M. Dutta, S. Z. Rahaman, R. Mahapatra, S. Maikap, *Nanoscale research letters* **2015**, *10*, 188-188.

[683] Y. Yang, P. Gao, S. Gaba, T. Chang, X. Pan, W. Lu, *Nature Communications* **2012**, *3*, 732.

[684] L. Zhong, L. Jiang, R. Huang, C. H. d. Groot, *Applied Physics Letters* **2014**, *104*, 093507.

[685] Z. Wang, S. Joshi, S. E. Savel'ev, H. Jiang, R. Midya, P. Lin, M. Hu, N. Ge, J. P. Strachan, Z. Li, Q. Wu, M. Barnell, G.-L. Li, H. L. Xin, R. S. Williams, Q. Xia, J. J. Yang, *Nature Materials* **2016**, *16*, 101.

[686] Q. Liu, J. Sun, H. Lv, S. Long, K. Yin, N. Wan, Y. Li, L. Sun, M. Liu, *Advanced Materials* **2012**, *24*, 1844-1849.

[687] S. Z. Rahaman, S. Maikap, W. S. Chen, H. Y. Lee, F. T. Chen, M. J. Kao, M. J. Tsai, *Applied Physics Letters* **2012**, *101*, 073106.

[688] W. Hu, X. Chen, G. Wu, Y. Lin, N. Qin, D. Bao, *Applied Physics Letters* **2012**, *101*, 063501.

[689] W. A. Hubbard, A. Kerelsky, G. Jasmin, E. R. White, J. Lodico, M. Mecklenburg, B. C. Regan, *Nano Letters* **2015**, *15*, 3983-3987.

[690] D. Liu, Q. Lin, Z. Zang, M. Wang, P. Wangyang, X. Tang, M. Zhou, W. Hu, *ACS Applied Materials & Interfaces* **2017**, *9*, 6171-6176.

[691] S. Gao, C. Song, C. Chen, F. Zeng, F. Pan, *The Journal of Physical Chemistry C* **2012**, *116*, 17955-17959.

[692] H. Wang, Y. Du, Y. Li, B. Zhu, W. R. Leow, Y. Li, J. Pan, T. Wu, X. Chen, *Advanced Functional Materials* **2015**, *25*, 3825-3831.

[693] Z. Xu, Y. Bando, W. Wang, X. Bai, D. Golberg, *ACS Nano* **2010**, *4*, 2515-2522.

[694] R. Bruchhaus, M. Honal, R. Symanczyk, M. Kund, *Journal of The Electrochemical Society* **2009**, *156*, H729-H733.

[695] N. Yamada, E. Ohno, N. Akahira, K. i. Nishiuchi, K. i. Nagata, M. Takao, *Japanese Journal of Applied Physics* **1987**, *26*, 61.

[696] R. E. Simpson, P. Fons, A. V. Kolobov, T. Fukaya, M. Krbal, T. Yagi, J. Tominaga, *Nature Nanotechnology* **2011**, *6*, 501.

[697] S. Raoux, W. Wełnic, D. Ielmini, *Chemical Reviews* **2010**, *110*, 240-267.

[698] Y. Li, X.-Y. Sun, C.-Y. Xu, J. Cao, Z.-Y. Sun, L. Zhen, *Nanoscale* **2018**, *10*, 23080-23086.

[699] T. N. Ng, D. E. Schwartz, L. L. Lavery, G. L. Whiting, B. Russo, B. Krusor, J. Veres, P. Bröms, L. Herlogsson, N. Alam, O. Hagel, J. Nilsson, C. Karlsson, *Scientific Reports* **2012**, *2*, 585.

[700] S.-T. Han, Y. Zhou, V. A. L. Roy, *Advanced Materials* **2013**, *25*, 5425-5449.

[701] A. S. Tayi, A. Kaeser, M. Matsumoto, T. Aida, S. I. Stupp, *Nature Chemistry* **2015**, *7*, 281.

[702] S. Majumdar, H. Tan, Q. H. Qin, S. van Dijken, *Advanced Electronic Materials* **2019**, *5, 1800795.*

[703] Y. Cao, Q. Li, M. Huijben, R. K. Vasudevan, S. V. Kalinin, P. Maksymovych, *Physical Review Materials* **2018**, *2*, 094401.

[704] J. Jiang, Z. L. Bai, Z. H. Chen, L. He, D. W. Zhang, Q. H. Zhang, J. A. Shi, M. H. Park, J. F. Scott, C. S. Hwang, A. Q. Jiang, *Nature Materials* **2017**, *17*, 49.

[705] aJ. Rödel, W. Jo, K. T. P. Seifert, E.-M. Anton, T. Granzow, D. Damjanovic, *Journal of the American Ceramic Society* **2009**, *92*, 1153-1177; bJ. Shieh, Y. C. Lin, C. S. Chen, *Journal of Physics D: Applied Physics* **2009**, *43*, 025404.

[706] J. Müller, T. S. Böscke, U. Schröder, S. Mueller, D. Bräuhaus, U. Böttger, L. Frey, T. Mikolajick, *Nano Letters* **2012**, *12*, 4318-4323.

[707] P. Polakowski, J. Müller, *Applied Physics Letters* **2015**, *106*, 232905.

[708] S. Mueller, J. Mueller, A. Singh, S. Riedel, J. Sundqvist, U. Schroeder, T. Mikolajick, *Advanced Functional Materials* **2012**, *22*, 2412-2417.

[709] B.-T. Lin, Y.-W. Lu, J. Shieh, M.-J. Chen, *Journal of the European Ceramic Society* **2017**, *37*, 1135-1139.

[710] Y. Zhou, S. Ramanathan, *Proceedings of the IEEE* **2015**, *103*, 1289-1310.

[711] K. Moon, E. Cha, D. Lee, J. Jang, J. Park, H. Hwang, in *2016 International Symposium on VLSI Technology, Systems and Application (VLSI-TSA)*, **2016**, pp. 1-2.

[712] S. Kumar, J. P. Strachan, R. S. Williams, *Nature* **2017**, *548*, 318.

[713] Y. Zhou, X. Chen, C. Ko, Z. Yang, C. Mouli, S. Ramanathan, *IEEE Electron Device Letters* **2013**, *34*, 220-222.

[714] N. Shukla, A. V. Thathachary, A. Agrawal, H. Paik, A. Aziz, D. G. Schlom, S. K. Gupta, R. Engel-Herbert, S. Datta, *Nature Communications* **2015**, *6*, 7812.

[715] J. del Valle, Y. Kalcheim, J. Trastoy, A. Charnukha, D. N. Basov, I. K. Schuller, *Physical Review Applied* **2017**, *8*, 054041.

[716] P. Stoliar, L. Cario, E. Janod, B. Corraze, C. Guillot-Deudon, S. Salmon-Bourmand, V. Guiot, J. Tranchant, M. Rozenberg, *Advanced Materials* **2013**, *25*, 3222-3226.

[717] J. Shi, Y. Zhou, S. Ramanathan, *Nature Communications* **2014**, *5*, 4860.

[718] S. Yamanouchi, Y. Taguchi, Y. Tokura, *Physical Review Letters* **1999**, *83*, 5555-5558.

[719] S. Lee, A. Fursina, J. T. Mayo, C. T. Yavuz, V. L. Colvin, R. G. Sumesh Sofin, I. V. Shvets, D. Natelson, *Nature Materials* **2007**, *7*, 130.

[720] A. Camjayi, C. Acha, R. Weht, M. G. Rodríguez, B. Corraze, E. Janod, L. Cario, M. J. Rozenberg, *Physical Review Letters* **2014**, *113*, 086404.

[721] Q. Hong, L. Zhao, X. Wang, *Neurocomputing* **2019**, *330*, 11-16.

[722] D. B. Strukov, G. S. Snider, D. R. Stewart, R. S. Williams, *Nature* **2008**, *453*, 80.

[723] Q. Xia, W. Robinett, M. W. Cumbie, N. Banerjee, T. J. Cardinali, J. J. Yang, W. Wu, X. Li, W. M. Tong, D. B. Strukov, G. S. Snider, G. Medeiros-Ribeiro, R. S. Williams, *Nano Letters* **2009**, *9*, 3640-3645.

[724] J. C. Gonzalez-Rosillo, R. Ortega-Hernandez, B. Arndt, M. Coll, R. Dittmann, X. Obradors, A. Palau, J. Suñé, T. Puig, *Advanced Electronic Materials* **2019**, *0*, 1800629.

[725] C. H. Cheng, A. Chin, F. S. Yeh, *IEEE Electron Device Letters* **2011**, *32*, 366-368.

[726] J. Yoon, H. Choi, D. Lee, J. Park, J. Lee, D. Seong, Y. Ju, M. Chang, S. Jung, H. Hwang, *IEEE Electron Device Letters* **2009**, *30*, 457-459.

[727] S. Yu, B. Gao, Z. Fang, H. Yu, J. Kang, H. S. P. Wong, *Advanced Materials* **2013**, *25*, 1774-1779.

[728] D. R. B. Ly, A. Grossi, C. Fenouillet-Beranger, E. Nowak, D. Querlioz, E. Vianello, *Journal of Physics D: Applied Physics* **2018**, *51*, 444002.

[729] Y. Dan, M.-M. Poo, *Physiological Reviews* **2006**, *86*, 1033-1048.

[730] F. Zeldenrust, W. J. Wadman, B. Englitz, *Frontiers in Computational Neuroscience* **2018**, *12*, 48. doi: 10.3389/fncom.2018.00048.

[731] R. Yang, H.-M. Huang, Q.-H. Hong, X.-B. Yin, Z.-H. Tan, T. Shi, Y.-X. Zhou, X.-S. Miao, X.-P. Wang, S.-B. Mi, C.-L. Jia, X. Guo, *Advanced Functional Materials* **2018**, *28*, 1704455.

[732] Daniel E. Feldman, *Neuron* **2012**, *75*, 556-571.

[733] M. P. Sah, H. Kim, L. O. Chua, *IEEE Circuits and Systems Magazine* **2014**, *14*, 12-36.

[734] P. Stoliar, J. Tranchant, B. Corraze, E. Janod, M.-P. Besland, F. Tesler, M. Rozenberg, L. Cario, *Advanced Functional Materials* **2017**, *27*, 1604740.

[735] J. Zhang, X. Liao, *AEU - International Journal of Electronics and Communications* **2017**, *75*, 82-90.

[736] A. Amirsoleimani, M. Ahmadi, A. Ahmadi, in *2017 International Joint Conference on Neural Networks (IJCNN)*, **2017**, pp. 3409-3414.

[737] B. Bao, A. Hu, H. Bao, Q. Xu, M. Chen, H. Wu, *Complexity* **2018**, *2018*, 3872573.

[738] Y. V. Pershin, *IEEE Transactions on Circuits and Systems II: Express Briefs* **2018**, 1-1. doi: 10.1109/TCSII.2018.2873635

[739] F. Tesler, C. Adda, J. Tranchant, B. Corraze, E. Janod, L. Cario, P. Stoliar, M. Rozenberg, *Physical Review Applied* **2018**, *10*, 054001.

[740] M. D. Pickett, G. Medeiros-Ribeiro, R. S. Williams, *Nature Materials* **2012**, *12*, 114.

[741] H.-M. Huang, R. Yang, Z.-H. Tan, H.-K. He, W. Zhou, J. Xiong, X. Guo, *Advanced Materials* **2019**, *31*, 1803849.

[742] C. Adda, L. Cario, J. Tranchant, E. Janod, M.-P. Besland, M. Rozenberg, P. Stoliar, B. Corraze, *MRS Communications* **2018**, *8*, 835-841.

[743] C. Adda, B. Corraze, P. Stoliar, P. Diener, J. Tranchant, A. Filatre-Furcate, M. Fourmigué, D. Lorcy, M.-P. Besland, E. Janod, L. Cario, *Journal of Applied Physics* **2018**, *124*, 152124.

[744] Y. Zhang, W. He, Y. Wu, K. Huang, Y. Shen, J. Su, Y. Wang, Z. Zhang, X. Ji, G. Li, H. Zhang, S. Song, H. Li, L. Sun, R. Zhao, L. Shi, *Small* **2018**, *14*, 1802188.

[745] W. Yi, K. K. Tsang, S. K. Lam, X. Bai, J. A. Crowell, E. A. Flores, *Nature Communications* **2018**, *9*, 4661.

[746] T. Tuma, A. Pantazi, M. Le Gallo, A. Sebastian, E. Eleftheriou, *Nature Nanotechnology* **2016**, *11*, 693.

[747] G. A. Kerchner, R. A. Nicoll, *Nature Reviews Neuroscience* **2008**, *9*, 813.

[748] J. M. Montgomery, P. Pavlidis, D. V. Madison, *Neuron* **2001**, *29*, 691-701.

[749] S. Panzeri, J. H. Macke, J. Gross, C. Kayser, *Trends in cognitive sciences* **2015**, *19*, 162-172.

[750] Y. He, S. Nie, R. Liu, Y. Shi, Q. Wan, *IEEE Electron Device Letters* **2019**, *40*, 139-142.

[751] F. Alibart, E. Zamanidoost, D. B. Strukov, *Nature Communications* **2013**, *4*, 2072.

[752] M. Prezioso, F. Merrikh-Bayat, B. D. Hoskins, G. C. Adam, K. K. Likharev, D. B. Strukov, *Nature* **2015**, *521*, 61.

[753] P. M. Sheridan, F. Cai, C. Du, W. Ma, Z. Zhang, W. D. Lu, *Nature Nanotechnology* **2017**, *12*, 784.

[754] C. Du, F. Cai, M. A. Zidan, W. Ma, S. H. Lee, W. D. Lu, *Nature Communications* **2017**, *8*, 2204.

[755] C. Li, M. Hu, Y. Li, H. Jiang, N. Ge, E. Montgomery, J. Zhang, W. Song, N. Dávila, C. E. Graves, Z. Li, J. P. Strachan, P. Lin, Z. Wang, M. Barnell, Q. Wu, R. S. Williams, J. J. Yang, Q. Xia, *Nature Electronics* **2018**, *1*, 52-59.

[756] S. Choi, P. Sheridan, W. D. Lu, *Scientific Reports* **2015**, *5*, 10492.

[757] Z. Wang, S. Joshi, S. Savel'ev, W. Song, R. Midya, Y. Li, M. Rao, P. Yan, S. Asapu, Y. Zhuo, H. Jiang, P. Lin, C. Li, J. H. Yoon, N. K. Upadhyay, J. Zhang, M. Hu, J. P.

Strachan, M. Barnell, Q. Wu, H. Wu, R. S. Williams, Q. Xia, J. J. Yang, *Nature Electronics* **2018**, *1*, 137-145.

[758] C. D. James, J. B. Aimone, N. E. Miner, C. M. Vineyard, F. H. Rothganger, K. D. Carlson, S. A. Mulder, T. J. Draelos, A. Faust, M. J. Marinella, J. H. Naegle, S. J. Plimpton, *Biologically Inspired Cognitive Architectures* **2017**, *19*, 49-64.

[759] G. W. Burr, R. M. Shelby, A. Sebastian, S. Kim, S. Kim, S. Sidler, K. Virwani, M. Ishii, P. Narayanan, A. Fumarola, L. L. Sanches, I. Boybat, M. Le Gallo, K. Moon, J. Woo, H. Hwang, Y. Leblebici, *Advances in Physics: X* **2017**, *2*, 89-124.

[760] J. Y. Seok, S. J. Song, J. H. Yoon, K. J. Yoon, T. H. Park, D. E. Kwon, H. Lim, G. H. Kim, D. S. Jeong, C. S. Hwang, *Advanced Functional Materials* **2014**, *24*, 5316-5339.

[761] V. Ravichandran, C. Li, A. Banagozar, J. J. Yang, Q. Xia, *Science China Information Sciences* **2018**, *61*, 060423.

[762] S. Yu, *Proceedings of the IEEE* **2018**, *106*, 260-285.

[763] S. Pi, C. Li, H. Jiang, W. Xia, H. Xin, J. J. Yang, Q. Xia, *Nature Nanotechnology* **2019**, *14*, 35-39.

[764] C. Li, D. Belkin, Y. Li, P. Yan, M. Hu, N. Ge, H. Jiang, E. Montgomery, P. Lin, Z. Wang, W. Song, J. P. Strachan, M. Barnell, Q. Wu, R. S. Williams, J. J. Yang, Q. Xia, *Nature Communications* **2018**, *9*, 2385.

[765] E. R. Kandel, J. H. Schwartz, T. M. Jessell, *Principles of neural science*, McGraw-Hill, Health Professions Division, New York, **2000**.

[766] P. Verghese, D. G. Pelli, *Vision Research* **1992**, *32*, 983-995.

[767] B. Sengupta, M. B. Stemmler, K. J. Friston, *PLoS computational biology* **2013**, *9*, e1003157-e1003157.

[768] F. Caravelli, J. P. Carbajal, *Technologies* **2018**, *6*, 118.

[769] A. K. Maan, D. A. Jayadevi, A. P. James, *IEEE Transactions on Neural Networks and Learning Systems* **2017**, *28*, 1734-1746.

[770] P. Wang, J. Wang, L. Fu, Y. Wu, T. van Ree, *2 - Metal oxides in fuel cells*, in *Metal Oxides in Energy Technologies* (Ed.: Y. Wu), Elsevier, **2018**, pp. 17-47.

[771] F. Wang, Y. Zhang, N. Yu, L. Fu, Y. Zhu, Y. Wu, T. van Ree, *6 - Metal oxides in batteries*, in *Metal Oxides in Energy Technologies* (Ed.: Y. Wu), Elsevier, **2018**, pp. 127-167.

[772] L. Zhou, C. Li, X. Liu, Y. Zhu, Y. Wu, T. van Ree, *7 - Metal oxides in supercapacitors*, in *Metal Oxides in Energy Technologies* (Ed.: Y. Wu), Elsevier, **2018**, pp. 169-203.

[773] aU. Rashid, S. Soltani, S. I. Al-Resayes, I. A. Nehdi, *11 - Metal oxide catalysts for biodiesel production*, in *Metal Oxides in Energy Technologies*, in *Metal Oxides in Energy Technologies* (Ed.: Y. Wu), Elsevier, **2018**, pp. 303-319; bB. Chen, Z. Liu, C. Li, Y. Zhu, L. Fu, Y. Wu, T. van Ree, *9 - Metal oxides for hydrogen storage*, in *Metal Oxides in Energy Technologies*, in *Metal Oxides in Energy Technologies* (Ed.: Y. Wu), Elsevier, **2018**, pp. 251-274.

[774] L. Ji, *3 - Metal oxide-based thermoelectric materials*, in *Metal Oxides in Energy Technologies* (Ed.: Y. Wu), Elsevier, **2018**, pp. 49-72.

[775] J. Matsuno, J. Fujioka, T. Okuda, K. Ueno, T. Mizokawa, T. Katsufuji, *Science and Technology of Advanced Materials* **2018**, *19*, 899-908.

[776] H. Ohta, *18 - Thermoelectrics based on metal oxide thin films*, in *Metal Oxide-Based Thin Film Structures* (Eds.: N. Pryds, V. Esposito), Elsevier, **2018**, pp. 441-464.

[777] Perovskite and Related Oxides for Energy Harvesting by Thermoelectricity in *Perovskites and Related Mixed Oxides* (eds P. Granger, V. I. Parvulescu, V. I. Parvulescu and W. Prellier). **2015** Wiley‑VCH Verlag, doi:10.1002/9783527686605.ch09.

[778] K. Uchino, *5 - Piezoelectric energy harvesting systems with metal oxides*, in *Metal Oxides in Energy Technologies* (Ed.: Y. Wu), Elsevier, **2018**, pp. 91-126.

[779] A. Datta, D. Mukherjee, S. Kar-Narayan, *19 - Ferroelectric and piezoelectric oxide nanostructured films for energy harvesting applications*, in *Metal Oxide-Based Thin Film Structures* (Eds.: N. Pryds, V. Esposito), Elsevier, **2018**, pp. 465-488.

[780] Y. Wang, C. Li, W. Zhou, Y. Zhu, L. Fu, Y. Wu, T. van Ree, *14 - Metal oxide-based superconductors in AC power transportation and transformation* in *Metal Oxides in Energy Technologies* (Ed.: Y. Wu), Elsevier, **2018**, pp. 361-390.

[781] F. Ren, J. C. Yang, C. Fares, S. J. Pearton, *MRS Communications* **2019**, 1-11.

[782] S. J. Pearton, J. Yang, P. H. CaryIV, F. Ren, J. Kim, M. J. Tadjer, M. A. Mastro, *Applied Physics Reviews* **2018**, *5*, 011301.

[783] J. Wang, T. van Ree, Y. Wu, P. Zhang, L. Gao, *8 - Metal oxide semiconductors for solar water splitting* in *Metal Oxides in Energy Technologies* (Ed.: Y. Wu), Elsevier, **2018**, pp. 205-249.

[784] Y. Chen, H. H. Li, I. Bayram, E. Eken, *IEEE Design & Test* **2017**, *34*, 8-22.

[785] H. Y. Lee, P. S. Chen, T. Y. Wu, Y. S. Chen, C. C. Wang, P. J. Tzeng, C. H. Lin, F. Chen, C. H. Lien, M. Tsai, in *2008 IEEE International Electron Devices Meeting*, **2008**, pp. 1-4.

[786] A. Wedig, M. Luebben, D.-Y. Cho, M. Moors, K. Skaja, V. Rana, T. Hasegawa, K. K. Adepalli, B. Yildiz, R. Waser, I. Valov, *Nature Nanotechnology* **2015**, *11*, 67.

[787] J. F. Scott, C. A. Paz de Araujo, *Science* **1989**, *246*, 1400-1405.

[788] A. Chanthbouala, A. Crassous, V. Garcia, K. Bouzehouane, S. Fusil, X. Moya, J. Allibe, B. Dlubak, J. Grollier, S. Xavier, C. Deranlot, A. Moshar, R. Proksch, N. D. Mathur, M. Bibes, A. Barthélémy, *Nature Nanotechnology* **2011**, *7*, 101.

[789] H. Tian, L. Zhao, X. Wang, Y.-W. Yeh, N. Yao, B. P. Rand, T.-L. Ren, *ACS Nano* **2017**, *11*, 12247-12256.

[790] H. Zhao, Z. Dong, H. Tian, D. DiMarzi, M.-G. Han, L. Zhang, X. Yan, F. Liu, L. Shen, S.-J. Han, S. Cronin, W. Wu, J. Tice, J. Guo, H. Wang, *Advanced Materials* **2017**, *29*, 1703232.

[791] D. Groh, R. Pandey, M. B. Sahariah, E. Amzallag, I. Baraille, M. Rérat, *Journal of Physics and Chemistry of Solids* **2009**, *70*, 789-795.

[792] S. Ouyang, J. Ye, *Journal of the American Chemical Society* **2011**, *133*, 7757-7763.

[793] T. Omata, H. Nagatani, I. Suzuki, M. Kita, H. Yanagi, N. Ohashi, *Journal of the American Chemical Society* **2014**, *136*, 3378-3381.

[794] X. Yu, Y. Li, X. Hu, D. Zhang, Y. Tao, Z. Liu, Y. He, M. A. Haque, Z. Liu, T. Wu, Q. J. Wang, *Nature Communications* **2018**, *9*, 4299.

[795] S. Trolier-McKinstry, in *Piezoelectric and Acoustic Materials for Transducer Applications* (Eds.: A. Safari, E. K. Akdoğan), Springer US, Boston, MA, **2008**, pp. 39-56.

[796] D. Damjanovic, *Reports on Progress in Physics* **1998**, *61*, 1267-1324.

[797] B. Kundys, *Applied Physics Reviews* **2015**, *2*, 011301.

[798] B. C.-K. Tee, A. Chortos, A. Berndt, A. K. Nguyen, A. Tom, A. McGuire, Z. C. Lin, K. Tien, W.-G. Bae, H. Wang, P. Mei, H.-H. Chou, B. Cui, K. Deisseroth, T. N. Ng, Z. Bao, *Science* **2015**, *350*, 313-316.

[799] B. Y. Lee, J. Zhang, C. Zueger, W.-J. Chung, S. Y. Yoo, E. Wang, J. Meyer, R. Ramesh, S.-W. Lee, *Nature Nanotechnology* **2012**, *7*, 351.

[800] X. Chen, K. Parida, J. Wang, J. Xiong, M.-F. Lin, J. Shao, P. S. Lee, *ACS Applied Materials & Interfaces* **2017**, *9*, 42200-42209.

[801] B. Kundys, M. Viret, D. Colson, D. O. Kundys, *Nature Materials* **2010**, *9*, 803-805.

[802] T.-C. Wei, H.-P. Wang, H.-J. Liu, D.-S. Tsai, J.-J. Ke, C.-L. Wu, Y.-P. Yin, Q. Zhan, G.-R. Lin, Y.-H. Chu, J.-H. He, *Nature Communications* **2017**, *8*, 15018.

[803] H. Tsai, R. Asadpour, J.-C. Blancon, C. C. Stoumpos, O. Durand, J. W. Strzalka, B. Chen, R. Verduzco, P. M. Ajayan, S. Tretiak, J. Even, M. A. Alam, M. G. Kanatzidis, W. Nie, A. D. Mohite, *Science* **2018**, *360*, 67-70.

[804] C. Lü, S. Wu, B. Lu, Y. Zhang, Y. Du, X. Feng, *Journal of Micromechanics and Microengineering* **2018**, *28*, 025010.

[805] H.-H. Chou, A. Nguyen, A. Chortos, J. W. F. To, C. Lu, J. Mei, T. Kurosawa, W.-G. Bae, J. B. H. Tok, Z. Bao, *Nature Communications* **2015**, *6*, 8011.

[806] Y. Wang, B. Chen, Y. Zhu, L. Fu, Y. Wu, T. van Ree, 13 - Metal oxides in energy-saving smart windows, in *Metal Oxides in Energy Technologies* (Ed.: Y. Wu), Elsevier, **2018**, pp. 341-360.

[807] S. Wang, W. Fan, Z. Liu, A. Yu, X. Jiang, *Journal of Materials Chemistry C* **2018**, *6*, 191-212.

[808] T. M. Bartol, Jr., C. Bromer, J. Kinney, M. A. Chirillo, J. N. Bourne, K. M. Harris, T. J. Sejnowski, *eLife* **2015**, *4*, e10778.

[809] E. Bullmore, O. Sporns, *Nature Reviews Neuroscience* **2009**, *10*, 312.

[810] A. Avena-Koenigsberger, B. Misic, O. Sporns, *Nature Reviews Neuroscience* **2017**, *19*, 17.

[811] C. E. Shannon, *Bell system technical journal* **1948**, *27*.

[812] A. Borst, F. E. Theunissen, *Nature Neuroscience* **1999**, *2*, 947.

[813] J. D. Victor, *Biological Theory* **2006**, *1*, 302-316.

[814] R. Quian Quiroga, S. Panzeri, *Nature Reviews Neuroscience* **2009**, *10*, 173.

[815] A. G. Dimitrov, A. A. Lazar, J. D. Victor, *Journal of Computational Neuroscience* **2011**, *30*, 1-5.

[816] N. M. Timme, C. Lapish, *eNeuro* **2018**, *5*, ENEURO.0052-0018.2018.

[817] M. Wibral, J. T. Lizier, V. Priesemann, *Frontiers in Robotics and AI* **2015**, *2*, 5. doi: 10.3389/frobt.2015.00005.

[818] D. Abasolo, R. Hornero, J. Escudero, C. Gomez, M. Garcia, M. Lopez, in *2006 IET 3rd International Conference On Advances in Medical, Signal and Information Processing - MEDSIP 2006*, **2006**, pp. 1-4.

[819] C. J. Stam, *Clinical Neurophysiology* **2005**, *116*, 2266-2301.

[820] C. Güdücü, B. O. Olcay, L. Schäfer, M. Aziz, V. A. Schriever, M. Özgören, T. Hummel, *Brain Research* **2019**, *1708*, 78-83.

[821] W. Bialek, F. Rieke, R. de Ruyter van Steveninck, D. Warland, *Science* **1991**, *252*, 1854-1857.

[822] S. P. S. Naama Brenner, Roland Koberle, William Bialek and Rob R. de Ruyter van Steveninck, *Neural Computation* **2000,** *12*, 1531-1552

[823] L. M. A. Bettencourt, V. Gintautas, M. I. Ham, *Physical Review Letters* **2008**, *100*, 238701.

[824] M. Li, J. Z. Tsien, *Frontiers in cellular neuroscience* **2017**, *11*, 236-236.

[825] J. T. Lizier, J. Heinzle, A. Horstmann, J.-D. Haynes, M. Prokopenko, *Journal of Computational Neuroscience* **2011**, *30*, 85-107.

[826] T. Berger, W. B. Levy, *IEEE Transactions on Information Theory* **2010**, *56*, 852-874.

[827] S. Ito, M. E. Hansen, R. Heiland, A. Lumsdaine, A. M. Litke, J. M. Beggs, *PLOS ONE* **2011**, *6*, e27431.

[828] Andre M. Bastos, W. M. Usrey, Rick A. Adams, George R. Mangun, P. Fries, Karl J. Friston, *Neuron* **2012**, *76*, 695-711.

[829] N. Timme, S. Ito, M. Myroshnychenko, F.-C. Yeh, E. Hiolski, P. Hottowy, J. M. Beggs, *PLOS ONE* **2014**, *9*, e115764.

[830] D. A. Butts, *Network: Computation in Neural Systems* **2003**, *14*, 177-187.

[831] M. R. Deweese, M. Meister, *Network: Computation in Neural Systems* **1999**, *10*, 325-340.

[832] S. Panzeri, R. S. Petersen, S. R. Schultz, M. Lebedev, M. E. Diamond, *Neuron* **2001**, *29*, 769-777.

[833] P. Wollstadt, K. K. Sellers, L. Rudelt, V. Priesemann, A. Hutt, F. Fröhlich, M. Wibral, *PLOS Computational Biology* **2017**, *13*, e1005511.

[834] G. Gómez-Herrero, W. Wu, K. Rutanen, M. C. Soriano, G. Pipa, R. Vicente, *Entropy* **2015**, *17*, 1958.

[835] W. F. Asaad, P. M. Lauro, J. A. Perge, E. N. Eskandar, *The Journal of Neuroscience* **2017**, *37*, 6995-7007.

[836] M. Wibral, N. Pampu, V. Priesemann, F. Siebenhühner, H. Seiwert, M. Lindner, J. T. Lizier, R. Vicente, *PLOS ONE* **2013**, *8*, e55809.

[837] S. Nigam, M. Shimono, S. Ito, F.-C. Yeh, N. Timme, M. Myroshnychenko, C. C. Lapish, Z. Tosi, P. Hottowy, W. C. Smith, S. C. Masmanidis, A. M. Litke, O. Sporns, J. M. Beggs, *The Journal of Neuroscience* **2016**, *36*, 670-684.

[838] J. Fan, *Frontiers in Human Neuroscience* **2014**, *8*, 680.

[839] K. Sayood, *Entropy* **2018**, *20*, 706.

[840] V. Crupi, J. D. Nelson, B. Meder, G. Cevolani, K. Tentori, *Cognitive Science* **2018**, *42*, 1410-1456.

[841] A. Zénon, O. Solopchuk, G. Pezzulo, *Neuropsychologia* **2019**, *123*, 5-18.

[842] Q. Ren, Q. Long, Z. Zhang, J. Zhao, *Information Transfer Characteristic in Memristic Neuromorphic Network*. Springer Berlin Heidelberg, Berlin, Heidelberg, **2013**, pp. 1-8.

[843] W. W. Lee, S. L. Kukreja, N. V. Thakor, *Frontiers in Neuroscience* **2017**, *11*, 5. doi: 10.3389/fnins.2017.00005

[844] H. D. Crane, *Proceedings of the IRE* **1962**, *50*, 2048-2060.

[845] L. O. Chua, K. Sung Mo, *Proceedings of the IEEE* **1976**, *64*, 209-223.

[846] L. Chua, V. Sbitnev, H. Kim, *International Journal of Bifurcation and Chaos* **2012**, *22*, 1230011.

[847] Y. Pan, T. Wan, H. Du, B. Qu, D. Wang, T.-J. Ha, D. Chu, *Journal of Alloys and Compounds* **2018**, *757*, 496-503.

[848] Y. Matveyev, R. Kirtaev, A. Fetisova, S. Zakharchenko, D. Negrov, A. Zenkevich, *Nanoscale Research Letters* **2016**, *11*, 147.

[849] Ella M. Gale, *Faraday Discussions* **2019**, *213*, 521-551.

[850] A. Chiolerio, M. Chiappalone, P. Ariano, S. Bocchini, *Frontiers in Neuroscience* **2017**, *11*, 70 doi: 10.3389/fnins.2017.00070

[851] H. An, J. Li, Y. Li, X. Fu, Y. Yi, *Computers & Electrical Engineering* **2017**, *63*, 99-113.

[852] Z. Mainen, T. Sejnowski, *Science* **1995**, *268*, 1503-1506.

[853] S. I. a. J. H. Manton, *Neural Computation* **2009**, *21*, 1714-1748

[854] D. A. Butts, C. Weng, J. Jin, C.-I. Yeh, N. A. Lesica, J.-M. Alonso, G. B. Stanley, *Nature* **2007**, *449*, 92.

[855] C. Koch, I. Segev, *Nature Neuroscience* **2000**, *3*, 1171.

[856] S. A. Prescott, T. J. Sejnowski, *The Journal of neuroscience : the official journal of the Society for Neuroscience* **2008**, *28*, 13649-13661.

[857] G. Chakma, M. M. Adnan, A. R. Wyer, R. Weiss, C. D. Schuman, G. S. Rose, *IEEE Journal on Emerging and Selected Topics in Circuits and Systems* **2018**, *8*, 125-136.

[858] C. Zhao, Y. Yi, J. Li, X. Fu, L. Liu, *IEEE Transactions on Very Large Scale Integration (VLSI) Systems* **2017**, *25*, 2193-2205.

[859] S. Moradi, R. Manohar, *Journal of Physics D: Applied Physics* **2018**, *52*, 014003.

[860] N. Zheng, P. Mazumder, *IEEE Transactions on Nanotechnology* **2018**, *17*, 520-532.

[861] C. R. Gallistel, *Trends in Cognitive Sciences* **2017**, *21*, 498-508.

[862] S. Ambrogio, S. Balatti, F. Nardi, S. Facchinetti, D. Ielmini, *Nanotechnology* **2013**, *24*, 384012.

[863] E. Covi, S. Brivio, A. Serb, T. Prodromakis, M. Fanciulli, S. Spiga, *Frontiers in neuroscience* **2016**, *10*, 482-482.

[864] M. S. Feali, A. Ahmadi, *Neural Processing Letters* **2017**, *45*, 1-14.

[865] G. Rachmuth, H. Z. Shouval, M. F. Bear, C.-S. Poon, *Proceedings of the National Academy of Sciences* **2011**, *108*, E1266-E1274.

[866] B. N. Ralston, L. Q. Flagg, E. Faggin, J. T. Birmingham, *Journal of Neurophysiology* **2016**, *115*, 2501-2518.

[867] D. Keun Lee, M.-H. Kim, T.-H. Kim, S. Bang, Y.-J. Choi, S. Kim, S. Cho, B.-G. Park, *Solid-State Electronics* **2019**, 154, 31-35.

[868] M. S. Feali, A. Ahmadi, M. Hayati, *Neurocomputing* **2018**, *309*, 157-167.

[869] A. Parihar, M. Jerry, S. Datta, A. Raychowdhury, *Frontiers in Neuroscience* **2018**, *12*, 210. doi: 10.3389/fnins.2018.00210

[870] T. Levi, T. Nanami, A. Tange, K. Aihara, T. Kohno, *IEEE Transactions on Circuits and Systems II: Express Briefs* **2018**, *65*, 577-581.

[871] K. Wang, S. Dai, Y. Zhao, Y. Wang, C. Liu, J. Huang, *Small* **2019**, 15, 1900010.

[872] Y. Shen, N. C. Harris, S. Skirlo, M. Prabhu, T. Baehr-Jones, M. Hochberg, X. Sun, S. Zhao, H. Larochelle, D. Englund, M. Soljačić, *Nature Photonics* **2017**, *11*, 441.

[873] J.-Y. Mao, L. Hu, S.-R. Zhang, Y. Ren, J.-Q. Yang, L. Zhou, Y.-J. Zeng, Y. Zhou, S.-T. Han, *Journal of Materials Chemistry C* **2019**, *7*, 48-59.

[874] B. Li, W. Wei, X. Yan, X. Zhang, P. Liu, Y. Luo, J. Zheng, Q. Lu, Q. Lin, X. Ren, *Nanotechnology* **2018**, *29*, 464004.

[875] S. Wang, C. Chen, Z. Yu, Y. He, X. Chen, Q. Wan, Y. Shi, D. W. Zhang, H. Zhou, X. Wang, P. Zhou, *Advanced Materials* **2019**, *31*, 1806227.

[876] Z. Wang, S.-R. Zhang, L. Zhou, J.-Y. Mao, S.-T. Han, Y. Ren, J.-Q. Yang, Y. Wang, Y. Zhai, Y. Zhou, *physica status solidi (RRL) – Rapid Research Letters*, *0*, 1800644.

[877] Q. Wu, J. Wang, J. Cao, C. Lu, G. Yang, X. Shi, X. Chuai, Y. Gong, Y. Su, Y. Zhao, N. Lu, D. Geng, H. Wang, L. Li, M. Liu, *Advanced Electronic Materials* **2018**, *4*, 1800556.

[878] P. Maier, F. Hartmann, M. Emmerling, C. Schneider, M. Kamp, S. Höfling, L. Worschech, *Physical Review Applied* **2016**, *5*, 054011.

[879] D.-C. Hu, R. Yang, L. Jiang, X. Guo, *ACS Applied Materials & Interfaces* **2018**, *10*, 6463-6470.

[880] S. Abbas, M. Kumar, D.-K. Ban, J.-H. Yun, J. Kim, *ACS Applied Electronic Materials* **2019**, *1*, 437-443.

[881] B. J. Shastri, A. N. Tait, T. Ferreira de Lima, M. A. Nahmias, H.-T. Peng, P. R. Prucnal, *Neuromorphic Photonics, Principles of*, in *Encyclopedia of Complexity and Systems Science* (Ed.: R. A. Meyers), Springer Berlin Heidelberg, Berlin, Heidelberg, **2018**, pp. 1-37.

[882] B. J. Shastri, M. A. Nahmias, A. N. Tait, T. F. d. Lima, H.-T. Peng, P. R. Prucnal, *Integrated neuromorphic photonics, Vol. 10721*, SPIE, **2018**.

[883] S. Abel, D. J. Stark, F. Eltes, J. E. Ortmann, D. Caimi, J. Fompeyrine, in *2017 IEEE International Conference on Rebooting Computing (ICRC)*, **2017**, pp. 1-3.

[884] J. M. Shainline, *The largest cognitive systems will be optoelectronic*, in *arXiv e-prints*, **2018**, arXiv:1809.02572.

[885] H. Peng, M. A. Nahmias, T. F. d. Lima, A. N. Tait, B. J. Shastri, *IEEE Journal of Selected Topics in Quantum Electronics* **2018**, *24*, 1-15.

[886] D. S. Reich, F. Mechler, J. D. Victor, *Science* **2001**, *294*, 2566-2568.

[887] A. Fairhall, E. Shea-Brown, A. Barreiro, *Current Opinion in Neurobiology* **2012**, *22*, 653-659.

[888] R. A. A. Ince, R. Senatore, E. Arabzadeh, F. Montani, M. E. Diamond, S. Panzeri, *Neural Networks* **2010**, *23*, 713-727.

[889] A. K. Tagantsev, G. Gerra, *Journal of Applied Physics* **2006**, *100*, 051607.

[890] K. Yoo, B. Koteswararao, J. Kang, A. Shahee, W. Nam, F. F. Balakirev, V. S. Zapf, N. Harrison, A. Guda, N. Ter-Oganessian, K. H. Kim, *npj Quantum Materials* **2018**, *3*, 45.

[891] J. T. Zhang, C. Ji, J. L. Wang, W. S. Xia, B. X. Guo, X. M. Lu, J. S. Zhu, *Physical Review B* **2017**, *96*, 235136.

[892] Y. Zhang, J. Wang, M. P. K. Sahoo, T. Shimada, T. Kitamura, *Physical Chemistry Chemical Physics* **2017**, *19*, 26047-26055.

[893] D. Lee, H. Lu, Y. Gu, S.-Y. Choi, S.-D. Li, S. Ryu, T. R. Paudel, K. Song, E. Mikheev, S. Lee, S. Stemmer, D. A. Tenne, S. H. Oh, E. Y. Tsymbal, X. Wu, L.-Q. Chen, A. Gruverman, C. B. Eom, *Science* **2015**, *349*, 1314-1317.

[894] D. O. Hebb, *The Organization of Behavior: A Neuropsychological Theory*, Wiley, **1949**.

[895] L. W. Martin, A. M. Rappe, *Nature Reviews Materials* **2016**, *2*, 16087.

[896] Y. A. Genenko, R. Khachaturyan, J. Schultheiß, A. Ossipov, J. E. Daniels, J. Koruza, *Physical Review B* **2018**, *97*, 144101.

[897] L. Baudry, I. Lukyanchuk, V. M. Vinokur, *Scientific Reports* **2017**, *7*, 42196.

[898] G. A. Boni, L. D. Filip, C. Chirila, I. Pasuk, R. Negrea, I. Pintilie, L. Pintilie, *Nanoscale* **2017**, *9*, 19271-19278.

[899] S. Manipatruni, D. E. Nikonov, I. A. Young, *Nature Physics* **2018**, *14*, 338-343.

[900] D. C. Vaz, A. Barthélémy, M. Bibes, *Japanese Journal of Applied Physics* **2018**, *57*, 0902A0904.

[901] S. Boyn, J. Grollier, G. Lecerf, B. Xu, N. Locatelli, S. Fusil, S. Girod, C. Carrétéro, K. Garcia, S. Xavier, J. Tomas, L. Bellaiche, M. Bibes, A. Barthélémy, S. Saïghi, V. Garcia, *Nature Communications* **2017**, *8*, 14736.

[902] R. Guo, Y. Zhou, L. Wu, Z. Wang, Z. Lim, X. Yan, W. Lin, H. Wang, H. Y. Yoong, S. Chen, Ariando, T. Venkatesan, J. Wang, G. M. Chow, A. Gruverman, X. Miao, Y. Zhu, J. Chen, *ACS Applied Materials & Interfaces* **2018**, *10*, 12862-12869.

[903] H. Mulaosmanovic, E. Chicca, M. Bertele, T. Mikolajick, S. Slesazeck, *Nanoscale* **2018**, *10*, 21755-21763.

[904] A. Q. Jiang, Y. Zhang, *NPG Asia Materials* **2019**, *11*, 2.

[905] F. Zayer, W. Dghais, M. Benabdeladhim, B. Hamdi, *AEU - International Journal of Electronics and Communications* **2019**, *100*, 56-65.

[906] Z. Fei, W. Zhao, T. A. Palomaki, B. Sun, M. K. Miller, Z. Zhao, J. Yan, X. Xu, D. H. Cobden, *Nature* **2018**, *560*, 336-339.

[907] J. Shen, Y.-q. Ma, *Journal of Applied Physics* **2001**, *89*, 5031-5035.

[908] J. Lin, S. Guha, S. Ramanathan, *Frontiers in Neuroscience* **2018**, *12*, 856. doi: 10.3389/fnins.2018.00856

[909] A. K. Friedman, J. J. Walsh, B. Juarez, S. M. Ku, D. Chaudhury, J. Wang, X. Li, D. M. Dietz, N. Pan, V. F. Vialou, R. L. Neve, Z. Yue, M.-H. Han, *Science* **2014**, *344*, 313-319.

[910] J. N. Campbell, R. A. Meyer, *Neuron* **2006**, *52*, 77-92.

[911] M. W. a. W. A. P. Steven M. Silverstein *Computational Psychiatry* **2017**, *1*, 82-101.

[912] B. Elevåg, P. W. Foltz, M. Rosenstein, R. Ferrer-i-Cancho, S. De Deyne, E. Mizraji, A. Cohen, *Schizophrenia Bulletin* **2017**, *43*, 509-513.

[913] J. Seitz, J. Goldstein, A. E. Lyall, M. Kubicki, M. E. Shenton, P. Savadjiev, E. C. del Re, L. J. Seidman, T. Petryshen, C.-F. Westin, L. J. O'Donnell, J. D. Wojcik, R. I. Mesholam-Gately, P. Nestor, M. Niznikiewicz, R. W. McCarley, **2018**.

[914] R. Wallace, *Acta Biotheoretica* **2018**, *66*, 79-112.

[915] A. Giersch, A. L. Mishara, *Frontiers in Psychology* **2017**, *8*, 1659.

[916] T. Kircher, H. Bröhl, F. Meier, J. Engelen, *The Lancet Psychiatry* **2018**, *5*, 515-526.

[917] E. Bullmore, O. Sporns, *Nature Reviews Neuroscience* **2012**, *13*, 336.

[918] J. E. Niven, S. B. Laughlin, *Journal of Experimental Biology* **2008**, *211*, 1792-1804.

[919] C. Cherniak, *The Journal of Neuroscience* **1994**, *14*, 2418-2427.

[920] C. Cherniak, *Trends in Neurosciences* **1995**, *18*, 522-527.

[921] V. Balasubramanian, P. Sterling, *The Journal of Physiology* **2009**, *587*, 2753-2767.

[922] R. H. Masland, *Nature Neuroscience* **2001**, *4*, 877.

[923] T. Zhai, X. Fang, M. Liao, X. Xu, H. Zeng, B. Yoshio, D. Golberg, *Sensors (Basel, Switzerland)* **2009**, *9*, 6504-6529.

[924] Q. Zhang, K. Zhang, D. Xu, G. Yang, H. Huang, F. Nie, C. Liu, S. Yang, *Progress in Materials Science* **2014**, *60*, 208-337.

[925] T. Zhai, L. Li, Y. Ma, M. Liao, X. Wang, X. Fang, J. Yao, Y. Bando, D. Golberg, *Chemical Society Reviews* **2011**, *40*, 2986-3004.

[926] S. Abbas, M. Kumar, J. Kim, *Materials Science in Semiconductor Processing* **2018**, *88*, 86-92.

[927] M. M. Y. A. Alsaif, S. Kuriakose, S. Walia, N. Syed, A. Jannat, B. Y. Zhang, F. Haque, M. Mohiuddin, T. Alkathiri, N. Pillai, T. Daeneke, J. Z. Ou, A. Zavabeti, *Advanced Materials Interfaces* **2019**, *6*, 1900007.

[928] L. Bao, J. Kang, Y. Fang, Z. Yu, Z. Wang, Y. Yang, Y. Cai, R. Huang, *Scientific Reports* **2018**, *8*, 13727.

[929] S. Yu, B. Gao, Z. Fang, H. Yu, J. Kang, H.-S. P. Wong, *Advanced Materials* **2013**, *25*, 1774-1779.

[930] H. Wang, Q. Zhao, Z. Ni, Q. Li, H. Liu, Y. Yang, L. Wang, Y. Ran, Y. Guo, W. Hu, Y. Liu, *Advanced Materials* **2018**, *30*, 1803961.

[931] S. Gao, G. Liu, H. Yang, C. Hu, Q. Chen, G. Gong, W. Xue, X. Yi, J. Shang, R.-W. Li, *ACS Nano* **2019**, *13*, 2634-2642.

[932] S. B. Laughlin, *Current Opinion in Neurobiology* **2001**, *11*, 475-480.

[933] D. Attwell, S. B. Laughlin, *Journal of Cerebral Blood Flow & Metabolism* **2001**, *21*, 1133-1145.

[934] B. Hille, *Ion Channels of Excitable Membranes (3rd Edition)*, Sinauer Associates Inc, **2001**.

[935] J. S. Lee, S. Lee, T. W. Noh, *Applied Physics Reviews* **2015**, *2*, 031303.

[936] X. Shi, Z. Zeng, L. Yang, Y. Huang, *IEEE Transactions on Emerging Topics in Computational Intelligence* **2018**, *2*, 359-370.

[937] J.-Y. Chen, C.-W. Huang, C.-H. Chiu, Y.-T. Huang, W.-W. Wu, *Advanced Materials* **2015**, *27*, 5028-5033.

[938] Z. Wang, M. Yin, T. Zhang, Y. Cai, Y. Wang, Y. Yang, R. Huang, *Nanoscale* **2016**, *8*, 14015-14022.

[939] M. M. Shirolkar, C. Hao, X. Dong, T. Guo, L. Zhang, M. Li, H. Wang, *Nanoscale* **2014**, *6*, 4735-4744.

[940] W. Xue, S. Gao, J. Shang, X. Yi, G. Liu, R.-W. Li, *Advanced Electronic Materials* **2019**, *0*, 1800854.

[941] R. P. N. Rao, D. H. Ballard, *Nature Neuroscience* **1999**, *2*, 79.

[942] A. Clark, *Behavioral and Brain Sciences* **2013**, *36*, 181-204.

[943] R. Hyman, *Journal of Experimental Psychology* **1953**, *45*, 188-196.

[944] G. N. Saxe, D. Calderone, L. J. Morales, *PLOS ONE* **2018**, *13*, e0191582.

[945] P. Lennie, *Current Biology* **2003**, *13*, 493-497.

[946] L. Itti, P. Baldi, *Vision Research* **2009**, *49*, 1295-1306.

[947] P. Baldi, L. Itti, *Neural Networks* **2010**, *23*, 649-666.

[948] K. Friston, *Nature Reviews Neuroscience* **2010**, *11*, 127.

[949] A. G. Volkov, J. Reedus, C. M. Mitchell, C. Tucket, V. Forde-Tuckett, M. I. Volkova, V. S. Markin, L. Chua, *Plant Signaling & Behavior* **2014**, *9*, e29056.

[950] V. S. Markin, A. G. Volkov, L. Chua, *Plant Signaling & Behavior* **2014**, *9*, e972887.

[951] Y. V. Pershin, S. La Fontaine, M. Di Ventra, *Physical Review E* **2009**, *80*, 021926.

[952] Y. V. Pershin, M. Di Ventra, *Neural Networks* **2010**, *23*, 881-886.

[953] D. Querlioz, O. Bichler, A. F. Vincent, C. Gamrat, *Proceedings of the IEEE* **2015**, *103*, 1398-1416.

[954] R. Naous, M. Al-Shedivat, K. N. Salama, *IEEE Transactions on Nanotechnology* **2016**, *15*, 15-28.

[955] J. S. Friedman, L. E. Calvet, P. Bessière, J. Droulez, D. Querlioz, *IEEE Transactions on Circuits and Systems I: Regular Papers* **2016**, *63*, 895-904.

[956] J. S. Friedman, J. Droulez, P. Bessière, J. Lobo, D. Querlioz, *International Journal of Approximate Reasoning* **2017**, *85*, 139-158.

[957] A. Ren, Z. Li, C. Ding, Q. Qiu, Y. Wang, J. Li, X. Qian, B. Yuan, *SIGARCH Comput. Archit. News* **2017**, *45*, 405-418.

[958] E. O. Neftci, B. U. Pedroni, S. Joshi, M. Al-Shedivat, G. Cauwenberghs, *Frontiers in Neuroscience* **2016**, *10*, 241. doi: 10.3389/fnins.2016.00241

[959] A. Serb, J. Bill, A. Khiat, R. Berdan, R. Legenstein, T. Prodromakis, *Nature Communications* **2016**, *7*, 12611.

[960] M. Hansen, F. Zahari, M. Ziegler, H. Kohlstedt, *Frontiers in Neuroscience* **2017**, *11*. 91. doi: 10.3389/fnins.2017.00091

[961] G. J. Berman, W. Bialek, J. W. Shaevitz, *Proceedings of the National Academy of Sciences* **2016**, *113*, 11943-11948.

[962] D. C. Knill, A. Pouget, *Trends in Neurosciences* **2004**, *27*, 712-719.

[963] M. Bar, *Trends in Cognitive Sciences* **2007**, *11*, 280-289.

[964] T. Monk, C. Savin, J. Lücke, *Scientific Reports* **2018**, *8*, 10038.

[965] F. Karl, *Entropy* **2012**, *14*, 2100.

[966] H. B. Barlow, *Possible principles underlying the transformation of sensory messages. Sensory communication* **1961**. doi: 10.7551/mitpress/9780262518420.003.0013

[967] R. Linsker, *Annual Review of Neuroscience* **1990**, *13*, 257-281.

[968] R. C. Smith, S. Seelecke, Z. Ounaies, J. Smith, *Journal of Intelligent Material Systems and Structures* **2003**, *14*, 719-739.

[969] M. E. Lines, A. M. Glass, *Principles and Applications of Ferroelectrics and Related Materials*, OUP Oxford, **2001**.

[970] F. Rubio-Marcos, A. Del Campo, P. Marchet, J. F. Fernández, *Nat Commun* **2015**, *6*, 6594.

[971] T. Li, A. Lipatov, H. Lu, H. Lee, J.-W. Lee, E. Torun, L. Wirtz, C.-B. Eom, J. Íñiguez, A. Sinitskii, A. Gruverman, *Nature Communications* **2018**, *9*, 3344.

[972] L. You, F. Zheng, L. Fang, Y. Zhou, L. Z. Tan, Z. Zhang, G. Ma, D. Schmidt, A. Rusydi, L. Wang, L. Chang, A. M. Rappe, J. Wang, *Science Advances* **2018**, *4*, eaat3438.

[973] A. B. Swain, M. Rath, S. Pal, M. S. R. Rao, V. Subramanian, P. Murugavel, *Applied Physics Letters* **2018**, *113*, 233902.

[974] M. Adachi, M. Seki, H. Yamahara, H. Nasu, H. Tabata, *Applied Physics Express* **2015**, *8*, 043002.

[975] K. J. Friston, J. Daunizeau, J. Kilner, S. J. Kiebel, *Biological Cybernetics* **2010**, *102*, 227-260.

[976] K. Friston, S. Samothrakis, R. Montague, *Biological Cybernetics* **2012**, *106*, 523-541.

[977] K. Friston, F. Rigoli, D. Ognibene, C. Mathys, T. Fitzgerald, G. Pezzulo, *Cognitive Neuroscience* **2015**, *6*, 187-214.

[978] K. Friston, T. FitzGerald, F. Rigoli, P. Schwartenbeck, J. O Doherty, G. Pezzulo, *Neuroscience & Biobehavioral Reviews* **2016**, *68*, 862-879.

[979] K. Friston, FitzGerald, Thomas, Rigoli, Francesco, Schwartenbeck, Philipp and Pezzulo, Giovanni *Neural Computation* **2017**, *29*, 1-49

[980] C. L. Buckley, C. S. Kim, S. McGregor, A. K. Seth, *Journal of Mathematical Psychology* **2017**, *81*, 55-79.

[981] G. Pezzulo, F. Donnarumma, P. Iodice, D. Maisto, I. Stoianov, *Entropy* **2017**, *19*, 266.

[982] G. Pezzulo, F. Rigoli, K. J. Friston, *Trends in Cognitive Sciences* **2018**, *22*, 294-306.

[983] R. A. Adams, S. Shipp, K. J. Friston, *Brain Structure and Function* **2013**, *218*, 611-643.

[984] A. Linson, A. Clark, S. Ramamoorthy, K. Friston, *Frontiers in Robotics and AI* **2018**, *5*, 21. doi: 10.3389/frobt.2018.00021

[985] M. Biehl, C. Guckelsberger, C. Salge, S. C. Smith, D. Polani, *Frontiers in neurorobotics* **2018**, *12*, 45-45.

[986] K. Friston, *Proceedings of the IEEE* **2014**, *102*, 446-446.

[987] B. Balaji, K. Friston, *Bayesian state estimation using generalized coordinates, Vol. 8050*, SPIE, **2011**.

[988] L. Pio-Lopez, A. Nizard, K. Friston, G. Pezzulo, *Journal of The Royal Society Interface* **2016**, *13*, 20160616.

[989] M. Botvinick, M. Toussaint, *Trends in Cognitive Sciences* **2012**, *16*, 485-488.

[990] N. F. Lepora, G. Pezzulo, *PLOS Computational Biology* **2015**, *11*, e1004110.

[991] G. Pezzulo, P. Cisek, *Trends in Cognitive Sciences* **2016**, *20*, 414-424.

[992] F. M. J. Verschure Paul, M. A. Pennartz Cyriel, G. Pezzulo, *Philosophical Transactions of the Royal Society B: Biological Sciences* **2014**, *369*, 20130483.

[993] P. Lanillos, G. Cheng, in *2018 IEEE/RSJ International Conference on Intelligent Robots and Systems (IROS)*, **2018**, pp. 4083-4090.

[994] S. Denève, R. Jardri, *Brain* **2013**, *136*, 3227-3241.

[995] C. D. Fiorillo, P. N. Tobler, W. Schultz, *Science* **2003**, *299*, 1898-1902.

[996] K. J. Friston, T. Shiner, T. FitzGerald, J. M. Galea, R. Adams, H. Brown, R. J. Dolan, R. Moran, K. E. Stephan, S. Bestmann, *PLOS Computational Biology* **2012**, *8*, e1002327.

[997] K. Hu, R. Xiong, H. Guo, R. Ma, S. Zhang, Z. L. Wang, V. V. Tsukruk, *Advanced Materials* **2016**, *28*, 3549-3556.

[998] H. E. Lee, S. Kim, J. Ko, H.-I. Yeom, C.-W. Byun, S. H. Lee, D. J. Joe, T.-H. Im, S.-H. K. Park, K. J. Lee, *Advanced Functional Materials* **2016**, *26*, 6170-6178.

[999] B. K. Sharma, J.-H. Ahn, *Advanced Electronic Materials* **2016**, *2*, 1600105.

[1000] N. Münzenrieder, G. Cantarella, C. Vogt, L. Petti, L. Büthe, G. A. Salvatore, Y. Fang, R. Andri, Y. Lam, R. Libanori, D. Widner, A. R. Studart, G. Tröster, *Advanced Electronic Materials* **2015**, *1*, 1400038.

[1001] Y. Park, M.-J. Park, J.-S. Lee, *Advanced Functional Materials* **2018**, *28*, 1804123.

[1002] Y. Kim, Y. J. Kwon, D. E. Kwon, K. J. Yoon, J. H. Yoon, S. Yoo, H. J. Kim, T. H. Park, J.-W. Han, K. M. Kim, C. S. Hwang, *Advanced Materials* **2018**, *30*, 1704320.

[1003] Y. Liu, Z. Liu, B. Zhu, J. Yu, K. He, W. R. Leow, M. Wang, B. K. Chandran, D. Qi, H. Wang, G. Chen, C. Xu, X. Chen, *Advanced Materials* **2017**, *29*, 1701780.